Transcriptional signatures of microglial innate immune memory in models of Parkinson's and Huntington's disease

Dissertation

zur Erlangung des Grades eines
Doktors der Naturwissenschaften

der Mathematisch-Naturwissenschaftlichen Fakultät
und
der Medizinischen Fakultät
der Eberhard-Karls-Universität Tübingen

vorgelegt
von

Ping Liu
aus Si Chuan, Land China

2022

Tag der mündlichen Prüfung: 11.07.2022

Dekan der Math.-Nat. Fakultät: Prof. Dr. Thilo Stehle
Dekan der Medizinischen Fakultät: Prof. Dr. Bernd Pichler

1. Berichterstatter: Dr. Jonas Neher

2. Berichterstatter: Prof. Dr. Alexander N.R. Weber

Prüfungskommission: Dr. Jonas Neher

Prof. Dr. Alexander N.R. Weber

Prof. Dr. Olga Garaschuk

PD Dr. Julia Schulze-Hentrich

Erklärung / Declaration:

Ich erkläre, dass ich die zur Promotion eingereichte Arbeit mit dem Titel:

"**Transcriptional signatures of microglial innate immune memory in models of Parkinson's and Huntington's disease**"

selbständig verfasst, nur die angegebenen Quellen und Hilfsmittel benutzt und wörtlich oder inhaltlich übernommene Stellen als solche gekennzeichnet habe. Ich versichere an Eides statt, dass diese Angaben wahr sind und dass ich nichts verschwiegen habe. Mir ist bekannt, dass die falsche Abgabe einer Versicherung an Eides statt mit Freiheitsstrafe bis zu drei Jahren oder mit Geldstrafe bestraft wird.

I hereby declare that I have produced the work entitled "Transcriptional signatures of microglial innate immune memory in models of Parkinson's and Huntington's disease", submitted for the award of a doctorate, on my own (without external help), have used only the sources and aids indicated and have marked passages included from other works, whether verbatim or in content, as such. I swear upon oath that these statements are true and that I have not concealed anything. I am aware that making a false declaration under oath is punishable by a term of imprisonment of up to three years or by a fine.

Tübingen, den 01.08.2022

Acknowledgement

First of all, I would like to thank my PhD supervisor, Dr. Jonas Neher, for his great help in life and in research during my PhD. 4 years ago, I was an immature PhD student who had just moved from clinical medicine to basic research and did not understand many of the experiments or research hypotheses. Thanks a lot for his support and encouragement during this period, which was very important to me. I will always remember his smile and patience, and I can't thank you enough for responding to my emails in the evenings and at weekends. Whether or if I am successful in the future, the four years I spent as a doctoral student in your research group was a pivotal decision in my life and a very memorable period.

I would like to appreciate my advisory board members, Prof. Alexander N.R. Weber and Prof. Olga Garaschuk, for their suggestions and support for my PhD project. Also, I would like to thank Prof. Alexander N.R. Weber for reviewing my thesis.

Thanks to all my collaborators in the EPIROM project, Dr. Julia Schulze-Hentrich, Dr. Thomas Hentrich, Reema Chowdhury, Dr. M. Sadman Sakib, Dr. Jonasz Weber, Jessica Cielenga and Dr. Yogesh Singh.

I am very happy to be a member of the AG Neher and AG Jucker family; everyone was so kind and nice, and every lab retreat and party were a moment I will never forget. I appreciate the assistance from Katleen Wild in our laboratory. Thanks to Desirée Brösamle for her help with data analysis, as well as our lunch times and exchanges. Thanks to Marius Lambert for his help with ELISA. I would like to thank Lisa Steinbrecher a lot. We sat together for 3 years, and you were so nice and take care of my emotions and stress. Thank you for your friendship and I hope your headache goes away. In addition, I appreciate the support and assistance from the other lab members, Jessica Wagner, Jian Sun, Nina Hermann, Marleen Veit, and everyone else. I like all of you and Tübingen.

I want to thank my parents, other family members and my friends. Most of all, thank you to the love of my life, Mengyan Jiang, for all your support and companionship over the years and for

making my PhD career more memorable. Thanks to my unborn baby, Zhiheng Liu, for making this year even better.

Lastly, thanks for my regretless and resilience along the academic journey.

Table of Contents

Summary

Due to the ever-increasing age of the human population, the absolute number of individuals impacted by neurodegenerative diseases has been growing globally for the last 25 years. As most of them are currently incurable, neurological disorders are the primary cause of disability and death worldwide (GBD 2016 Neurology Collaborators, 2019). Thus, a detailed understanding of the underlying processes of neurodegenerative disorders and the search for therapies are becoming increasingly urgent tasks.

Parkinson's disease (PD) and Huntington's disease (HD) are chronic neurodegenerative conditions with neuronal loss in the motor, sensory, and cognitive systems. Both disorders share a progressive intracellular deposition of proteins in insoluble aggregates, which are thought to play a critical role in disease pathogenesis and finally result in significant neuronal damage. The cause of sporadic PD is unclear; however, the histological hallmarks of PD are termed Lewy bodies (LBs) and Lewy neurites (LNs), which are both composed mostly of aggregated a-synuclein (aSyn) (Wakabayashi et al., 2007). In comparison, HD is a hereditary disorder with a well-characterized causal gene and protein, namely mutant Huntingtin (mHTT), that results in extensive early neuronal damage and death across the brain (Martin and Gusella, 1986).

Increasing evidence indicates that neuroinflammation plays a substantial role in the pathogenesis of various neurodegenerative disorders. Therefore, it is crucial to understand how exactly the brain's immune system affects neuropathology and whether environmental factors that change the immune system response could be risk factors for neurodegenerative diseases. Recent research revealed that innate immune memory in microglia could shape cerebral β-amyloidosis in an AD mouse model and can modify brain cytokine levels, microglial epigenetic and gene expression profiles, metabolism, and phagocytic activity for at least 6 months (Wendeln et al., 2018). However, whether microglial immune memory influences disease pathogenesis in models of PD and HD remains unknown.

Therefore, the aim of this thesis was to investigate the effect of innate immune memory on microglial transcriptomic profiles in PD and HD rat models. To this end, two well-characterized rat models of a-synucleinopathy or mutant huntingtin (mHTT) pathology, the neuropathological hallmarks of PD or HD, respectively, were used. Those two rat models were previously generated

using a bacterial artificial chromosome (BAC) that contains the entire human SNCA or HTT genomic sequence as well as all regulatory regions (Nuber et al., 2013; Yu-Taeger et al., 2012).

The first set of experiments of my thesis focused on investigating whether immune memory can be induced in the blood and brain by peripheral immune stimuli (using one, two or four injections of bacterial lipopolysaccharides) and a high-fat diet in PD and HD rat models. This was done by multiplex Enzyme-linked immunosorbent assay (ELISA), quantifying nine cytokines (IFN-γ, IL-1β, IL-4, IL-5, IL-6, KC/GRO, IL-10, IL-13, and TNF-α) in 4 animal cohorts (with a total of 330 animals) across different treatments and genotypes. Results from these analyses confirmed an acute immune response in the periphery and brain after acute LPS injections in 3-month-old rat models that were indistinguishable amongst all genotypes. Testing the long-term effects of peripheral immune stimulation in 9-month-old animals, a possible synergy of the peripheral immune stimulation (6 months earlier) and pathology-associated inflammatory responses was found because cytokine levels were differentially regulated by different peripheral immune stimuli in the PD and HD models. This indicated that also in these models, microglial innate immune memory induced by peripheral stimuli may persist for the long term (at least 6 months).

The second set of experiments of my thesis focused on investigating whether immune memory triggered by peripheral stimuli and a high-fat diet is apparent in the microglial transcriptomic profiles in PD and HD rat models. Bulk RNA-sequencing of sorted microglia from the forebrain (olfactory bulb, cortex, striatum, and hippocampus) in 3- as well as 9-month-old cohorts was used to examine gene co-expression networks of microglial profiles across the various conditions (wildtype vs transgenic with different immune stimuli). In young, 3-month-old animals without pathology, the acute microglial transcriptomic responses were not significantly different between transgenic rats (BAC SNCA or BAC HD) and wild-type animals in PD and HD cohorts. However, in the 9-month cohort (WT vs BAC SNCA or HD), apparent differences in microglial transcriptomic profiles were found between the control group (PBS), and between different treatment groups (1 x LPS, 4 x LPS, HFD) of the same genotype. Interestingly, different pathways were modulated in microglia from the PD and HD models, even in response to the same peripheral immune stimulus. These data corroborate the capacity of microglia for innate immune memory and demonstrate for the first time that not only the initial immune stimulus but also the secondary stimulus (here PD and HD brain pathology) significantly affects the microglial phenotype.

The third set of experiments of my thesis focused on the heterogeneity of microglial cells in 9-month-old BAC HD and BAC SNCA rats using single-cell RNA-sequencing (scRNA-seq). Analysing 34,914 individual microglial cells, 11 subpopulations were identified, but pathology-specific microglial subclusters were not apparent in BAC HD or BAC SNCA animals (contrary to what has been observed, for example, in AD models). However, a shift in the proportions of cells within the different microglial subpopulations was found for microglia from PD and HD models, highlighting some genes and related pathways that may play an essential role in the development of α-synuclein or Htt pathology.

In conclusion, the findings of my thesis support the existence of innate immune memory in microglia across a variety of disease models and species and provide the first evidence that the same initial immune stimulus causes brain pathology-specific modulation of transcriptomic responses in microglia (as evidenced by different molecular pathways being modulated in PD vs HD models here); whether specific immune memory states exert beneficial or detrimental effects on PD and HD pathology should therefore be tested in future experiments. The results of the single-cell experiments suggest for the first time that only specific microglial subpopulations react in the early stages of PD and HD pathology; whether these cells are associated with driving or preventing pathology requires further investigation.

Nomenclature

ARM	activated response microglia
BAC	bacterial artificial chromosome
CNS	central nervous system
CT	cortex
Cyc-M	proliferating microglia
DAM	disease-associated microglia
DEGs	differentially expressed genes
ELISA	Enzyme-linked immunosorbent assay
FACS	Fluorescence-activated cell sorting
GBE	Gel Beads in Emulsion
GO	Gene Ontology
GWAS	genome-wide association studies
HBSS	Hank's buffered salt solution
HP	hippocampus
HD	Huntington's disease
HFD	high-fat diet
HTT	Huntingtin
IFN	interferon
Il-6	interleukin 6
IRM	interferon response microglia
KEGG	Kyoto Encyclopedia of Genes and Genomes
LPS	lipopolysaccharide
NK cells	Natural killer cells
OB	olfactory bulb
ORA	over-representation analysis

PAMPs	pathogen-associated molecular patterns
PCA	principal component analysis
PCR	Polymerase chain reaction
PD	Parkinson's disease
PET	Positron emission tomography
PFA	paraformaldehyde
PRRs	pattern recognition receptors
RT	reverse transcription
SEM	standard error of the mean
ST	striatum
SV	surrogate variables
TLR4	Toll-like receptor 4
TNF	Tumor necrosis factor
VST	variance-stabilizing transformation
WAM	white matter–associated microglia
WGCNA	weighted gene co-expression network analysis
WT	wildtype / control

1. Introduction

1.1 Innate immune memory

The immune system is a network of biological processes, which is made up of many types of cells, organs, proteins, and tissues. The critical role of the immune system in host defence is best demonstrated by its dysfunction. Immunodeficiency leads to severe infections and tumours, while overactivity leads to autoimmune diseases, such as rheumatoid arthritis, systemic lupus erythematosus, and other conditions (Parkin and Cohen, 2001). In mammals, two distinct types of immunity exist: innate and adaptive immunity.

Innate immunity is present in the immune system of both vertebrates and invertebrates, which is the first response to infection and tissue damage. Unlike adaptive immune responses, which are unique to a certain pathogen, but relatively slow, innate immune responses are rapid but show much less specificity. Innate immune cells, such as macrophages, dendritic cells, and natural killer cells (Akira et al., 2006), recognise pathogens and tissue damage via germline-encoded pattern recognition receptors (PRRs), which detect a variety of pathogen-associated molecular patterns (PAMPs) and damage-associated molecular patterns (Lanier, 2005; Medzhitov and Janeway, 2000). Phagocytosis, chemotaxis, killing of pathogens or dying cells, and cytokine secretion are the main mechanisms engaged by PRR activation. These innate immune responses are typically quite effective at eliminating invading pathogens (O'Neill et al., 2013). Furthermore, innate immunity also plays an important role in promoting adaptive immunity. For example, macrophages activate adaptive immune cells (i.e., antigen-specific B and T lymphocytes) through antigen presentation. In turn, activated B and T lymphocytes proliferate and differentiate into effector cells; eventually, effector B cells and activated T cells participate in the immune response along with innate immune cells. After cessation of the acute immune response, some of the remaining effector cells (B / T cells) are conserved as memory T and B cells. When these memory cells are exposed to the same antigen again, they can rapidly proliferate. This enables the immune system to launch a more effective and rapid immune response than during the first exposure (Dempsey et al., 2003; Iwasaki and Medzhitov, 2015). Thus, the innate and adaptive immune responses cooperate to offer long-lasting protection to the organism.

Immune memory has been thought to be a unique feature of the adaptive immune system for a long time. However, a growing number of studies indicate that innate immune cells can also exhibit adaptive properties (Bowdish et al., 2007; Christ et al., 2018; Lay et al., 2018; Naik et al., 2017). For example, continuous protection against reinfection has been found in plants and invertebrates that lack adaptive immunity (Conrath et al., 2015; Gourbal et al., 2018; Kurtz, 2005). Furthermore, mice deficient in functioning adaptive immune cells still show enhanced protection against specific pathogens following particular types of vaccines (Bistoni et al., 1986; van 't Wout et al., 1992). Another study also showed that mice pre-treated with β-glucan were resistant to Staphylococcus aureus infection (Marakalala et al., 2013). These findings support the concept that the innate immune system has adaptive properties as well.

Different types of adaptations in innate immune responses have been demonstrated in the peripheral immune system, such as priming, tolerance, and trained immunity. This indicates that innate immune cells are highly plastic and adapt to different insults such as trauma, infections, and immunisation with long-term modifications. For example, after a second stimulus with a pathogen, monocytes and macrophages show memory features with an enhanced non-specific innate immune protection, termed "*trained immunity*" (Kleinnijenhuis et al., 2012; Quintin et al., 2012). In contrast to trained immunity, high-dose lipopolysaccharide (LPS) activation of the Toll-like receptor 4 (TLR4) has been known for decades to reduce the inflammatory response to a second stimulation, termed "*LPS tolerance*" (Dobrovolskaia and Vogel, 2002; Fan and Cook, 2004). The classical innate immune paradigm holds that the first stimulus induces persistent changes in the functional state of innate immune cells (priming), which then mediate a differential response to a secondary immune stimulus (**Figure 1**). Compared to the naive immune response, this differentiated response can be enhanced (known as *trained immunity* or *immune training*) or reduced (known as *tolerance*) (Ifrim et al., 2014). The potential mechanism of immune memory is epigenetic reprogramming, especially in the repertoire of so-called enhancers, i.e. cis-regulatory elements that (when activated) interact with promoters to increase gene expression (Novakovic et al., 2016; Ostuni et al., 2013; Saeed et al., 2014; Wendeln et al., 2018).

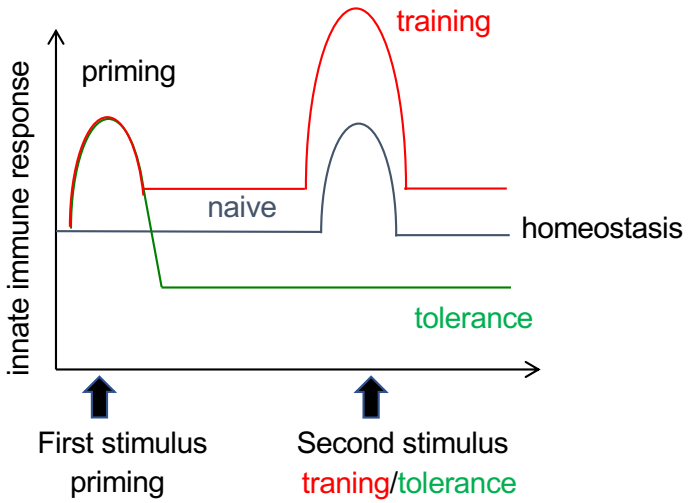

Figure 1. The concept of innate immune memory. The cellular activation state of innate immune cells is modified long-term after the first stimulation (priming). Cells respond to secondary stimulation with an adapted immune response, which can be enhanced (training) or suppressed (tolerance). The figure was adapted from Ifrim et al. (Clinical and Vaccine Immunology 2014).

Recently, our lab has shown that microglia, the major brain-resident macrophages, are also capable of innate immune memory (Wendeln et al., 2018). In this study, different numbers of LPS injections resulted in the differential immune response of microglia in adult mice. In line with the concept of innate immune memory in peripheral macrophages, the LPS stimuli modified the microglial response (immune priming) in a way, which then mediated either an enhanced (immune training) or reduced (immune tolerance) response to a following inflammatory stimulus, even after a long-term stage (6 months later). Specifically, in response to the acute stimulation, a single LPS injection (0.5 mg/kg, i.p.) resulted in immune training one day later, but repeated LPS injections on four consecutive days (0.5 mg/kg, i.p.) caused immune tolerance in the brain with increased and suppressed levels in several cytokines, respectively (IL-1β; TNF-α; IL-10). The authors also examined the long-term effects of single and repeated LPS treatments given at 9 months of age. They found that training and tolerizing stimuli can modify brain cytokine levels, microglial epigenetic and gene expression profiles, metabolic and phagocytic activity for at least six months. This innate immune memory in microglia was also sufficient to modulate cerebral β-amyloidosis in a model of AD pathology (APP23 transgenic mice).

1.2 Microglia

The central nervous system (CNS) comprises the brain and spinal cord, where billions of cells participate in the brain's and spinal cord's function and are individually interconnected to thousands more. Rudolf Virchow first described glial cells in 1856, and the Spanish neuroscientist Pio del Rio Hortega distinguished astrocytes, microglia, and oligodendrocytes in the brain's non-neural cell types in 1919 (Del Río-Hortega Bereciartu, 2020). In the CNS, all glial cells comprise approximately 90%, and microglia constitute 10% of all cells (Lawson et al., 1990). Microglia are the tissue-resident macrophages of the central nervous system in the parenchyma and originate entirely from the yolk sac during embryogenesis (Ginhoux et al., 2010). Additionally, other macrophages exist at the CNS interfaces, such as meningeal, perivascular and choroid plexus macrophages, and these populations receive varying contributions from bone marrow progenitors (Lopez-Atalaya et al., 2018).

Microglia are critical for maintaining tissue homeostasis during development, health, and disease. During development, microglia contribute to shaping neural circuits by regulating synaptic pruning. During CNS damage, microglia are essential for phagocytosis and removal of pathogens, cell debris, and protein aggregates. Additionally, microglia release various soluble substances, including chemokines, cytokines, and neurotrophic factors, which contribute to many aspects of immune responses and tissue repair in the central nervous system (Colonna and Butovsky, 2017; Ginhoux and Guilliams, 2016). In contrast, the absence of microglia leads to learning deficits and impaired synapse formation (Badimon et al., 2020; Parkhurst et al., 2013). Moreover, microglia can influence the development of other glial cell types and their functions in the brain. For example, microglia have an important role in regulating the growth and remyelination activities of oligodendrocytes (Hagemeyer et al., 2017; Lloyd and Miron, 2019; Miron et al., 2013). Microglia also monitor and regulate neuronal activity through specific receptors, such as the purinergic receptor P2RY12 (Badimon et al., 2020; Li and Barres, 2018). P2RY12 is highly expressed in microglia (Butovsky et al., 2014; Haynes et al., 2006; Hickman et al., 2013), is activated by ATP and enables microglia to respond rapidly to microenvironmental changes (Haynes et al., 2006). Some studies also found decreased gene expression levels of *P2ry12* in microglia in neurodegenerative diseases (Badimon et al., 2020; Mildner et al., 2017; Parhizkar et al., 2019), and P2RY12-deficient animals exhibit decreased excitability in the CA1 and impaired fear

memory (Peng et al., 2019). Recent single-cell RNA-sequencing studies revealed that downregulation of the homeostatic gene expression (such as *P2ry12*, *Cx3cr1*, and *Tmem119*) is a characteristic of specific microglial subpopulations in models of brain disease, so-called disease-associated microglia (DAM) and microglial neurodegenerative phenotype (MGnD) (Deczkowska et al., 2018; Keren-Shaul et al., 2017; Wang, 2021). These findings imply that microglia P2RY12 may play a key role in maintaining brain homeostasis.

In the steady-state, tissue-resident macrophages can autonomously maintain self-renewal, whereas monocytes do not contribute significantly (Hashimoto et al., 2013). However, the capacity of self-renewal of some tissue-resident macrophages (including lung, renal, and cardiac macrophages) declines with age and cells are eventually replaced by monocyte-derived macrophages (Perdiguero and Geissmann, 2016). In contrast to other short-lived macrophages in peripheral tissues, microglia were initially considered to be long-lived cells with a low turnover (Lawson et al., 1992), implying that microglia are rarely regenerated. However, several later studies indicated that microglia are a dynamic population and provided insight into the molecular underpinnings of the repopulation response (Bruttger et al., 2015; Elmore et al., 2014; Gomez-Nicola and Perry, 2015; Varvel et al., 2012). Furthermore, in the adult mouse and human brain, a recent study indicated that microglia undergo several rounds of population renewal during the lifetime of the organism (Askew et al., 2017). A similar study reported that human microglia, as distinct from most other hematopoietic lines, have a slow renewal rate with a median turnover of 28% per year, with some microglia persisting for more than 20 years (Réu et al., 2017). In mouse models, genetic labelling of individual microglia in living mice combined with tracking of these cells over time by multiphoton microscopy revealed that under homeostatic conditions, neocortical microglia were very long-lived, with a median lifespan of over 15 months; hence, roughly half of these cells survive the whole lifetime of the mouse (Füger et al., 2017). Therefore, due to their relative longevity, microglia are susceptible to environmental stresses and neurodegenerative disorders but capable of long-lasting immune memory.

Microglia are considered a heterogeneous population, which may enable them to respond to environmental changes to maintain CNS homeostasis in a variety of ways. Some early studies already showed regional microglial heterogeneity based on cell shape, density, electrophysiological properties, and surface expression of immune markers (De Biase et al., 2017; Lawson et al., 1990;

Schmid et al., 2002). Grabert et al. first described differences in gene expression across microglia in the cerebral cortex, hippocampus, cerebellum, and striatum at the transcriptome level (Ayata et al., 2018). The human brain has also been found to have regional heterogeneity in microglia. For example, different gene expression profiles were detected in microglia isolated from the post-mortem tissue of control and multiple sclerosis (MS) donors in grey and white matter (van der Poel et al., 2019). In addition to regional heterogeneity, sex-dependent heterogeneity in microglial gene expression has also been observed (Erny et al., 2015; Guneykaya et al., 2018; Hanamsagar et al., 2017; Thion et al., 2018). Moreover, based on molecular markers, an old nomenclature categorised microglia into two opposite types: M1 phenotype and M2 phenotype. According to this categorisation, M1 microglia would produce pro-inflammatory cytokines and were potentially cytotoxic, while the M2 phenotype would produce anti-inflammatory cytokines and show clearance and regeneration functions (Kigerl et al., 2009; Tang and Le, 2016). However, it is now evident that this perspective no longer properly captures the diversity of microglia (or macrophage) phenotypes. As the brain microenvironment is highly dynamic, so is the adaptive response of microglia to the microenvironment (Hanisch and Kettenmann, 2007; Ransohoff and Perry, 2009). With the advancement of technology, emerging methods such as single-cell RNA sequencing (scRNA-seq) have allowed the profiling of single cells with high-throughput datasets, helping us investigate microglial heterogeneity at the single-cell level. Now, more and more microglia subpopulations were identified by different single-cell RNA seq datasets, such as disease-associated microglia (DAM), activated response microglia (ARM), interferon responsive microglia (IRM), MHC expressing microglia (MHC), proliferating microglia (Cyc-M), and white matter-associated microglia (WAM) (Ellwanger et al., 2021; Friedman et al., 2018; Hammond et al., 2019; Keren-Shaul et al., 2017; Li et al., 2019; Mathys et al., 2017; Parhizkar et al., 2019; Safaiyan et al., 2021; Sala Frigerio et al., 2019; Wang et al., 2020b; Zhou et al., 2020). Those results from single-cell analysis can contribute to establishing more comprehensive molecular maps of microglia, allowing for the identification of new gene markers, functional pathways, and regulatory factors during development, health, and disease.

1.3 Microglia in Parkinson's disease

Parkinson's disease (PD) was initially discovered in 1817 by James Parkinson, who reported the symptoms in his elderly patients, including tremor, stiffness, and postural instability in his publication (Parkinson, 2002). PD is the second most prevalent neurodegenerative disorder, affecting 1.2% of people over 65 years of age. Most incidents are sporadic, with 5–10% inherited (Deng et al., 2018). From 1990 to 2015, the number of patients diagnosed with Parkinson's disease was more than 6 million, and the number of PD patients is expected to increase to almost 12 million by 2040 due to the ageing society (Dorsey et al., 2018). In the substantia nigra, degeneration of dopaminergic neurons develops due to the deposition of Lewy bodies containing aggregated a-synuclein, leading to dopaminergic denervation of the striatum (Dickson, 2018). The SNCA gene encodes α-synuclein and is a genetic risk factor for both sporadic and familial Parkinson's disease (Devine et al., 2011). It has been well established that missense mutations, duplications, or triplication of the SNCA gene can cause PD, and there is a strong gene dosage impact (Ibáñez et al., 2004, 2009; Polymeropoulos et al., 1997; Singleton et al., 2003). Meanwhile, the accumulation of misfolded proteins in the brain is a common feature of neurodegenerative diseases (Soto and Pritzkow, 2018). α-synuclein proteins are also believed to have a crucial role in the etiology of Parkinson's disease (Koros et al., 2017; Stefanis, 2012). During the pathogenesis of Parkinson's disease, α-synuclein gradually converts from soluble to insoluble fibrillar complexes, causing neuronal degeneration (Cremades et al., 2017; Eschbach and Danzer, 2014; Villar-Piqué et al., 2016). Autophagic failure, mitochondrial dysfunction, endoplasmic reticulum stress, and calcium dysregulation have been proposed as potential mechanisms of α-synuclein-induced neurodegeneration (Benskey et al., 2016; Wong and Krainc, 2017).

Although the exact cause of Parkinson's disease is uncertain, growing evidence shows that PD's pathogenesis is not limited to changes in neuronal cells but also includes the immune system, as indicated by a neuroinflammatory response in PD patients (Kannarkat et al., 2013; Tansey and Goldberg, 2010). For example, many HLA-DR-positive reactive microglia were found in the substantia nigra of PD patients (McGeer et al., 1988). Similarly, reactive microglia have been observed in various preclinical models of Parkinson's disease (Alam and Schmidt, 2002; Goetz, 2011; Meredith and Rademacher, 2011; Tieu, 2011). Two positron emission tomography (PET) imaging analyses of PD patients demonstrated an increase in microglial activation (Gerhard

et al., 2006; Stokholm et al., 2017). Another post-mortem investigation on PD patients also described microgliosis in the brain (Imamura et al., 2003). Both microgliosis and chronic microglial immune activation have been reported that may contribute to the degeneration of dopaminergic neurons in PD (Mosley et al., 2012; Stone et al., 2009). Furthermore, it has been shown that aggregation of α-synuclein induces neuronal toxicity as well as neuroinflammation in the brain by activating microglia, thereby exacerbating the pathogenic process of PD (Daniele et al., 2015). With regard to molecular pathways, microglia were found to be activated near a-synuclein deposits with a dependence on the receptors CD36 and TLR2 (Croisier et al., 2005; Kim et al., 2013; Su et al., 2008). In addition, increased levels of several pro-inflammatory cytokines, such as IL-1β, TGF-α, and TGF-β (Nagatsu et al., 2000) and upregulation of TNF-α in nigrostriatal microglia (Boka et al., 1994), have also been found in human PD brains. All these findings support the existence of a chronic pro-inflammatory environment in the brain of PD patients that is closely associated with microglia activation.

Mutations in the leucine-rich repeat kinase 2 (LRRK2) gene are one of the most common causes of familial PD and a risk factor for sporadic PD (Healy et al., 2008; Kumari and Tan, 2009; Paisán-Ruíz et al., 2008). LRRK2 is a serine/threonine kinase that has been shown to be closely associated with immune cell function (Islam and Moore, 2017). Mutations in LRRK2 that result in PD increase its kinase activity and lead to neurodegeneration (Berwick et al., 2019; Cookson, 2015). Moreover, a strong association between LRRK2, the pathogenesis of PD, and the immune system have been observed in several studies (Brockmann et al., 2016, 2017; Dzamko et al., 2012, 2017). Regulating the autophagy/lysosomal degradation pathway is one of the primary functions of LRRK2 (Alegre-Abarrategui et al., 2009; Gómez-Suaga et al., 2012; Schapansky et al., 2014). S-chapansky et al discovered autophagic deficits in LRRK2 knockdown mice in macrophages and microglia (Schapansky et al., 2014). Therefore, proper LRRK2 activity may be essential for maintaining microglial lysosomal function (Berger et al., 2010; Biskup et al., 2006), and failure of this microglial pathway may contribute to PD pathogenesis.

Recently, Chang et al. performed a meta-analysis of genome-wide association studies (GWAS) to find 17 novel risk loci for Parkinson's disease, which are significantly enriched in the pathways of lysosomal biology and autophagy, which (as outlined above) may both be related to the degradation of protein aggregates and microgliosis (Chang et al., 2017). Another meta-analysis of

GWAS has shown many PD risk loci linked with key microglial functions. For example, an overrepresentation of the immune signal pathways and interferon-gamma response were found among PD risk loci by protein-protein and gene expression enrichment analysis (Nalls et al., 2019). Those studies provide substantial evidence that microglial function and associated neuroinflammation may play an important role in the development of PD pathology.

1.4 Microglia in Huntington's disease

Huntington's disease (HD) was described in detail by the American medical scientist George Huntington in 1872 (Lanska 2000). HD is a neurodegenerative disease that is autosomal dominantly inherited and is caused by mutations in the *HTT* gene (mHTT), leading to increases in the trinucleotide CAG stretch in the HTT protein (Bates, 2005). The mutation leads to progressive neurodegeneration throughout the brain, exhibiting significant atrophy and loss of medium spiny neurons in the striatum (Vonsattel and DiFiglia, 1998; Vonsattel et al., 1985; Waldvogel et al., 2015). The magnitude of CAG amplification is inversely related to the age of onset of HD. Carriers with 36-39 CAG repeats may never acquire HD; however, in the extremely rare case of CAG repeats longer than 55, HD can develop in patients younger than 20 years of age. Huntington's disease exhibits a combination of motor (choreiform movements), cognitive, and/or psychiatric symptoms, with progressive loss of the ability to speak, move, think, and swallow, which continues to progress for approximately 10 to 20 years and ultimately results in death (Bates et al., 2015). Scientists have proposed several hypotheses regarding the pathogenesis of Huntington's disease, such as the toxicity of mutant HTT protein (mHTT) (Bennett et al., 2007; Martinez-Vicente et al., 2010), the formation of mHTT fibrils and large inclusions (DiFiglia et al., 1997; Hoffner et al., 2005), and mitochondrial dysfunction (Polyzos and McMurray, 2017; Shirendeb et al., 2011), but its exact pathogenesis is still unclear.

Microglial activation is also a prominent feature in HD patients. For example, PET imaging revealed proinflammatory microglia in HD patients and was linked with disease development at a subclinical stage. The extensive microglial activation in preclinical HD was associated with striatal neuronal impairment (Tai et al., 2007). Moreover, the degree of microglial activation was found to correspond to the severity of HD, providing evidence that microglia contribute to the persistent neuronal degeneration in HD patients (Pavese et al., 2006; Sapp et al., 2001). Similarly, in HD

patients' plasma, increased levels of TNFα and IL-6 have been detected, indicating that inflammation may play a key role in the pathogenesis of HD (Björkqvist et al., 2008; Dalrymple et al., 2007). However, microglia may also contribute to neuroprotection in HD. For example, the co-culture of mHTT-expressing neurons with wild-type microglia enhances neuronal survival (Kraft et al., 2012). On the other hand, microglia expressing mHTT have a decreased ability of migration and a decreased motility of cellular processes, indicating that mHTT can also directly affect microglial cells (Kwan et al., 2012).

Similar immune dysfunctions were reported in common mouse models of HD reviewed by Creus-Muncunill & Ehrlich (Creus-Muncunill and Ehrlich, 2019). mHTT nuclear inclusions were found in cortical and striatal microglia in three distinct HD mouse strains (Jansen et al., 2017), and age-related alterations in striatal microglial morphology were reported in mouse models of HD (Franciosi et al., 2012). In addition, there is accumulating evidence that cell-autonomous dysfunction of microglia is caused by the expression of mHTT in microglia (Björkqvist et al., 2008; Kwan et al., 2012). Although all cell types express *HTT*, the incidence of inclusion bodies is significantly lower in microglia (Jansen et al., 2017). This may be due to an increase in immunoproteasome activity (Orre et al., 2013) and autophagosomes (Su et al., 2016), which gives microglia a greater capacity to digest mHTT. Nevertheless, mHTT may eventually cause microglial dysfunction. Indeed, a recent *in vivo* study showed that supplementing transgenic R6/2 HD mice with normal human glial cells resulted in neuronal protection and phenotypic improvement (Benraiss et al., 2016).

Moreover, microglial function and gene expression profiles are directly affected by mHTT. By enhancing the expression and transcriptional activity of the myeloid lineage-determining proteins PU.1 and C/EBPs, *mHTT* expression in microglia enhanced cell-autonomous pro-inflammatory transcriptional activation. Notably, the upregulation of PU.1 and its target genes were observed in the brains of HD patients and mice models, which were associated with elevated IL6 and TNF expression. Additionally, in the context of sterile inflammation, microglia expressing *mHTT* had a greater potential to trigger neuronal death both in vitro and in vivo. (Crotti et al., 2014). Accordingly, suppression of microglial responses in HD mice models can be protective (Paldino et al., 2020; Siew et al., 2019).

In summary, these studies have provided evidence that neuroinflammation mediated by microglia modulates the development of HD in a variety of ways.

2. Materials and Methods

2.1 Animal models

This study used two well-characterized rat models of Parkinson's disease and Huntington's disease developed at the Institute of Medical Genetics and Applied Genomics in Tübingen. The rat models are generated using a bacterial artificial chromosome (BAC) that contains the entire human SNCA or HTT genomic sequence and all regulatory regions. BAC SNCA rats exhibit early changes in novelty-seeking, avoidance, and olfactory perception. It is important to note that the identified pathological changes were accompanied by a substantial loss of dopaminergic integrity (Nuber et al., 2013). BAC HD transgenic rats develop an early-onset and progressive HD-like phenotype in motor impairments and anxiety-related symptoms. Accumulations of mHTT aggregates occur more commonly in the cortex than in the striatum (Yu-Taeger et al., 2012).

Only male rats were used for this study. All rats were housed (four rats per cage, two wild-type and two transgenic rats) in a standard light-dark cycle (12 hours of light and 12 hours of darkness) and given unlimited access to food and drink. Across the study, all methods followed the regulations established by standards for the animal care and use committee. All operations were authorized (TVA: HG 02/19) by the local authority (Regierungspräsidium Tübingen, Germany).

2.2 Peripheral immune stimulation

LPS (Lipopolysaccharide from Salmonella typhimurium, L6511, Sigma-Aldrich) was injected intraperitoneally (i.p.) into three-month-old rats in various treatment groups with a daily dose of 500 ug per kg bodyweight. In the short-term cohort (three-month cohort), the rats were injected with a single LPS injection (1 x LPS), two consecutive days with LPS injection (2 x LPS), or four consecutive days with LPS injection (4 x LPS). In the long-term cohort (9-month cohort), the rats received either four LPS injections on four consecutive days (4 x LPS), a single LPS injection followed by three vehicle injections on the following three days (1 x LPS), or four vehicle injections on four consecutive days (PBS). The rats in the high-fat diet (HFD) group received high-fat diet chow for 30 days (TD 88137: Fat % 21.3, Sugars % 34.0, Cholesterol mg/kg 1972.4) between the age of 2 and 3 months old.

2.3 Tissue collection

Anaesthesia was achieved by administering xylazine and ketamine (**20 mg/kg and 750 mg/kg**, respectively) at the given time points to achieve deep and surgical anaesthesia. Blood samples were taken from the heart's right ventricle, and the animals were perfused with ice-cold PBS through the left ventricle for 5 mins. The brain was isolated and sagitally divided into two hemispheres, either preserved in 4% paraformaldehyde (PFA) or prepared for microglia isolation after being removed from the animal.

Blood samples were centrifuged at 2000 rcf at room temperature for 10 mins, and serum was collected and stored at -80℃. Fixed hemispheres were preserved in 4% PFA (15ml 4% PFA in a 50ml Falcon tube) for 24 hours, continued with 30% sucrose for another 48 hours, then frozen in 2-methylbutane, and sagitally cut at 25 µm thickness with a freezing-sliding microtome (Leica). Cryoprotectant medium was used to store cut brain sections at -20°C.

2.4 Microglia isolation and fluorescence-activated cell sorting (FACS)

To isolate microglia, the olfactory bulb, cortex, striatum, and hippocampus of one brain hemisphere were dissected and finely minced in ice-cold Hank's buffered salt solution (HBSS) with 15 mM HEPES, 0.54 % D-glucose, and 0.1 mg/ml DNase (Sigma). After homogenisation of minced tissue in glass Dounce (7 ml and 5 ml) and Potter homogenisers, the final homogenates were filtered with a 200-um cell strainer and centrifugated at 300g without a break for 10 minutes at 4 °C. The pellet was resuspended in 70% isotonic Percoll solution and then covered with 37% and 30% isotonic Percoll layers. The pellet was then centrifuged without a break for 30 minutes at 800g and 4 °C. Cells were collected from the gradient interface at 70/37 % and washed in FACS buffer (PBS, 2% FCS, 10 mM EDTA). Then, cells were resuspended, and Fc receptors were blocked with Fc-block (1:400, BD Bioscience) for 10 min on ice, followed by 20 minutes at 4 °C with anti-rat CD11b/c Alexa Fluor 647 (1:100, BioLegend) and anti-rat CD45 Alexa Fluor 488 (1:100, BioLegend) antibodies. After washing and centrifugation, dead cells were stained with Zombie VioletTM Fixable Viability Kit (1:400, BioLegend) for 5 minutes before loading on the FACS machine. Finally, the cells were sorted using a Sony SH800 instrument.

2.5 Enzyme-linked immunosorbent assay (ELISA)

To quantify cytokine levels, brain homogenates were centrifuged at 25,000g for 30 minutes at 4°C. The V-PLEX Proinflammatory Panel 2 Rat Kit (Mesoscale Discovery) was used to analyse the supernatants of brain homogenates and blood serum, performed by the manufacturer's instructions. To assess cytokines in both the blood and the brain, serum samples were diluted at 1:4, and brain homogenates were used without dilution before measurements. The investigator was blinded to the treatment groups. Protein concentrations in brain homogenates were adjusted against total protein concentrations as determined by the BCA protein assay kit (Pierce).

2.5 RNA sequencing

2.5.1 RNA isolation

For RNA isolation, 15,000 microglia were instantly sorted into RNase-free PCR strips containing 30 µl of RNase-free water with 0.2% Triton X-100 and 0.8U/µl RNase inhibitor (Clontech), and samples were promptly frozen on dry ice. Extraction of RNA was performed according to the manufacturer's recommendations using a NucleoSpin RNA XS kit (Macherey-Nagel). Following RNA isolation, a 2ul aliquot of each sample was taken to determine the RNA quantity and quality utilising High Sensitivity RNA kits (Agilent) on an Agilent 4200 TapeStation System or a 2100 Bioanalyzer Instrument. Only RNA samples with an RNA integrity number (RIN) $\geqslant$ 7.0 were used for library preparation.

2.5.2 Library preparation and Sequencing

The NEBNext Single Cell/Low Input RNA Library Prep Kit for Illumina (NEB #E6421) was employed to generate high-quality sequencing data from ultra-low input RNA. Sequencing libraries were prepared by the NGS Facility of the University of Tübingen at a depth of 10–20 million reads using an Illumina HiSeq 2500 platform.

2.5.3 Data processing and analysis

The read quality of RNA-seq data in FASTQ files was analysed using *FastQC* (v0.11.9) (LaMar, 2015) to identify sequencing cycles with low average quality, adaptor contamination, or

repeated PCR amplification sequences. Reads were aligned using *rna-STAR*7.7a against a custom-built reference genome based on the *Rattus norvegicus* Ensembl v102 assembly (GRCm38.p6) and the human transgene locus (*HTT* or *SNCA*) with gapped alignments to account for splicing. The alignment quality in terms of read distribution in specific genomic features was assessed using RNA-SeQC (v2.4.2). The read counts for all genes were calculated using the software *Rsubread* (v6.4) and normalised using the package *DESeq2* (v1.32.0) (Love et al., 2014). Only rows with at least ten reads were retained after pre-filtering. A variance-stabilizing transformation (VST) was used to normalise the expression matrix, as recommended by the author of the WGCNA R package (Langfelder and Horvath, 2008). Detecting and estimating surrogate variables (SV) for hidden sources of variation using the sva package (3.4.2.) (Leek et al., 2019), such as batch and preparation date, and then removing all proposed surrogate variables using the limma package's function *removeBatchEffect* (Ritchie et al., 2015). After removing batch effects, 25% of genes with the lowest variance were filtered out (50% of genes were filtered out based on WGCNA's detection in the BAC HD 3-month cohort), as low-variable genes are frequently associated with noise.

Weighted gene correlation network analysis (WGCNA) was used to discover clusters (modules) of highly associated genes using filtered count matrixes from the four cohorts of animals (Langfelder and Horvath, 2008). The power parameter was determined using the 'pickSoftThreshold' function. A soft threshold was chosen based on automatic detection. Following that, modules and a network were formed using the network type "signed hybrid" and dynamic branch cutting with a merge threshold of 0.25. After network construction, the genes were ranked by the value of intramodular connectivity (kWithin) within each module using the function "softConnectivity". The genes with a higher value of kWithin are more critical and the potential hub genes within the modules.

Finally, a gene list of kWithin more than 10 will be input for functional analysis. The clusterProfiler package (4.2.2) (Wu et al., 2021; Yu et al., 2012) was used to perform the over-representation analysis (ORA) on Kyoto Encyclopedia of Genes and Genomes (KEGG) pathways and Gene Ontology (GO) terms for our list of significant genes in each module. To focus on the most important KEGG pathways and GO terms, only pathways with a p.adjust value (FDR) <0.1,

and GO terms p.adjust value (FDR) <0.05 were considered. I only focused on some top pathways and GO terms in my thesis.

2.6 Single-cell RNA sequencing

2.6.1 Sample & library preparation & sequencing

Microglia were isolated (as described above) from 8 rats (3 BAC HD, 3 BAC SNCA, and 2 wildtypes) for single-cell RNA-seq experiments. The viability of each sample was determined using CellDrop-Automated Cell Counters, with samples showing a viability > 70% processed for the construction of a 10x Genomics chromium single-cell 3' library. Between 5,612 and 15,312 cells were loaded onto the Chromium GEM Chip from 10x Genomics (Pleasanton, CA).

A Chromium Controller was then used for cell capture and library preparation. In brief, on a microfluidic chip, single cells, reverse transcription (RT) reagents, Gel Beads with barcoded oligonucleotides, and oil are mixed to generate reaction vesicles known as Gel Beads in Emulsion (GEMs). The GEMs are then incubated to generate barcoded, full-length cDNA from polyadenylated messenger RNA. The GEMs are broken, and the pooled portions are recovered following incubation. Following that, full-length, barcoded cDNA is amplified using PCR to provide enough material for library construction. Before library formation, enzymatic fragmentation and size selection is utilized to maximise the cDNA amplicon size. As a result, all cDNAs derived from a single cell will share the same barcode, allowing sequencing reads to be traced back to their single cell of origin. The constructed libraries were then sequenced in paired-end mode on an Illumina NovaSeq 6000.

2.6.2 Data processing and analysis

SeqPurge (Sturm et al., 2016) was used to trim the read adapter of FASTQs as part of the in-house NGS-bits pipeline (v2020 12). CellRanger (v6.0.1) software aligned reads to the Rat genome Ensembl v104 plus transgene (10x Genomics) (Zheng et al., 2017). The normalisation of count matrices, scaling, dimensionality reduction, and selection of variable features are all based on Seurat (v4.0.1) (Hao et al., 2021). Cells with more than 1000 but fewer than 4800 genes and with

more than 6% mitochondrial genes were filtered out. Finally, 34,914 cells were used for further analysis; and a standard pipeline was executed on the integrated dataset in Seurat.

10 principal components were used to construct a shared nearest neighbour's graph with k=20 using Seurat's FindNeighbors function. The modularity function was set to a resolution of 0.5, and clusters were detected using Seurat's FindClusters function. The dimension of the clusters was reduced using the RunUMAP function. Cell types were identified manually for clusters using some well-known gene markers (Bakken et al., 2018; Chen and Colonna, 2021; Hodge et al., 2019; Mathys et al., 2019). The sub-clusters' differential gene expression analysis was performed on the Seurat object's RNA assay using Seurat's FindAllMarkers function and the MAST algorithm. Differentially expressed genes (DEGs) were defined as those with a fold change of more than 0.5 and a corrected p-value of 0.05. The functional analysis was performed using ClusterProfiler (Wu et al., 2021; Yu et al., 2012).

2.7 Statistics

The statistical studies were conducted using the R package rstatix (0.7.0), which provides a simple and straightforward framework for performing basic statistical tests. The Shapiro–Wilk test was used to determine the normal distribution of the data. If the normality requirement was satisfied, data were analysed using a one-way ANOVA (for multiple groups), followed by pairwise comparisons with post-hoc Tukey correction (if p-value<0.05). If the normality criteria were not met, the Kruskal–Wallis test was used, followed by pairwise comparisons with the Wilcoxon test and Holm-Bonferroni correction (if p-value<0.05) (e.g., cytokine data of 3-month cohort). For the pairwise comparison with selected groups (e.g., the boxplot for gene expression), the t-test was used, followed by Holm-Bonferroni correction.

2.8 R packages for bioinformatics and data visualization

R version 4.1.2 (2021-11-01) (Team, 2013);
Platform: x86_64-apple-darwin17.0 (64-bit);
Running under: macOS Big Sur 11.3.1.

R packages for bulk RNA-seq

enrichplot_1.14.2 (Yu et al., 2015)

DOSE_3.20.1 (Yu et al., 2015)

DESeq2_1.34.0 (Love et al., 2014)

WGCNA_1.70-3 (Langfelder and Horvath, 2008)

SummarizedExperiment_1.24.0 (Morgan et al., 2017)

GenomicRanges_1.46.1 (Lawrence et al., 2013)

matrixStats_0.61.0

org.Rn.eg.db_3.14.0 (Carlson et al., 2019)

S4Vectors_0.32.3

Biobase_2.54.0

stringr_1.4.0

RColorBrewer_1.1-2

writexl_1.4.0

readxl_1.3.1

forcats_0.5.1

cluster_2.1.2

fastcluster_1.2.3

dynamicTreeCut_1.63-1

GenomeInfoDb_1.30.1

MatrixGenerics_1.6.0

AnnotationDbi_1.56.2

IRanges_2.28.0

BiocGenerics_0.40.0

clusterProfiler_4.2.2 (Wu et al., 2021; Yu et al., 2012)

pheatmap_1.0.12

ggplot2_3.3.5 (Wickham, 2016)

tidyr_1.2.0

R packages for single-cell RNA-seq

BiocManager_1.30.16

pheatmap_1.0.12

SingleR_1.8.1 (Aran et al., 2019)

SummarizedExperiment_1.24.0

GenomeInfoDb_1.30.1

IRanges_2.28.0

MatrixGenerics_1.6.0

matrixStats_0.61.0

dplyr_1.0.7

purrr_0.3.4

tibble_3.1.6

Seurat_4.1.0

EnhancedVolcano_1.12.0

Biobase_2.54.0

S4Vectors_0.32.3

forcats_0.5.1

readr_2.1.2

tidyverse_1.3.1

ggplot2_3.3.5

usethis_2.1.5

ggrepel_0.9.1

GenomicRanges_1.46.1

BiocGenerics_0.40.0

stringr_1.4.0

tidyr_1.2.0

SeuratObject_4.0.4 (Hao et al., 2021)

R packages Functional analysis

enrichplot_1.14.2

AnnotationDbi_1.56.2

BiocGenerics_0.40.0

readxl_1.3.1

forcats_0.5.1

S4Vectors_0.32.3

ggplot2_3.3.5

DOSE_3.20.1

IRanges_2.28.0

clusterProfiler_4.2.2

tidyr_1.2.0

org.Rn.eg.db_3.14.0

Biobase_2.54.0

writexl_1.4.0

3. Results

3.1 Experimental design

To investigate whether immune memory can affect PD and HD pathology, different peripheral immune stimuli (1 x LPS, 2 x LPS, 4 x LPS) and a high-caloric diet were applied in PD and HD rat models. To induce immune memory, LPS was injected intraperitoneally (i.p.) into 3-month-old rats with a daily dose of 500 g per kg bodyweight. In the short-term cohort (3-month cohort), rats were injected either with a single LPS dose (1 x LPS), two doses on consecutive days (2 x LPS), or on four consecutive days (4 x LPS). In the long-term cohort (9-month cohort), the rats received either four LPS injections on four consecutive days (4 x LPS), or a single LPS injection followed by three vehicle injections on the following three days (1 x LPS), or four vehicle injections on four consecutive days (PBS). The rats in the high-fat diet (HFD) group got a one-month feeding of high-fat diet chow when they were two months old (**Figure 2. A, B**).

Next, to investigate whether immune memory triggered by peripheral stimuli and a high-caloric diet alter immune responses in PD and HD rat models, we performed ELISA measurements of 9 cytokines in the brain and serum and bulk RNA-sequencing of microglia in 3- as well as 9-month-old groups. For RNA-seq, microglia were sorted based on $CD11b^{high}$ and $CD45^{low}$ from the forebrain, where pathology develops with age in both rat models (**Figure 2. C, D**).

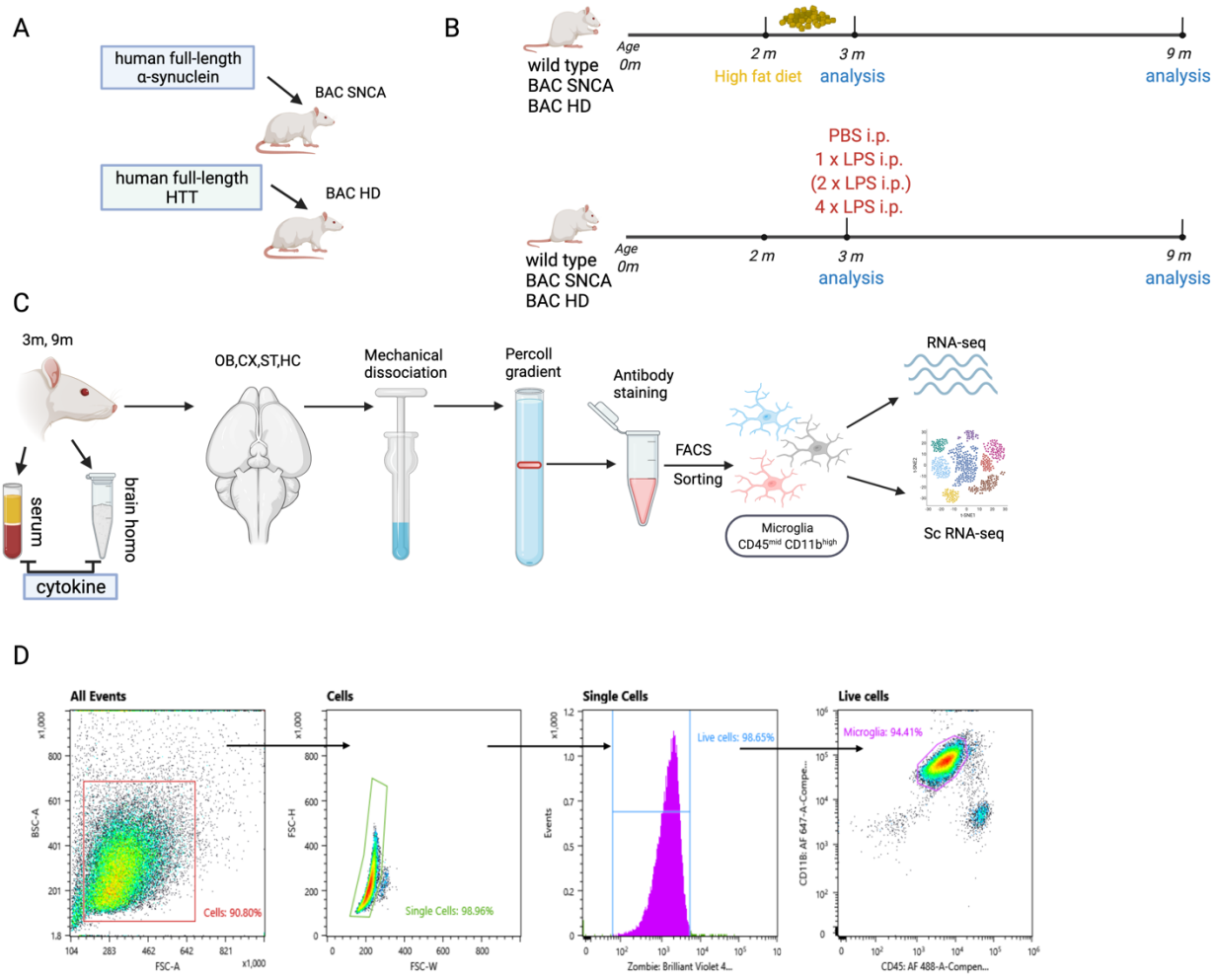

Figure 2. Experimental design & workflow. A. Rat models: BAC SNCA rats and BAC HD rats carry the complete gene for human SNCA or mutant human HTT, respectively, resulting in overexpression and progressive aggregation of α-synuclein or huntingtin. **B.** Experimental design: rats received a one-month high-fat diet or injections of lipopolysaccharide (LPS) at different times to induce innate immune memory. **C.** Microglia isolation workflow in this study. OB, olfactory bulb; CX, cortex; ST, striatum; HC, hippocampus. **D.** The sorting strategy of microglia in this study. Panel **A**, **B** and **C** of this figure are created with BioRender.com.

3.2 Acute and long-term cytokine profiles in PD and HD models

In the 3-month cohort (acute immune response), compared to the PBS group, three hours after the first LPS injection (1 x LPS), there was a significant increase in blood and brain pro-inflammatory cytokine levels (IL-1β, IFN-γ, KC/GRO and TNF-α) in both PD and HD models, confirming an acute immune response in the periphery and brain. After consecutive LPS injections (2 x LPS, 4 x LPS), the blood and brain levels of the pro-inflammatory cytokines (IL-1β, IFN-γ, KC/GRO and

TNF-α) were decreased compared to their levels after 1 x LPS in the PD model (**Figure 3. A**; **Figure 4. A**), showing the effect of immune tolerance in the periphery and brain. However, in the HD model, as compared to the 1 x LPS group, the 2 x LPS group showed a moderate increase in blood and brain levels of KC/GRO, while the 4 x LPS group showed a significant decrease in blood and brain levels of most pro-inflammatory cytokines (**Figure 3. C**; **Figure 4. C**).

In the 3-month cohort that received a high-fat diet, the blood level of IFN-γ decreased in comparison to animals on a standard diet (**Figure 3. A**), but no significant changes were detected for brain cytokines.

In the 9-month cohort (long-term effect), the impact of innate immune memory (induced by immune stimuli at 3 months of age) was still apparent both in the serum and brain in wild-type rats for some cytokines (IFN-γ, **Figure 3. B**; IL-1β, **Figure 4. B**), indicating that innate immune memory induced by peripheral stimuli may persist for a long term. In the BAC HD rats, the brain level of IFN-γ was decreased in the 1 x LPS group and HFD group compared to the PBS group (**Figure 4. D**), indicating a possible interaction of the peripheral immune stimulation and pathology-associated inflammatory responses. Moreover, the brain levels of IL-13 and TNF-α showed a significant difference between 1 x LPS group and 4 x LPS group in both wild-type rats and BAC HD rats (IL-13, TNF-α, **Figure 4. D**), indicating long-lasting alterations of the brain's immune response following peripheral immune stimulation.

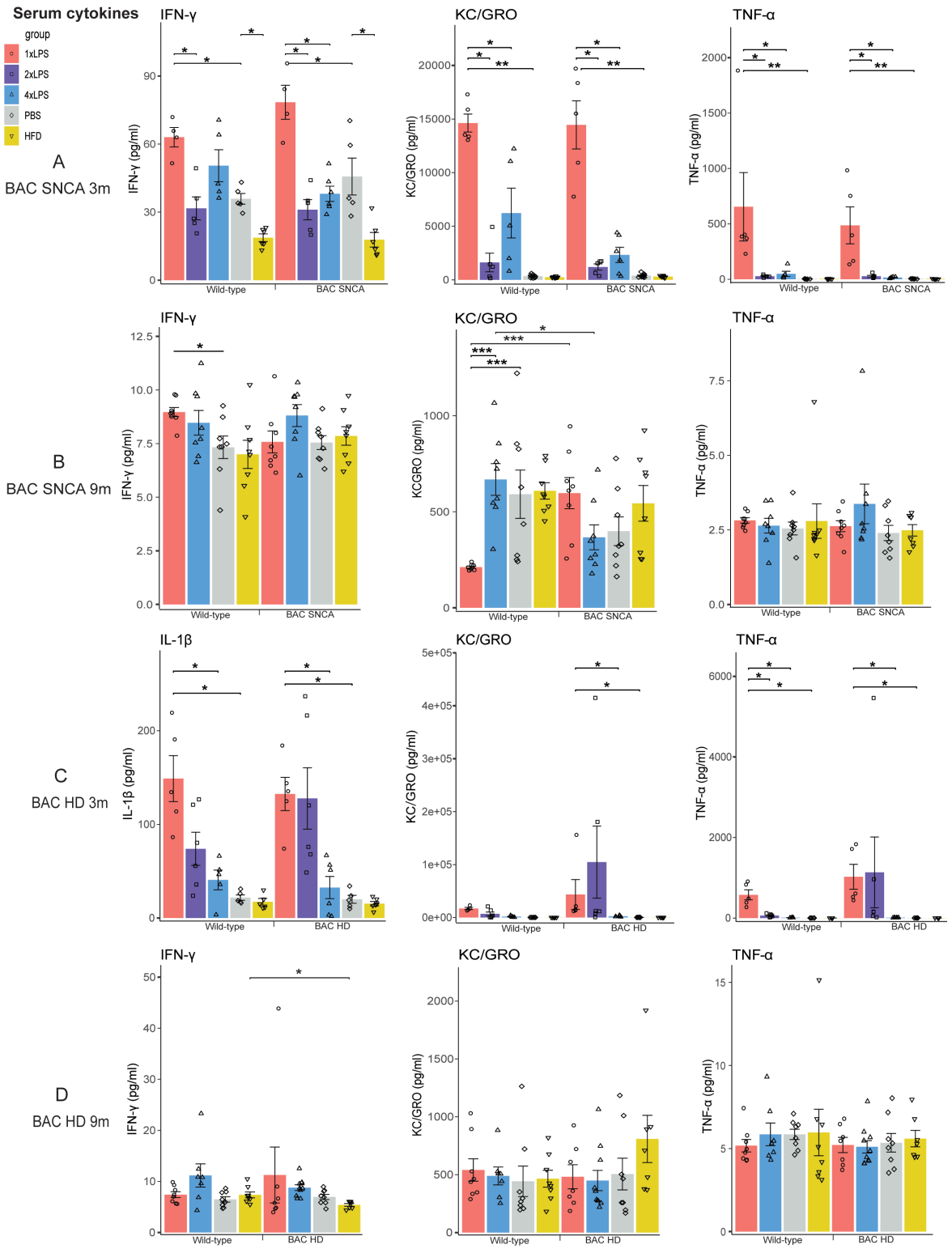

Figure 3. Serum cytokine levels after LPS injections or HFD feeding in the 3 or 9-month-old rat models. Cytokines were measured in the serum of animals 3h after each injection in 3-month-old animals or at 9 months of age. Error bars are SEM (standard error of the mean). *P < 0.05, **P < 0.051, ***P < 0.001 for Wilcox-test with Holm–Bonferroni correction. In A, number of rats, n = 4, 5, 5, 9(5), 9(5), 4, 5, 6, 9, 9 from left to right. 9(5) means 9 rats were measured, but IFN- γ was not detectable for four animals. In B and D, 8 rats for each condition. In C, n = 5, 6, 5, 5, 5, 5, 6, 6, 5, 5 from left to right.

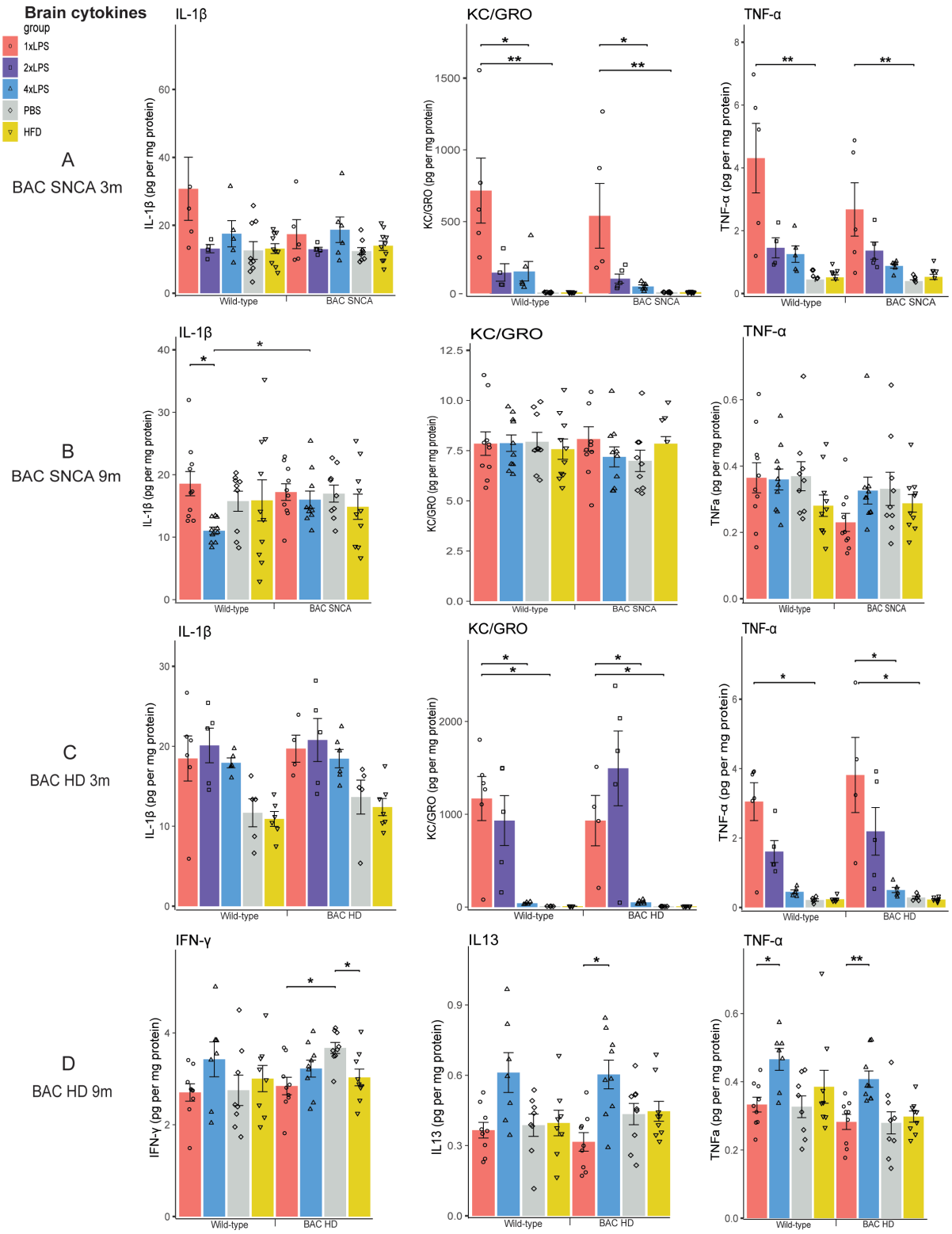

Figure 4. Brain cytokine levels after acute LPS injections or HFD feeding in the 3 or 9-month-old rat models. Cytokines were measured in the brain homogenate of animals 3h after each injection in 3-month-old animals or at 9 months of age. Error bars are SEM (standard error of the mean). *P < 0.05, **P < 0.01 for Wilcox-test with Holm–Bonferroni correction. In A, n = 4, 5, 5, 9, 9, 4, 5, 6, 9, 9 rats from left to right. In B, n = 10, 10, 9, 10, 10, 10, 9, 10 rats from left to right. In C, n = 6, 5, 5, 5, 6, 4, 5, 6, 5, 7 rats from left to right. In D, 9, 7, 8, 8, 9, 9, 9, 9 rats from left to right.

3.3 Microglial gene expression across different conditions

Next, I investigated whether immune memory triggered by peripheral stimuli and a high-caloric diet would shape the microglial transcriptomic profiles in PD and HD rat models. Bulk RNA-seq was performed on sorted microglia (based on CD11b^{high} and CD45^{low}) from the forebrain (olfactory bulb, cortex, striatum, and hippocampus), where pathology develops with age in both rat models (**Figure 2. C, D**).

To compare the gene expression level across the various conditions (wildtype vs transgenic, different immune stimuli), weighted correlation network analysis (WGCNA) was applied to discover clusters (modules) of highly associated genes using filtered count matrixes and associate each module with different treatments groups (1 x LPS, 2 x LPS, 4 x LPS, PBS or HFD) in both genotypes (wild type or BAC SNCA) by calculating the module–trait correlation for each condition. For functional analysis, genes with a high value of intramodular connectivity within each module were used. Finally, potential hub genes were identified for enriched KEGG pathways or GO terms in each module.

3.3.1 Microglial gene expression and function after acute immune stimulation in the PD model

First, principal component analysis (PCA) was performed to assess the data quality based on sample clustering. After pre-filtering, normalisation and removal of batch effects from the raw count matrix, the PCA plot displayed all 49 samples in different treatments (1 x LPS, 2 x LPS, 4 x LPS, PBS and HFD) in both genotypes (WT: wild type; TG: BAC SNCA) along PC1 (25% variance) and PC2 (8% variance) (**Figure 5. A**). Notably, PCA clearly separated LPS groups (1 x LPS, 2 x LPS, 4 x LPS) from PBS groups. 11,214 genes across all conditions were then used as the input for WGCNA analysis to identify gene clusters associated with wild-type or BAC SNCA rats following various treatments at 3 months of age. WGCNA unbiasedly clusters genes with similar expression patterns into one module; Using stepwise network construction and a minimum module size of 100 genes, this dissected the organised count matrix into 10 gene modules.

Then, the interaction relationships of the 10 modules were examined, and the network heatmap was generated (**Figure 5. B**). The hierarchical clustering and heatmap revealed that each module

was independent. Some modules are highly correlated with the same condition (e.g., both green and blue modules correlate negatively with gene expression in the 2 x LPS group, while the turquoise module correlates positively with gene expression in the 2 x LPS group). WGCNA was then used to associate each module with the five different treatments (1 x LPS, 2 x LPS, 4 x LPS, PBS or HFD) in both genotypes (wild type or BAC SNCA) by calculating the module–trait correlation for each condition. Following a search for significant correlations between all modules and traits, I discovered that the genes in the yellow and brown modules had a stronger correlation with 1 x LPS for microglia from both genotypes than other modules; genes in the blue, green, and turquoise modules showed a stronger correlation with 2 x LPS group for microglia from both genotypes (**Figure 5. C**). The heatmap and boxplot of gene expression within modules (**Figure 5. D. E**) made it clear that the 2 x LPS had a greater level of gene expression for both genotypes in the turquoise module; 1 x LPS had a higher gene expression for both genotypes in the brown module; 1 x LPS and 2 x LPS had a lower gene expression for both genotypes in the green module; 4 x LPS had a relatively higher level of gene expression for both genotype in the green and pink module. Overall, this analysis revealed no apparent difference in acute microglial immune responses between the BAC SNCA and wild-type animals, indicating that at this pre-pathological stage, microglial responses are comparable between genotypes.

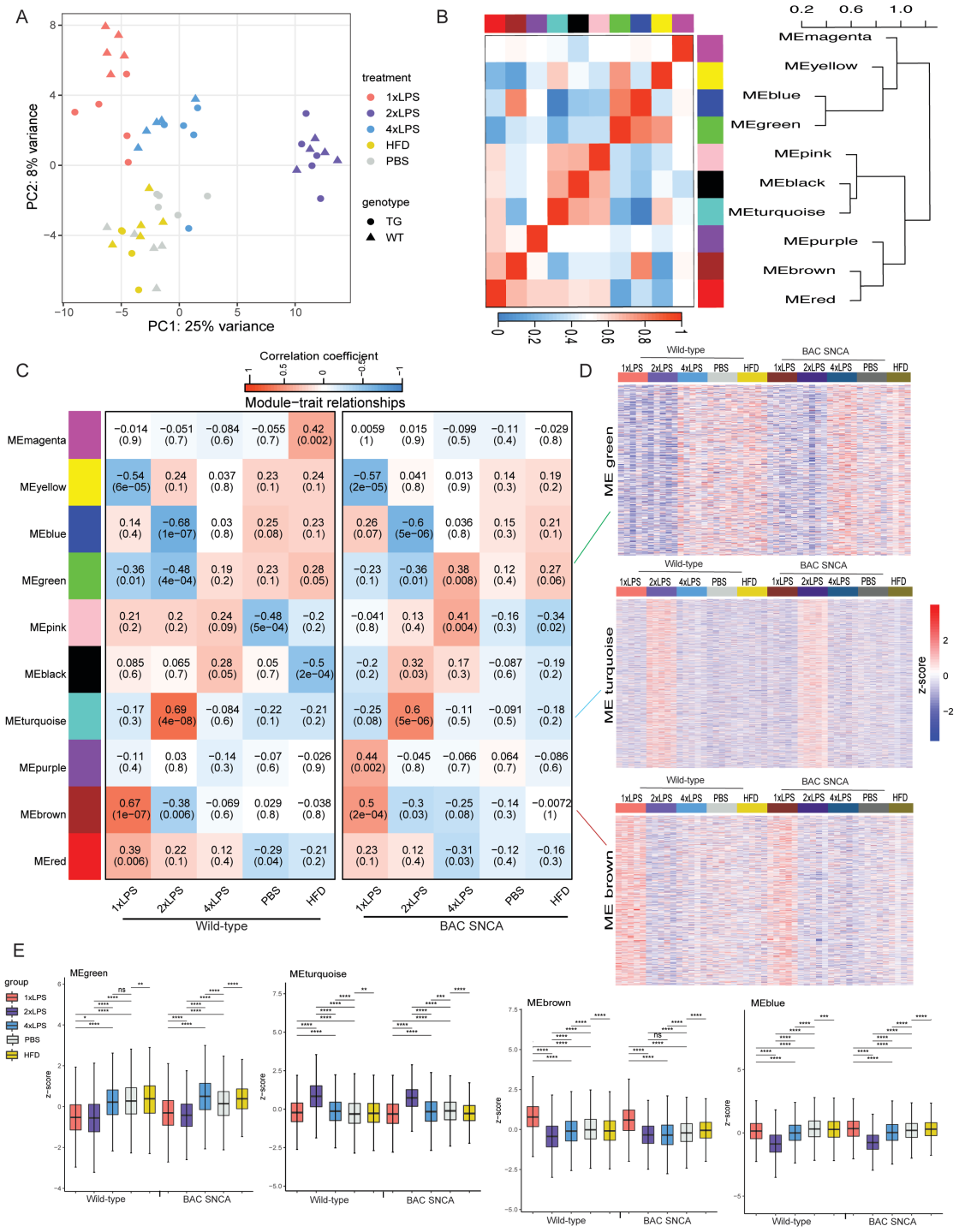

Figure 5. Gene expression analysis (WGCNA) in microglia from the BAC SNCA 3-month cohort.

A. Principal component analysis (PCA) clearly separates treatment groups. **B**. Hierarchical clustering and heatmap to highlight relationships between modules. **C**. Heatmap of the correlation between module eigengenes and treatment groups (in each colour module, the top value is the correlation coefficient, and the bottom is the P-value, n = 5, 5, 5, 5, 5, 5, 5, 5, 5, 4 rats from left to right). **D**. Heatmap of normalised gene expression within selected modules. The colours indicate z - scores, with a score of 0 being the average gene expression across samples. A positive z-score indicates the gene's expression is above the mean, whereas a negative value indicates the gene's expression is below the mean **E.** Boxplot of normalised gene expression for all genes within selected modules (n = 678, 3936, 940 and 3210 genes in green, turquoise, brown and blue module, respectively). *P < 0.05, **P < 0.01, ***P < 0.001, ****P < 0.0001 for one-way ANOVA with Holm–Bonferroni correction.

For functional analysis (KEGG pathway and GO term enrichment analysis), 6692 genes were selected based on the highest values of intramodular connectivity (kWithin > 10) within each module. The input gene list was ranked by weightFactor (kWithin / 100), where a higher value of weightFactor indicated that the gene has more connections to other genes and therefore plays a more important role in the enrichment analysis. The top terms for KEGG and GO enrichment analysis are presented in **Figure 6** and **Figure 8**, respectively. To consider the potentially biological complexities that may exist when a gene is annotated in several categories and the connectivity of genes in the modules, a cnetplot was used (**Figure 7**) to visualise the relationships between the ranked gene list by connectivity (weightFactor) and KEGG pathways as a network. With this method, we may identify some potential hub genes under each enriched pathway. Briefly, the genes in the blue module, which correlate with the 1 x LPS treatment, were significantly enriched in pathways associated with antigen processing and presentation (potential key genes: *Cd74*, *Cd4*, *Ctss*), phagosome (potential key genes: *Tlr2, C3, Itga5*), lysosome (potential key genes: *Tpp1, Ppt1, Ctsa*, *Acp2, Ctsd*), endocytosis and phagocytosis (potential key genes: *Lyn, Ptprc*). The genes in the brown module which correlate with the 2 x LPS treatment were significantly enriched in pathways associated with phagosome, TNF signalling pathway (potential key genes: *Irf1, Ifi47*), Toll-like receptor signalling pathway (potential key genes: *Il1b, Rela*), and NOD-like receptor signalling pathway (potential key genes: *Il1b, Rela, Irf7*), NF-kappa B signalling pathway (potential key genes: *Ccl4, Cd40*), which are related to innate immune responses and induction of inflammation (Wajant, H., Pfizenmaier, K. and Scheurich, P., 2003; Kawasaki, T. and Kawai, T., 2014; Saxena, M. and Yeretssian, G., 2014; Liu, T., Zhang, L., Joo, D. and Sun, S.C., 2017;). Furthermore, to characterise the cellular or physiological functions associated with the genes within the modules, GO enrichment analysis was performed on the same gene set, which revealed that genes in the blue module (which correlate with 2 x LPS) and brown module (which correlate with 1 x LPS) were significantly associated with immune response terms. The results from these enrichment analyses indicate that different acute immune stimuli may induce distinct immune responses (at the transcriptome level) in microglia. Of these, 1 x LPS and 2 x LPS caused the most pronounced alterations in the microglial transcriptome (**Figure 8**).

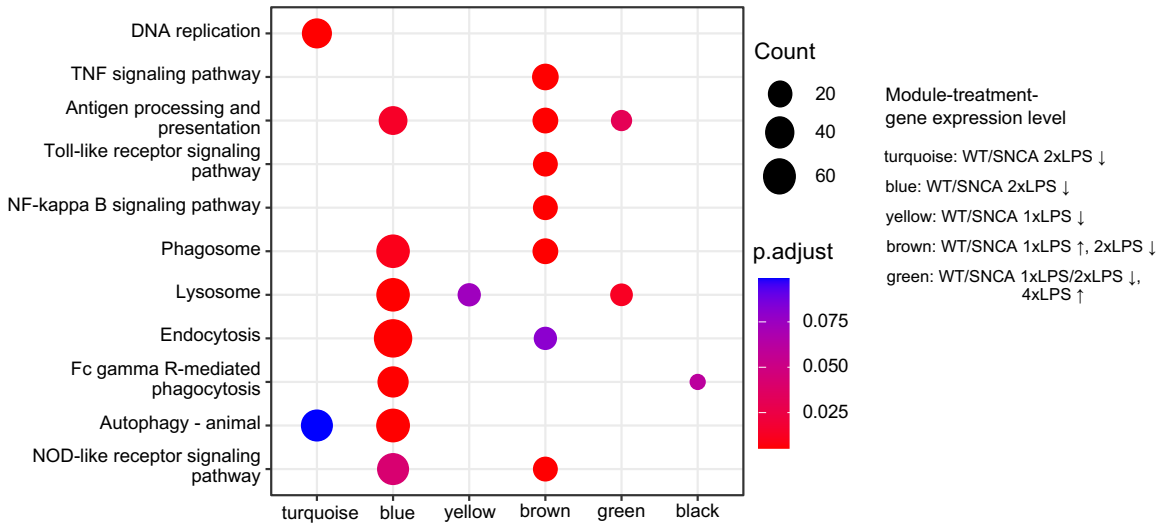

Figure 6. **Dot plot of selected KEGG pathways enriched in modules in microglia from the BAC SNCA 3-month cohort**. **Count:** the gene number enriched in the pathway. **p.adjust:** adjusted P-values for multiple comparisons. (Please note that only modules are shown where significant pathway enrichment was found). ↑ Increased average gene expression level; ↓ decreased average gene expression level.

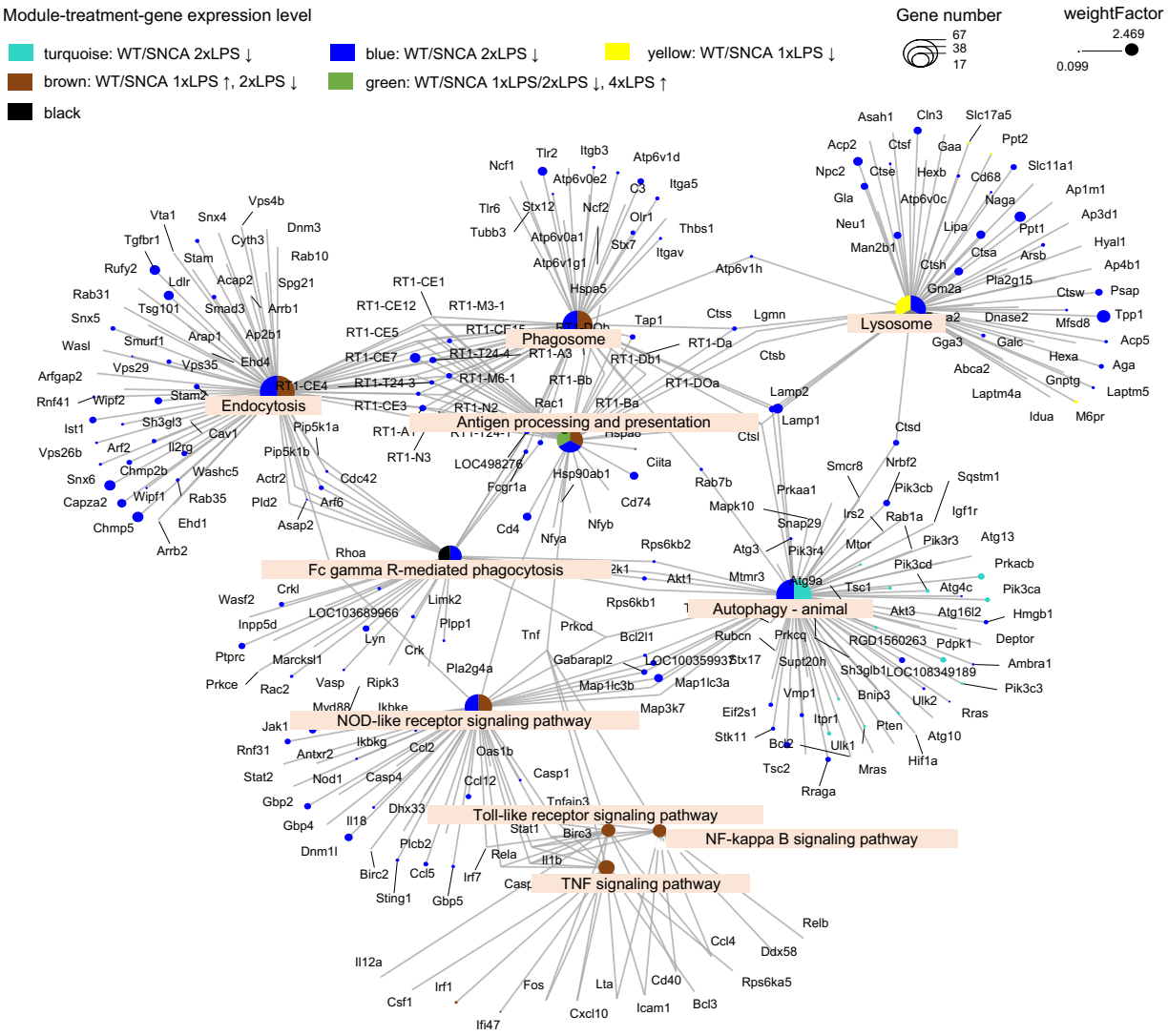

Figure 7. Network plot of selected KEGG pathways enriched in modules in microglia from the BAC SNCA 3-month cohort. The pie size for each category reflects the number of genes enriched in the respective pathway. Coloured dots label the genes within the respective module and pathway. The dot size (weightFactor, see Methods) represents the connectivity of genes in each module (where a higher value means the gene has more connections to other genes). ↑ Increased average gene expression level; ↓ decreased average gene expression level.

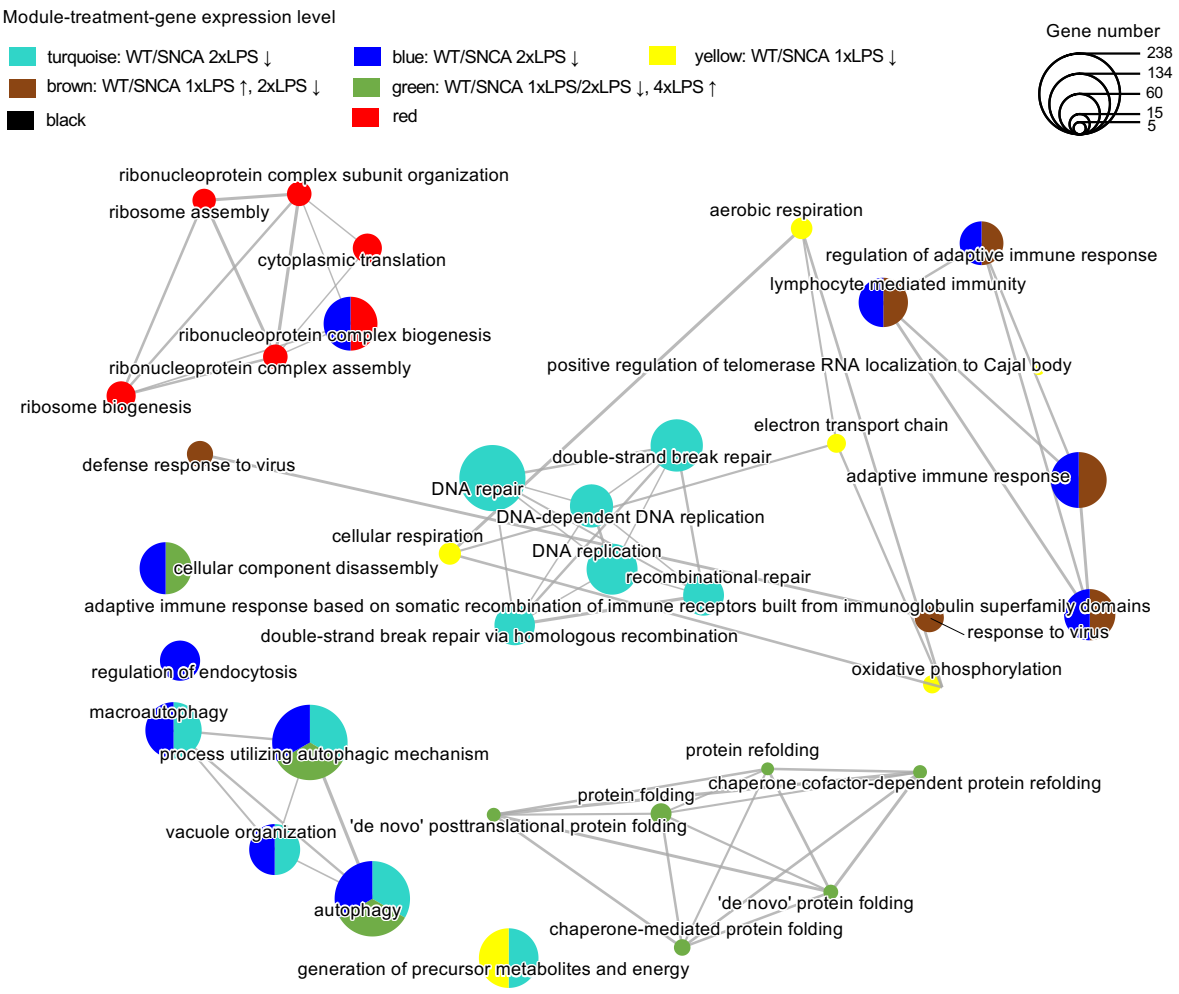

Figure 8. Network plot of the top 6 GO terms enriched in modules in microglia from the BAC SNCA 3-month cohort. The pie size for each category indicates the gene numbers enriched in the respective GO term. ↑ Increased average gene expression level; ↓ decreased average gene expression level.

3.3.2 Microglial gene expression and function 6 months after immune stimulation in the PD model

Analogous to the analysis of the acute immune response at 3 months of age, the long-term changes in gene expression were also analysed in microglia isolated from 9-month-old wild-type (WT) and BAC SNCA animals to assess a) if pathology would result in alterations of the microglial phenotype and b) if such pathology-associated responses would be differentially altered by the peripheral immune stimuli applied 6 months earlier.

First, principal component analysis (PCA) was performed to assess sample clustering. The PCA plot displays all 44 samples along PC1 (10% variance) and PC2 (10% variance) (**Figure 9. A**) for the different treatments (1 x LPS, 4 x LPS, PBS or HFD) applied in 3-month-old rats of both genotypes. As expected, the variance amongst samples of the same and of different groups was considerably higher compared to the acute immune stimulation. Nevertheless, microglia from the 1 x LPS group in WT animals were separated from the 1 x LPS group in BAC SNCA rats, indicating that 1 x LPS-induced innate immune memory in microglia altered their response to a-synuclein pathology.

10,569 genes were used as input for WGCNA analysis to identify gene clusters associated with wild-type or BAC SNCA rats in the various treatment groups. Using stepwise network construction and a minimum module size of 100 genes, this dissected the organised count matrix into 13 gene modules. Next, the interaction relationships of the 13 modules were examined, and the network heatmap and hierarchical clustering were created (**Figure 9. B**). WGCNA was then used to associate each module with the four different treatments (1 × LPS, 2 × LPS, 4 × LPS, PBS or HFD) in both genotypes (wild-type or BAC SNCA). Examining significant correlations between all modules and traits, I discovered that the genes in the green and red modules showed significant correlations with microglia from the BAC SNCA control group (PBS), indicating that they may reflect microglial responses to α-synuclein pathology (in the absence of a peripheral immune stimulus; **Figure 9. C**). Notably, WGCNA also highlighted immune memory effects, as genes in the magenta and purple modules showed an opposite correlation between 1 x LPS group and 4 x LPS group in BAC SNCA rats, while genes in the turquoise module had a significant correlation with the 4 x LPS group both in wild-type and BAC SNCA rats. Heatmaps and boxplots of normalised gene expression within modules (**Figures 9. D, E**) made it clear that microglia from the 4 x LPS group had higher levels of gene expression in the turquoise module in BAC SNCA rats; 1 x LPS had higher gene expression levels for both genotypes in the brown module, and 1 x LPS and 2 x LPS had lower gene expression levels for both genotypes in the green module.

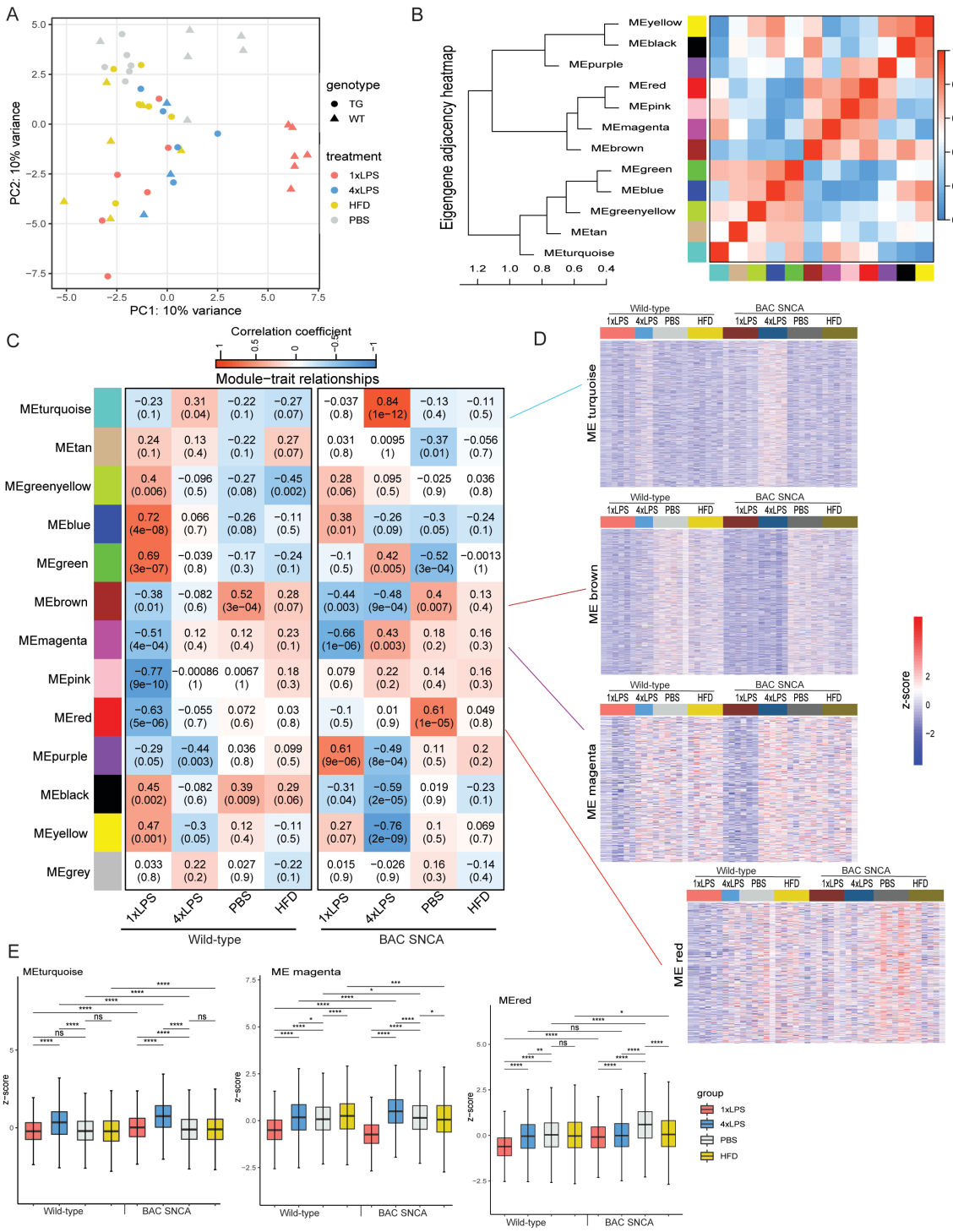

Figure 9. Gene expression analysis (WGCNA) in microglia from the BAC SNCA 9-month cohort. A. Principal component analysis (PCA) of the microglial transcriptomes across different conditions. **B.** Hierarchical clustering and heatmap to highlight relationships between modules. **C.** Heatmap of the correlation between module eigengenes and treatment groups (in each colour module, the top value is the correlation coefficient, and the bottom is the P-value, n = 6, 3, 6, 6, 6, 5, 6, 6 rats from left to right). **D.** Heatmap of normalised gene expression within selected modules. The colours indicate z - scores, with a score of 0 being the average gene expression across samples. A positive z-score indicates the gene's expression is above the mean, whereas a negative value indicates the gene's expression is below the mean. **E.** Boxplot of normalised gene expression for all genes within selected modules (n = 2094, 489 and 616 genes in turquoise, magenta and red modules, respectively). *P < 0.05, **P < 0.01, ***P < 0.001, ****P < 0.0001 for one-way ANOVA with Holm–Bonferroni correction.

For functional enrichment analysis (KEGG pathway and GO enrichment), 2,669 genes with the highest value of connectivity within modules were used. The input gene list was then ranked by the weightFactor, representing the number of connections with other genes and therefore their importance for the enrichment analysis. The top terms from each enrichment analysis are presented in **Figure 10. A** and **Figure 11** for KEGG and GO terms, respectively. Moreover, a cnetplot to illustrate individual genes within pathways is shown in **Figure 10. B, C**, which visualized the relationships between the ranked gene list by connectivity and KEGG pathways as a network. These analyses highlighted some very interesting pathways directly related to Parkinson's disease, protein aggregation and microglial activation states. Briefly, the genes in the red module, which reflect a microglial response to the development of α-synuclein pathology, were primarily enriched in pathways of protein processing in the endoplasmic reticulum and an unfolded protein response, as well as antigen processing and presentation and Il-17 signalling pathways (Hspa8, Hspa5, Hsp90aa1, Hsp90ab1); the genes in the turquoise module which are increased in microglia from 4 x LPS-treated BAC SNCA rats were significantly enriched in pathways of Parkinson's disease and Oxidative phosphorylation (potential key genes: *ATP6, ATP8, CYTB, Cox2*); the genes in the brown module which are downregulated in microglia from BAC SNCA rats that received either 1 x LPS or 4 x LPS were significantly enriched in pathways of NOD-like receptor signalling pathway (potential key genes: *Il6, Nlrp3, P2rx7, Xiap*), HIF-1 signalling pathway (potential key genes: *Akt2, Rps6kb1*) and P13K-Akt signalling pathway (potential key genes: *Syk, Nras*). Furthermore, GO enrichment analysis revealed that the genes in the red and turquoise modules enriched in pathways relating to protein folding, while the purple and magenta module genes, which showed opposite regulation by 1 x LPS and 4 x LPS in microglia from BAC SNCA rats, were significantly associated with metabolic processes and transmembrane transport terms (**Figure 11**).

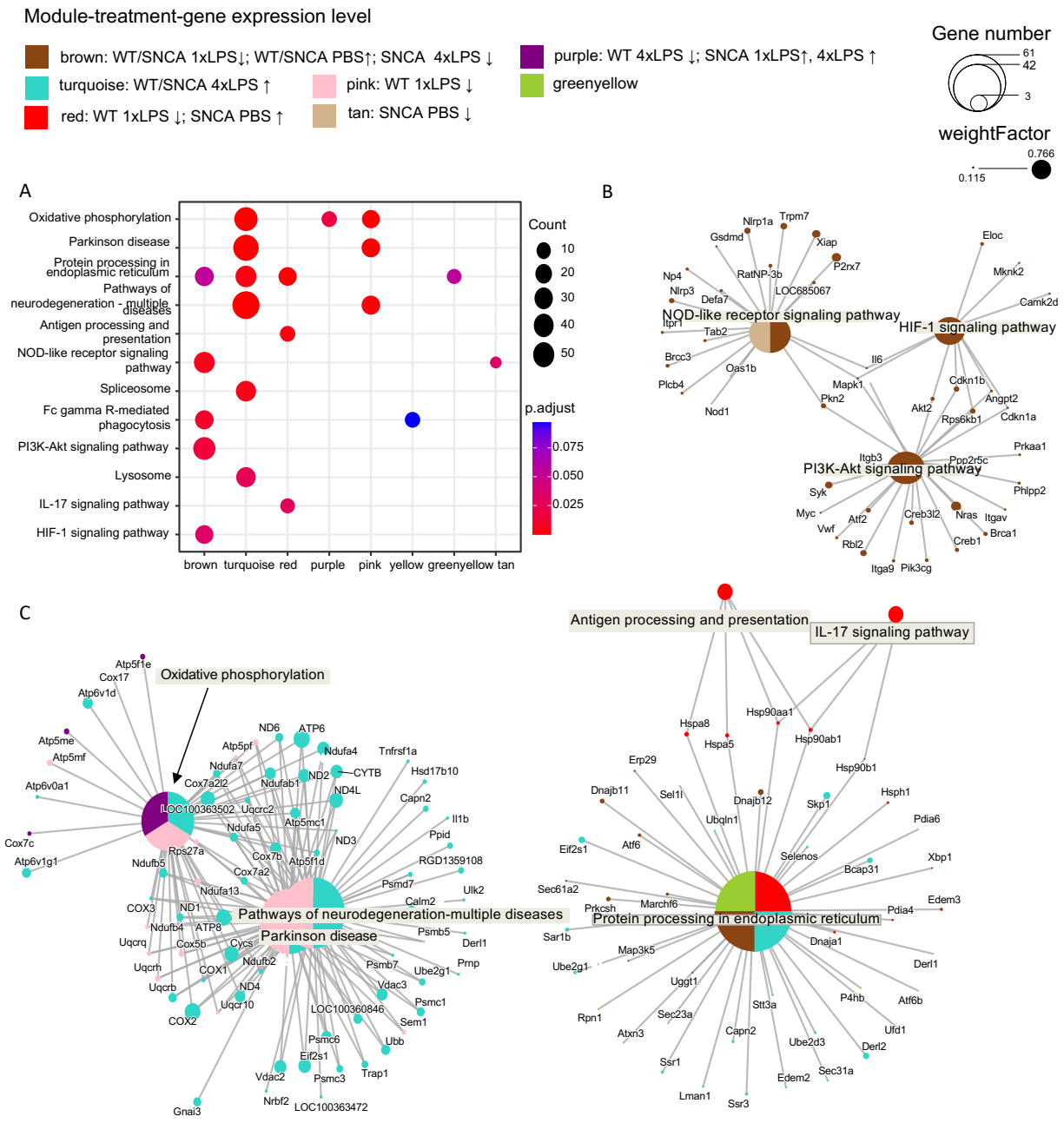

Figure 10. KEGG enrichment analysis in modules in microglia from the BAC SNCA 9-month cohort. A. Dot plot of selected KEGG pathways enriched in modules. **B, C.** Network plot of selected KEGG pathways enriched in modules. The pie size for each category reflects the number of genes enriched in the respective pathway. Coloured dots label the genes within the respective pathway and module. The dot size (weightFactor, see Methods) represents the connectivity of genes in each module (where a higher value means the gene has more connections to other genes). ↑ Increased average gene expression level; ↓ decreased average gene expression level.

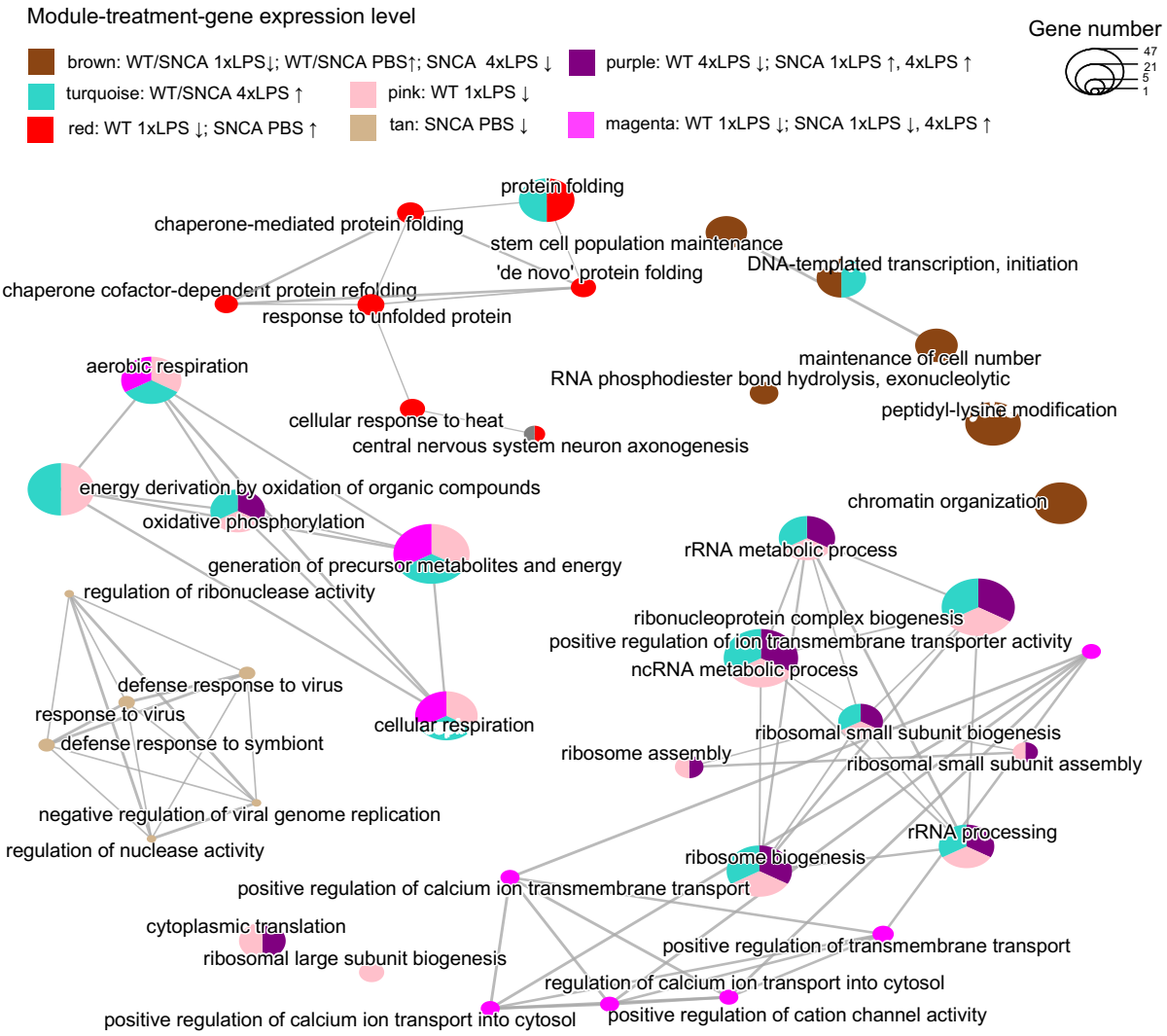

Figure 11. Network plot of top 6 GO terms enriched in modules in microglia from the BAC SNCA 9-month cohort. The pie size for each category reflects the gene numbers enriched in the respective GO term. ↑ Increased average gene expression level; ↓ decreased average gene expression level.

3.3.3 Microglial gene expression and function after acute immune stimulation in the HD model

The same analyses as described above for the BAC SNCA animals (and their WT controls) were performed for the BAC HD cohorts. In the 3-month cohort, the PCA plot displayed all 50 samples in different treatments (1 x LPS, 2 x LPS, 4 x LPS, PBS or HFD) in both genotypes (WT: wild-type; TG: BAC HD) along PC1 (38% variance) and PC2 (24% variance) (**Figure 12. A**). Very similar to the BAC SNCA cohort, 2 x LPS and 4 x LPS treatment groups were clearly separated from PBS and 1 x LPS groups in the PCA plot.

After filtering low variance genes, 7,179 genes were used as input for WGCNA analysis to identify gene clusters associated with wild-type or BAC HD rats following with different treatments at 3 months. Using stepwise network construction and a minimum module size of 100 genes, this dissected the organised count matrix into 8 gene modules. Next, I examined the interaction relationships of the 8 modules, and then created the hierarchical clustering and network heatmap (**Figure 12. B**). WGCNA was then used to associate each module with the five different treatments (1 x LPS, 2 x LPS, 4 x LPS, PBS or HFD) in both genotypes (wild-type or BAC HD). Examining modules with significant correlations, microglial genes in the yellow and black modules were found to correlate with 1 x LPS and 4 x LPS in both genotypes; genes in the turquoise, blue and brown modules showed a correlation with the 2 x LPS treatment for microglia from both genotypes (**Figure 12. C**). The heatmap and boxplot of gene expression within modules (**Figure 12. D, E**) made it clear that microglia from animals receiving 2 x LPS had a greater level of gene expression for both genotypes in the turquoise module and a lower level of gene expression in the blue module; 1 x LPS had a higher gene expression for both genotypes in the black module, and a lower level of gene expression in the yellow module. Interestingly, microglia from 4 x LPS-treated animals showed an opposite correlation with gene expression compared to the 1 x LPS group in the yellow and black modules. Very similar to the analysis in the BAC SNCA cohort, this analysis revealed no apparent difference in acute microglial immune responses between the BAC HD and wild-type animals, confirming that at this pre-pathological stage, microglial responses are comparable between genotypes.

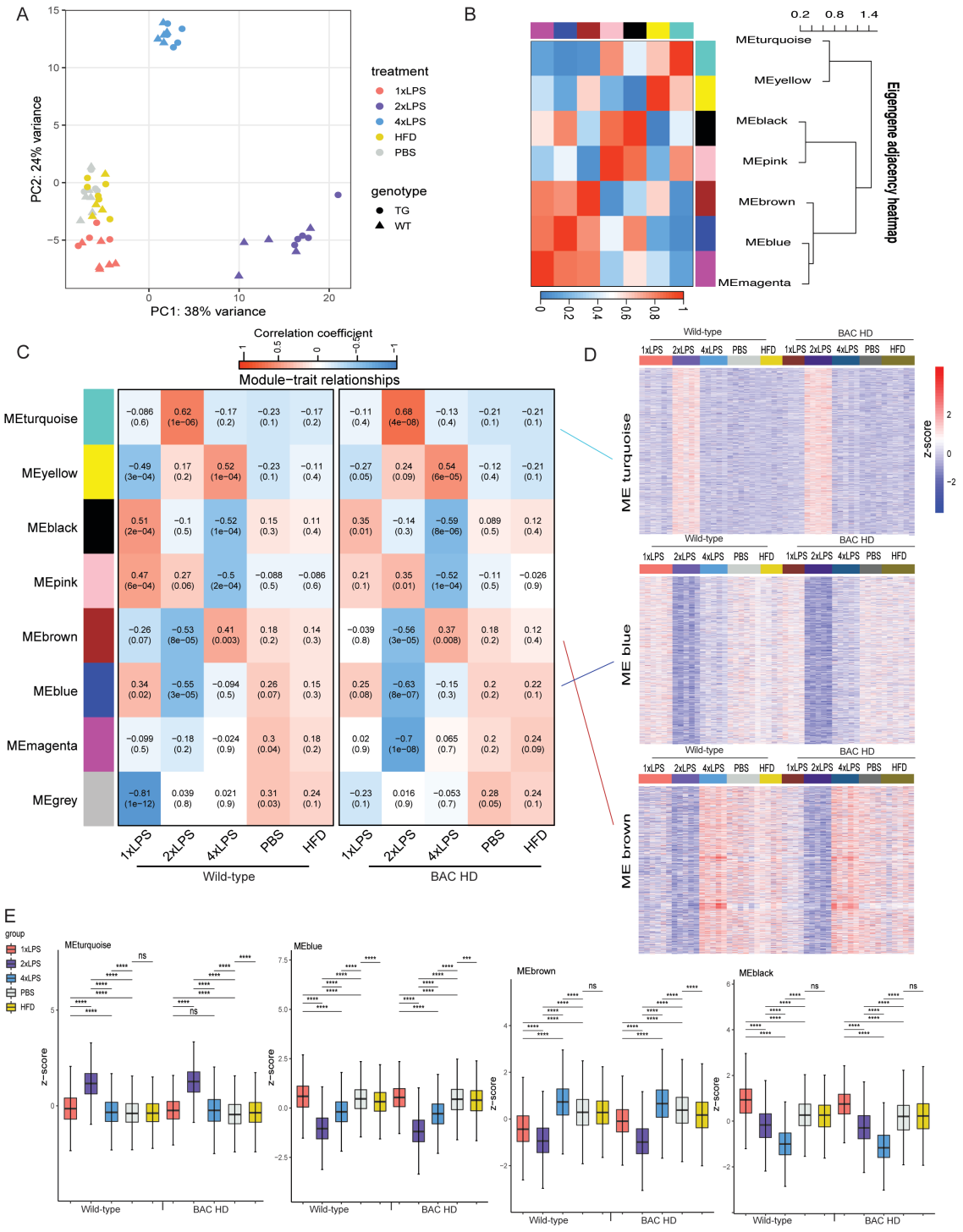

Figure 12. Gene expression analysis (WGCNA) in microglia from the BAC HD 3-month cohort. **A**. Principal component analysis (PCA) of the microglial transcriptomes across different conditions. **B.** Hierarchical clustering and heatmap to highlight relationships between modules. **C.** Heatmap of the correlation between module eigengenes and treatment groups (in each colour module, the top value is the correlation coefficient, and the bottom is the P-value, n = 6, 5, 5, 6, 4, 4, 4, 5, 5, 4, 6 rats from left to right). **D.** Heatmap of normalised gene expression within selected modules. The colours indicate z - scores, with a score of 0 being the average gene expression across samples. A positive z-score indicates the gene's expression is above the mean, whereas a negative value indicates the gene's expression is below the mean. **E.** Boxplot of genes expression level within modules. (n = 1911, 1404, 1338 and 206 genes in turquoise, blue, brown, and black modules, respectively). *P < 0.05, **P < 0.01, ***P < 0.001, ****P < 0.0001 for one-way ANOVA with Holm–Bonferroni correction.

For functional analysis (KEGG pathway and GO enrichment), all genes were input for enrichment analysis and again ranked by their weightFactor. The top terms from KEGG and GO enrichment analysis are presented in **Figure 13** and **Figure 15**, respectively. A cnetplot of KEGG pathways is shown in **Figure 14,** and a network plot of GO terms in **Figure 15**. Briefly, the genes in the black and yellow module, which correlate with the 1 x LPS treatment, were significantly enriched in pathways associated with antigen processing and presentation (potential key genes: *Cd74, Cd4, Ctss*), phagosome (potential key genes: *Ctss, C3, Itgam*), and endocytosis (potential key genes: *Il2rg, Ehd1*). The genes in the turquoise, brown, and blue modules which correlate with the 2 x LPS treatment groups were significantly enriched in pathways associated with protein processing in the endoplasmic reticulum (potential key genes: *Hsp90aa1, Ssr1, Canx*), lysosome (potential key genes: *Npc2, Tpp1, Ctsa, Hexb*), TNF signalling pathway (potential key genes: *Il1b, Traf2*), and NOD-like receptor signalling pathway (potential key genes: *Il1b, Ccl12, Irf7*), NF-kappa B signalling pathway (potential key genes: *Ccl4, Tnfaip3*), which are related to innate immune responses and induction of inflammation (Figure 14). Furthermore, GO enrichment analysis revealed that the black and yellow module genes, which correlate with gene expression in microglia from the 1 x LPS treatment groups, were significantly associated with antigen processing and immune response terms; the blue and brown modules that relate to 2 x LPS treatments were significantly associated with antigen processing and immune response terms **(Figure 15)**.

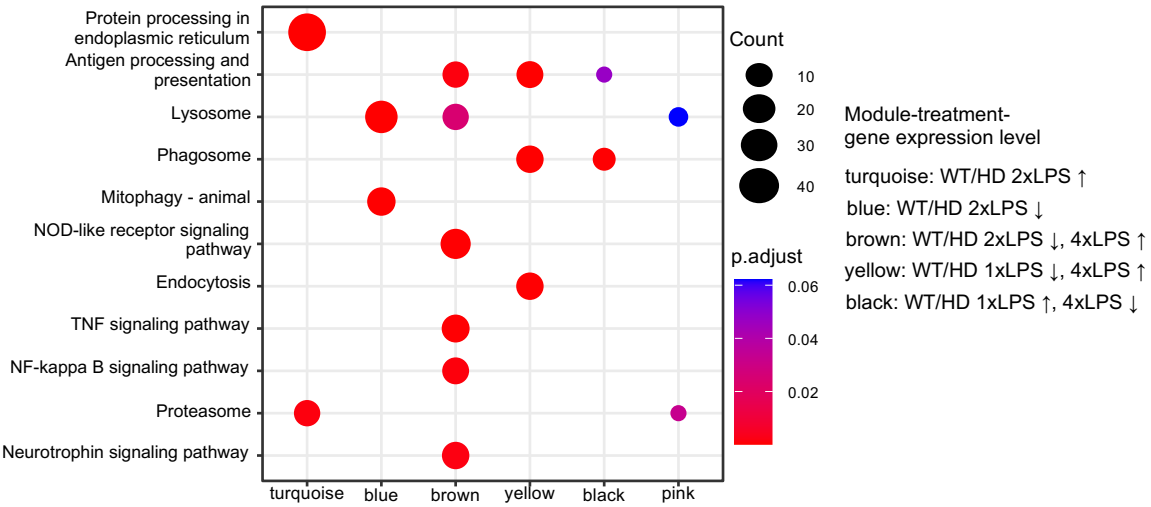

Figure 13. Dot plot of selected KEGG pathways enriched in modules in microglia from the BAC HD 3-month cohort.

(Please note that only modules are shown where significant pathway enrichment was found). ↑ Increased average gene expression level; ↓ decreased average gene expression level.

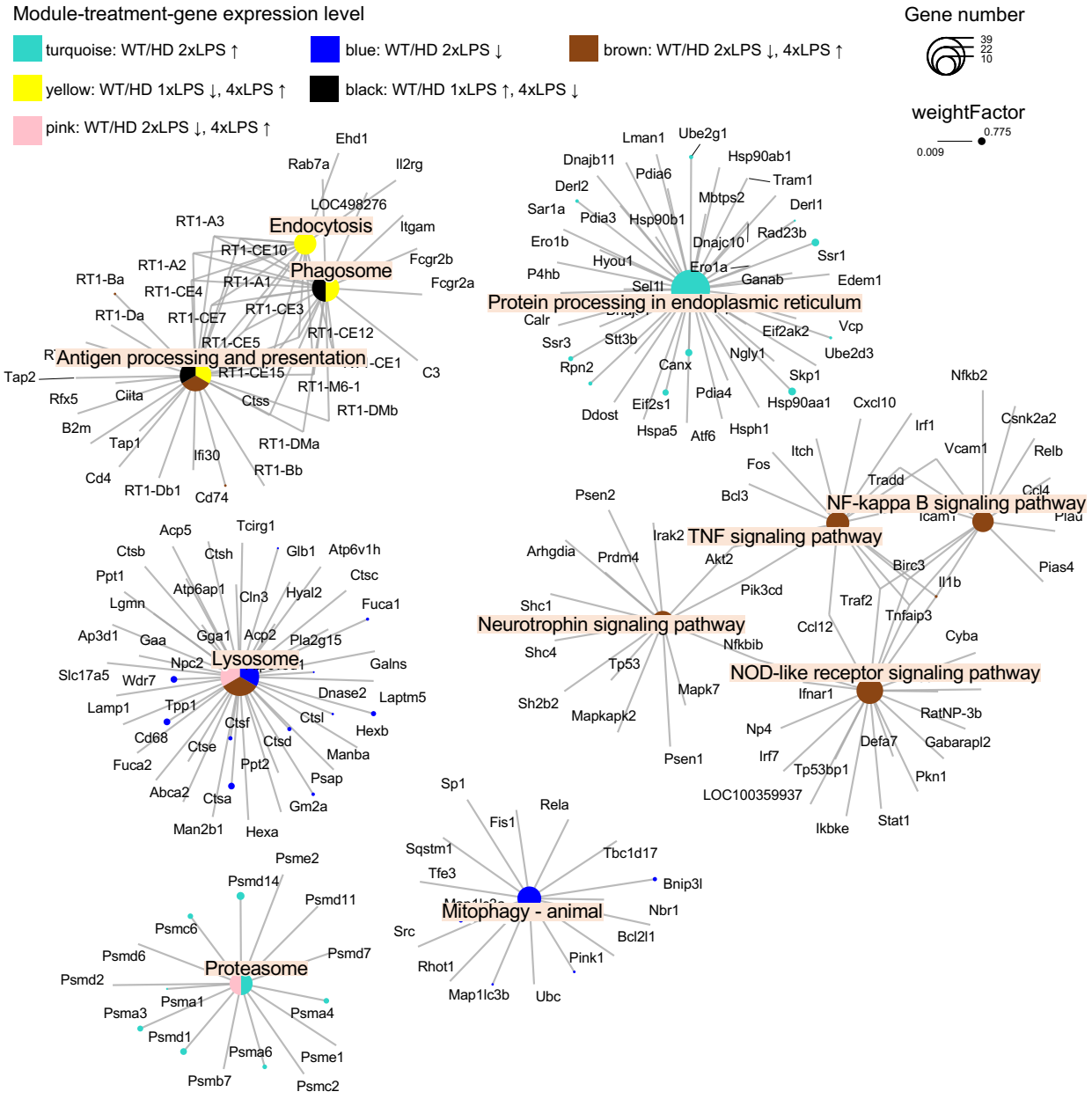

Figure 14. Network plot of selected KEGG pathways enriched in modules in microglia from the BAC HD 3-month cohort. The pie size for each category reflects the number of genes enriched in the respective pathway. Coloured dots label the genes within the respective module and pathway. The dot size (weightFactor, see Methods) represents the connectivity of genes in each module (where a higher value means the gene has more connections to other genes). ↑ Increased average gene expression level; ↓ decreased average gene expression level.

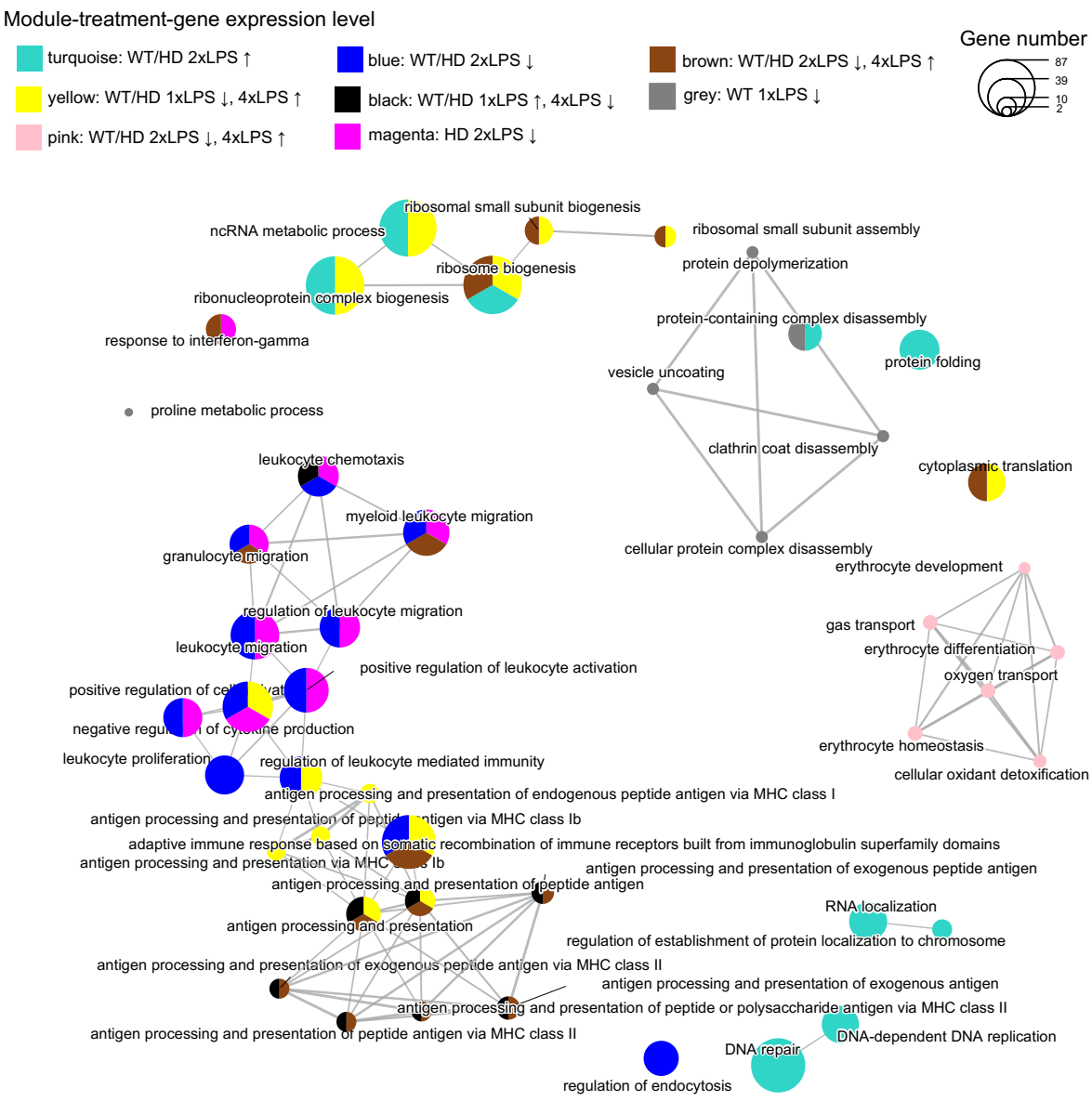

Figure 15. Network plot of top 6 GO terms enriched in modules in microglia from BAC HD 3-month cohort. The pie size for each category indicates the number of genes enriched in the respective GO term. ↑ Increased average gene expression level; ↓ decreased average gene expression level.

3.3.4 Microglial gene expression and function 6 months after immune stimulation in the HD model

First, samples were again clustered by PCA, displaying all 41 samples along PC1 (12% variance) and PC2 (9% variance) (**Figure 16. A**) for the different treatments (1 x LPS, 4 x LPS, PBS or HFD) in both genotypes (WT: wild type; TG: BAC HD). In the PCA plot, the PBS and 1 x LPS

groups were separated by genotypes, indicating that both the development of Htt pathology and innate immune memory affected microglial responses.

After filtering low variance genes, 10,508 genes were used as input for WGCNA to identify gene clusters associated with wild-type or BAC HD rats following the different treatments at 3 months. Using stepwise network construction and a minimum module size of 100 genes, this dissected the organised count matrix into 12 gene modules. Next, I examined the interaction relationships of the 12 modules, and then created the hierarchical clustering and network heatmap (**Figure 16. B**). WGCNA was then used to associate each module with the four different treatments (1 x LPS, 4 x LPS, PBS or HFD) in both genotypes (wild-type or BAC HD).

Examining significant correlations between all modules and conditions, both pathology- as well as immune memory-associated changes were also apparent in this model of HD pathology. In particular, genes in the blue module had a significant correlation with microglia from BAC HD rats as compared to wild-type rats in PBS, and 1 x LPS group; the turquoise, magenta, purple and brown modules showed a significant correlation in microglia from wild-type rats but not from BAC HD rats in PBS group, indicating the genes in those modules may respond to the development of pathology (**Figure 16. C**); the genes in the red, black, pink, and yellow modules showed an opposite correlation for microglia from the 1 x LPS group and 4 x LPS groups in BAC SNCA rats, highlighting differential immune memory effects (**Figure 16. C**). The heatmaps and boxplot of normalised gene expression within modules (**Figures 16. D, E**) revealed that microglia from the PBS group had lower gene expression levels in the turquoise module in wild-type rats than in BAC HD rats; microglia from the 1 x LPS and 4 x LPS group had higher gene expression level in the pink and magenta module in BACHD rats than wild-type rats, respectively. In BAC HD rats, although 4xLPS did not exhibit a strong correlation with any modules (correlation coefficient < 0.5 or P-value >0.05), it still showed opposite correlations to 1 x LPS, such as the red, black, pink, and yellow modules. Moreover, the average gene expression level in these modules was also significantly different between the 1 x LPS and 4 x LPS groups (pink module in **Figure 16. E**; the boxplots for other modules were not shown here).

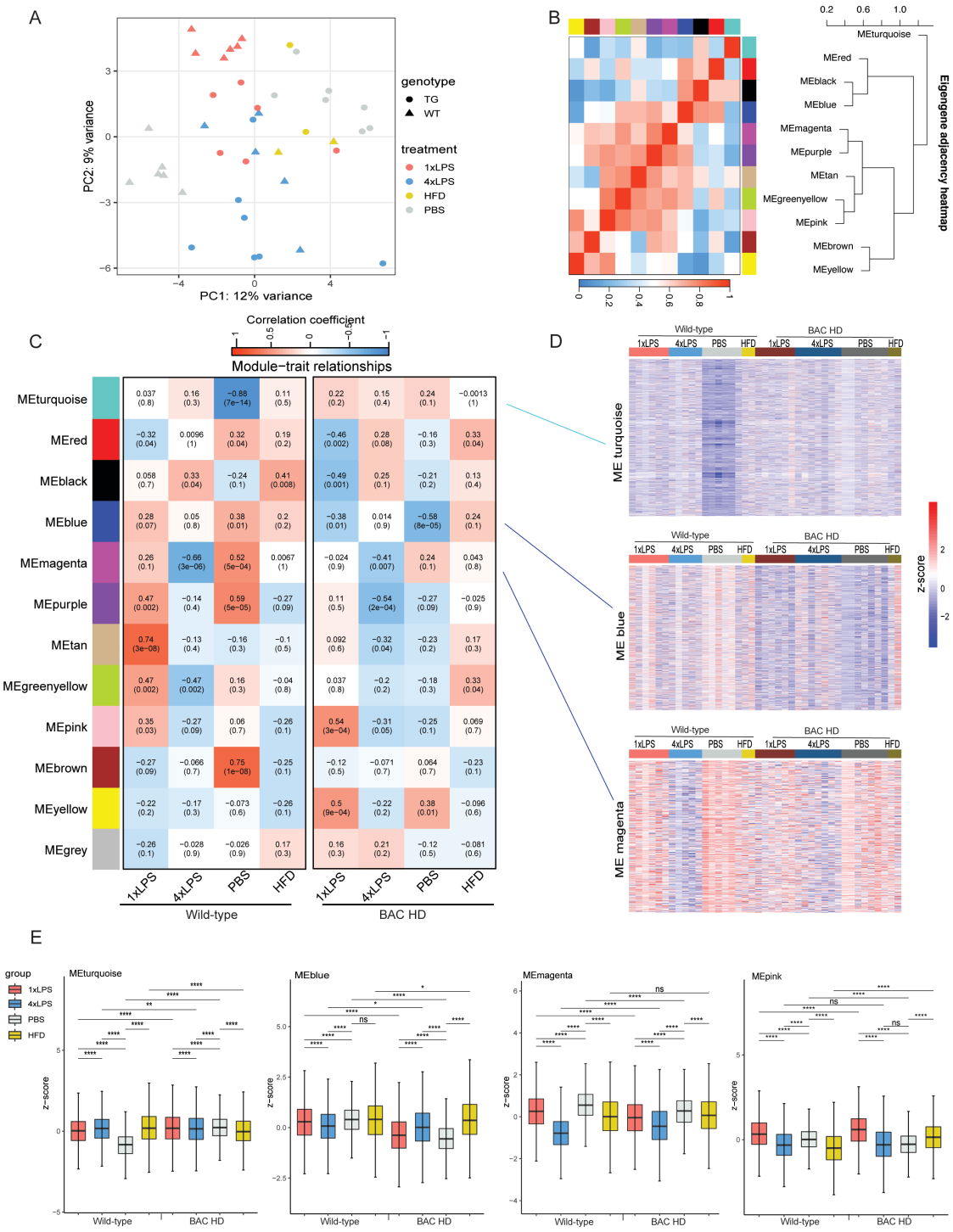

Figure 16. Gene expression analysis (WGCNA) in microglia from the BAC HD 9-month cohort. **A**. Principal component analysis (PCA) of the microglial transcriptomes across different conditions. **B.** Hierarchical clustering and heatmap to highlight relationships between modules. **C.** WGCNA heatmap of the correlation between module eigengenes and treatment groups (in each colour module, the top value is correlation coefficient, and the bottom is P-value, n = 6, 5, 6, 2, 6, 7, 7, 2 rats from left to right). **D.** Heatmap of normalised gene expression within selected modules. The colours indicate z - scores, with a score of 0 being the average gene expression across samples. A positive z-score indicates the gene's expression is above the mean, whereas a negative value indicates the gene's expression is below the mean. **E.** Boxplot of normalised gene expression for all genes within selected modules (n = 2784, 1369, 519 and 604 genes in turquoise, blue, magenta, and pink modules, respectively). *P < 0.05, **P < 0.01, ***P < 0.001, ****P < 0.0001 for one-way ANOVA with Holm–Bonferroni correction.

For functional enrichment analysis (KEGG pathway and GO enrichment), 2,623 genes with the highest connectivity values within modules were extracted and again ranked by their weightFactor. The top terms from KEGG and GO enrichment analysis are presented in **Figure 17. A** and **Figure 18**, respectively. A cnetplot of KEGG to illustrate individual genes within pathways is shown in **Figure 17. B** and a network plot of GO terms in **Figure 18**. Again, this analysis identified the regulation of highly relevant molecular pathways relating both to Huntington's disease and microglial immune activation. Briefly, the genes in the blue module which were down-regulated in microglia in response to the development of Htt pathology (comparing PBS-treated WT and BAC HD animals) were primarily enriched in the pathways of protein processing in the endoplasmic reticulum (potential key genes: *Os9, Rpn2, Hspa5, Vcp*); the genes in the turquoise module, which showed significantly lower expression in microglia from the PBS group in wild-type rats were enriched in pathways of Huntington disease and Oxidative phosphorylation; the genes in the red module which were down-regulated in microglia from the 1 x LPS in BAC SNCA rats were significantly enriched in mTOR, NOD-like receptor, Toll-like receptor and NF-kappa B signalling pathway. Furthermore, GO enrichment analysis revealed that the genes in the turquoise module (showing significantly lower expression in microglia from the PBS group in wild-type rats) were enriched in metabolic process terms, which were associated with mitochondrial function, while genes in the black module, which were down-regulated in microglia from 1xLPS BAC HD animals, were significantly associated with antigen processing and presentation (**Figure 18**).

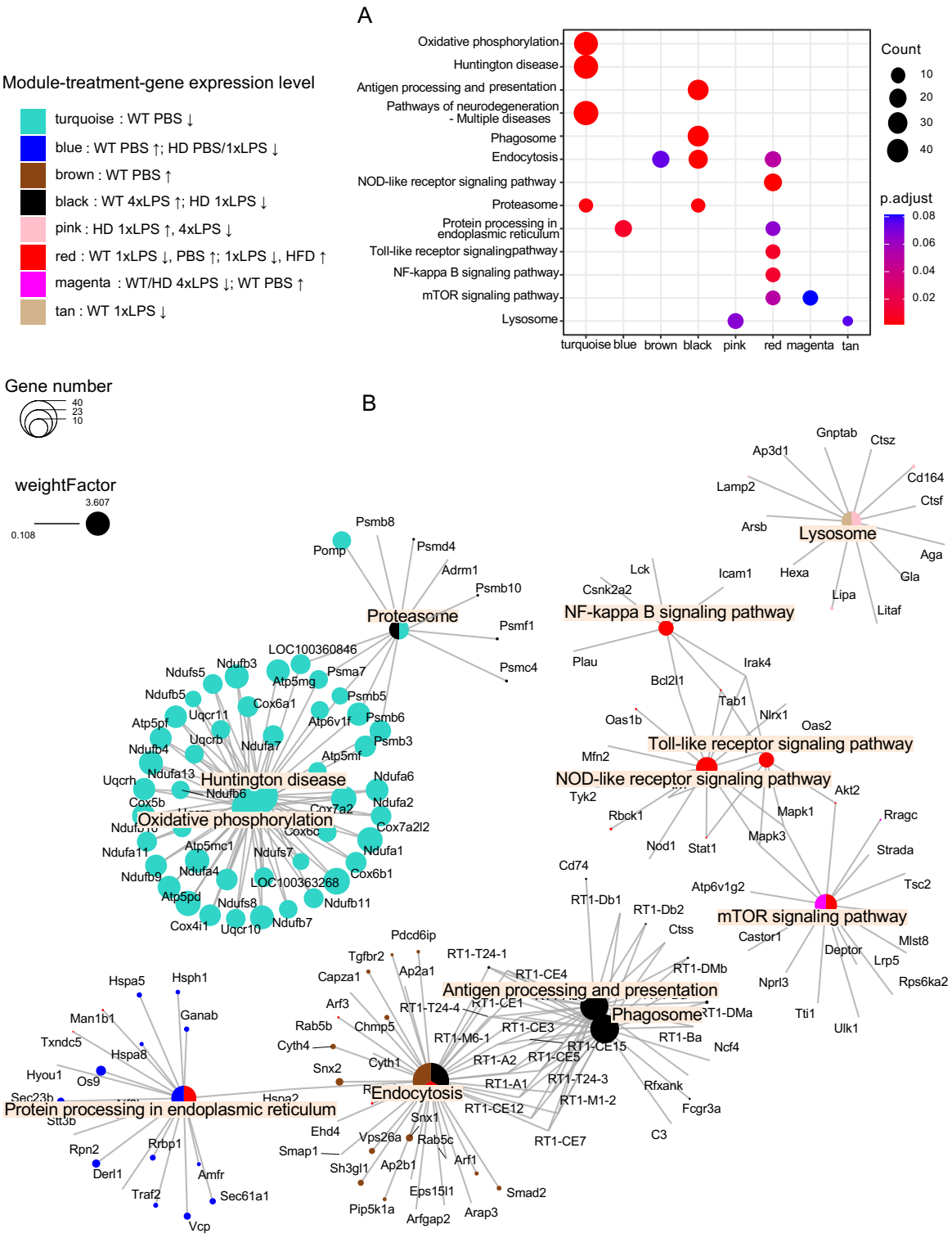

Figure 17. KEGG enrichment analysis in modules in microglia from the BAC HD 9-month cohort. A. Dot plot of selected KEGG pathways enriched in modules. **B.** Network plot of selected KEGG pathways enriched in modules. The pie size for each category reflects the number of genes enriched in the respective pathway. Coloured dots label the genes within the respective pathway and module. The dot size (weightFactor, see Methods) represents the connectivity of genes in each module (where a higher value means the gene has more connections to other genes). ↑ Increased average gene expression level; ↓ decreased average gene expression level.

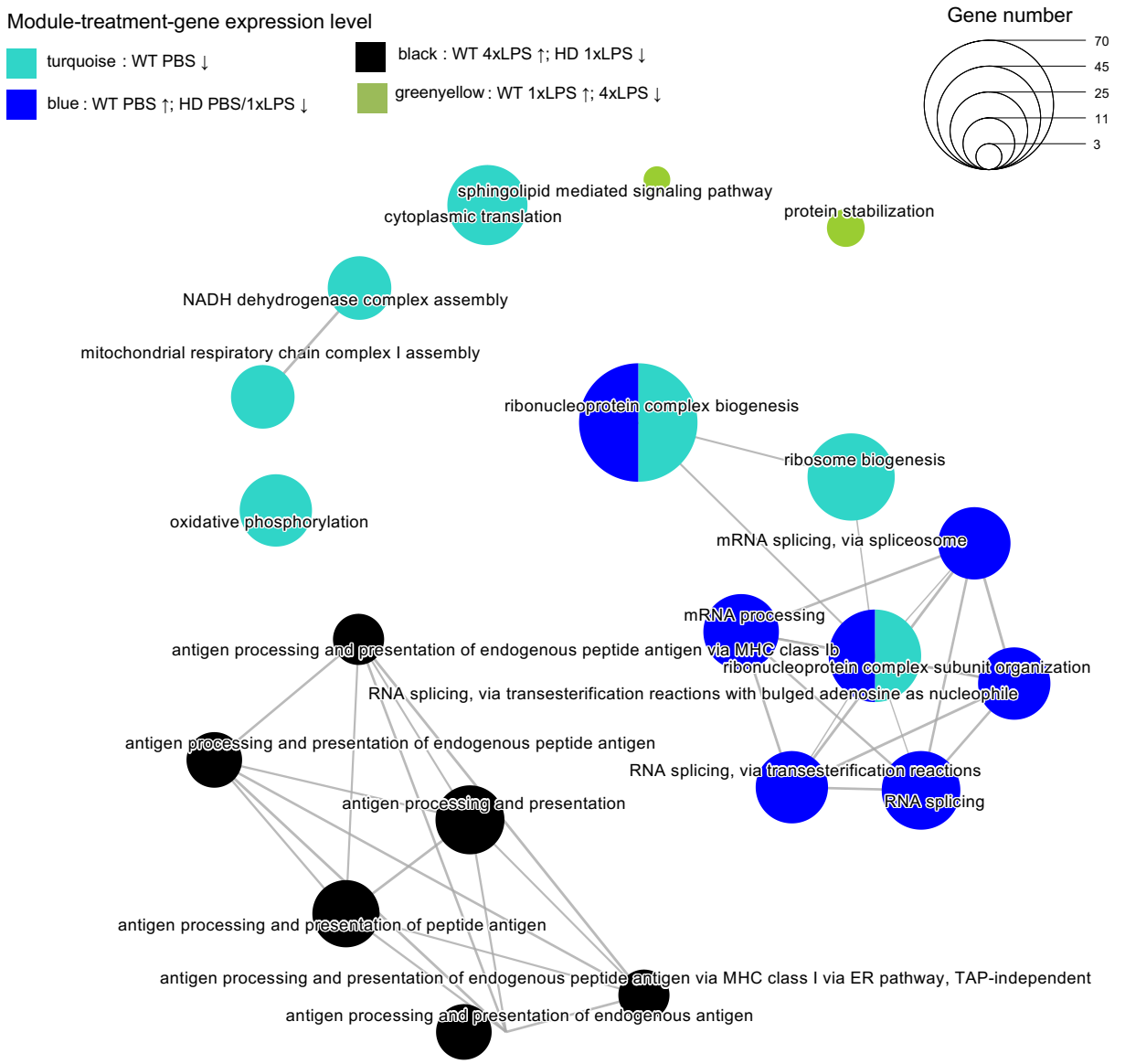

Figure 18. Network plot of top 6 GO terms enriched in modules in microglia from the BAC HD 9-month cohort. The pie size for each category indicates the gene numbers enriched in the respective GO term. ↑ Increased average gene expression level; ↓ decreased average gene expression level.

3.3.5 Summary table of pathway enrichment analysis

To compare the effects of different genotypes and different treatments for acute and long-term cohorts, and to identify common or distinct regulated pathways, the results of WGCNA and KEGG enrichment analyses are summarised for the four animal cohorts in **Table 1** for the 3-month cohort and **Table 2** for the 9-month cohort. Most of the signalling pathways could be classified into 3 categories: metabolism, inflammation, and phagocytosis related pathways.

As shown in Table 1, at 3 months of age, highly consistent regulation of molecular pathways was found between WT and transgenic animals within the same cohort, while some differences were found for BAC SNCA vs BAC HD cohorts. For example, in the BAC SNCA cohort, 1 x LPS significantly upregulated inflammation-related pathways (NOD-like receptor, Toll-like receptor, NF-kappa B and TNF signalling pathway), while 2 x LPS significantly downregulated these inflammation-related pathways, which is consistent with the cytokine results (Figure 3, Figure 4). Additionally, 1 x LPS significantly upregulated phagocytosis-related pathways (Antigen processing and presentation and Phagosome), whereas 2 x LPS significantly downregulated these pathways. In some pathways (Autophagy and Phagosome), the same treatment group exhibited opposite regulation, as the genes enriched in these pathways were from different co-expressed modules, suggesting that the same treatment may have opposing effects on different genes within the same functional pathways.

Table 1: Summary of enriched pathways in the 3-month cohort.

Double arrows, i.e., ↑↑ or ↓↓, indicate a strong correlation with a significant p-value (the correlation coefficient of modules is >0.5 or < -0.5 with a significant P-value p<0.05 in WGCNA, respectively). Single arrows, i.e., ↑ or ↓, indicate a less strong correlation with a significant P-value p< 0.05 (The modules' correlation coefficient are < 0.5 or > -0.5 but still show a significant P-value p<0.05.). Red font indicates opposing regulation of different genes within the same pathway.

KEGG PATHWAYS	WT (SNCA)	BAC SNCA	WT (HD)	BAC HD
METABOLISM PATHWAYS				
Citrate cycle (TCA cycle)	1xLPS↓↓	1xLPS↓↓	2xLPS↑,4xLPS↓	2xLPS↑,4xLPS↓
Autophagy - animal	2xLPS↓↓/↑↑	2xLPS↓↓/↑↑	2xLPS↓↓,4xLPS↑	2xLPS↓↓,4xLPS↑
Mitophagy - animal	2xLPS↓↓	2xLPS↓↓,4xLPS↑	2xLPS↓↓	2xLPS↓↓
Glycolysis / Gluconeogenesis			2xLPS↑↑	2xLPS↑↑
mTOR signalling pathway	2xLPS↑↑	2xLPS↑↑		
HIF-1 signalling pathway	2xLPS↑↑	2xLPS↑↑		
AMPK signalling pathway	2xLPS↓↓	2xLPS↓↓		
Oxidative phosphorylation	1xLPS↓↓	1xLPS↓↓		
INFLAMMATION PATHWAYS				
NOD-like receptor signalling pathway	1xLPS↑↑,2xLPS↓↓	1xLPS↑↑,2xLPS↓↓	2xLPS↓↓,4xLPS↑	2xLPS↓↓,4xLPS↑
TNF signalling pathway	1xLPS↑↑,2xLPS↓	1xLPS↑↑,2xLPS↓	2xLPS↓↓,4xLPS↑	2xLPS↓↓,4xLPS↑
Toll-like receptor signalling pathway	1xLPS↑↑,2xLPS↓	1xLPS↑↑,2xLPS↓	2xLPS↓↓,4xLPS↑	2xLPS↓↓,4xLPS↑
NF-kappa B signalling pathway	1xLPS↑↑,2xLPS↓	1xLPS↑↑,2xLPS↓	2xLPS↓↓,4xLPS↑	2xLPS↓↓,4xLPS↑
IL-17 signalling pathway	1xLPS↑↑,2xLPS↓	1xLPS↑↑,2xLPS↓		
MAPK signalling pathway	1xLPS↑↑,2xLPS↓↓	1xLPS↑↑,2xLPS↓↓		
JAK-STAT signalling pathway	1xLPS↑↑,2xLPS↓	1xLPS↑↑,2xLPS↓		
PHAGOCYTOSIS PATHWAYS				
Antigen processing and presentation	1xLPS↑↑,2xLPS↓	1xLPS↑↑,2xLPS↓, 4xLPS↑	1xLPS↓,2xLPS↓↓, 4xLPS↑↑	1xLPS↓,2xLPS↓↓, 4xLPS↑↑

Phagosome	1xLPS↑↑,2xLPS↓↓	1xLPS↑↑,2xLPS↓↓	1xLPS↓/↑↑, 4xLPS↑↑/↓↓	1xLPS↓/↑, 4xLPS↑↑/↓↓
Lysosome	1xLPS↓↓,2xLPS↓↓	1xLPS↓↓,2xLPS↓↓, 4xLPS↑	2xLPS↓↓,4xLPS↑	2xLPS↓↓,4xLPS↑
Endocytosis			1xLPS↓,4xLPS↑↑	1xLPS↓,4xLPS↑↑
Fc epsilon RI signalling pathway	2xLPS↑↑	2xLPS↑↑	1xLPS↑↑,4xLPS↓↓	1xLPS↑,4xLPS↓↓
PROLIFERATION PATHWAYS				
DNA replication	2xLPS↑↑	2xLPS↑↑	2xLPS↑↑	2xLPS↑↑

As shown in **Table 2** for 9-month-old animals, the microglial signalling pathways enriched in the control group (PBS) for BAC SNCA and BAC HD are distinct, indicating that the effects of microglia on PD (α-synuclein) or HD (Htt)-related pathology may be mediated through different pathways. For example, in the PD model, microglia in BAC SNCA upregulated pathways related to protein processing (Antigen processing and presentation and Protein processing in endoplasmic reticulum), whereas in BAC HD, microglia downregulated mitochondrial-related metabolic pathways (Glycolysis / Gluconeogenesis and HIF-1 signalling pathway) and phagocytosis-related pathways (Lysosome and Endocytosis).

Moreover, the influence of immune memory triggered by different immune stimuli was clearly distinct for the PD and HD models. In the PD model, 1 x LPS and 4 x LPS treatments (6 months earlier) primarily affected metabolic pathways such as Oxidative phosphorylation, Parkinson's disease, “Pathways of neurodegeneration - multiple diseases”, and TCA cycle, as well as inflammatory pathways such as NOD-like receptor and TNF signalling pathway. However, in the HD model, 1 x LPS and 4 x LPS treatments (6 months earlier) mainly impacted metabolic pathways such as Mitophagy, AMPK, Glycolysis/Gluconeogenesis and mTOR signalling pathway, as well as inflammation-related pathways, such as NOD-like receptor, Toll-like receptor, and Chemokine signalling pathway. In both rat models, 1 x LPS and 4 x LPS-induced immune memory influenced microglial phagocytosis-related pathways.

Table 2: Summary of enriched pathways in the 9-month cohort.

Double arrows, i.e., ↑↑ or ↓↓, indicate a strong correlation with a significant p-value (the correlation coefficient of modules is >0.5 or < -0.5 with a significant P-value p<0.05 in WGCNA, respectively). Single arrows, i.e., ↑ or ↓, indicate a less strong correlation with a significant P-value p<0.05. (The correlation coefficient of modules is <0.5 or > -0.5, but modules still show a significant P-value p<0.05.) Red font indicates opposing regulation of different genes within the same pathway.

KEGG PATHWAYS	WT (SNCA)	BAC SNCA	WT (HD)	BAC HD
METABOLISM PATHWAYS				
Oxidative phosphorylation	1xLPS↓↓, 4xLPS↑	1xLPS↑, 4xLPS↓/↑↑	PBS↓↓	
Parkinson disease	1xLPS↓, 4xLPS↑	4xLPS↑↑		
Pathways of neurodegeneration – multiple diseases	4xLPS↑, 1xLPS↓	4xLPS↑↑	PBS↓↓	
Huntington disease			PBS↓↓	
Citrate cycle (TCA cycle)	4xLPS↑	4xLPS↑↑	PBS↑↑	
HIF-1 signalling pathway		4xLPS↓	PBS↑	PBS↓↓,1xLPS↓
Mitophagy - animal			PBS↓↓/↑, 1xLPS↓	1xLPS↓, HFD↑
Autophagy - animal			PBS↑↑	
AMPK signalling pathway			PBS↑	PBS↓↓,1xLPS↓
Glycolysis / Gluconeogenesis			PBS↑	PBS↓↓,1xLPS↓
mTOR signalling pathway			1xLPS↓, PBS↑	1xLPS↓, HFD↑
INFLAMMATION PATHWAYS				
NOD-like receptor signalling pathway		PBS↓;4xLPS↓	1xLPS↓, PBS↑	1xLPS↓, HFD↑
Toll-like receptor signalling pathway			1xLPS↓, PBS↑↑	1xLPS↓, HFD↑
Chemokine signalling pathway			1xLPS↓, PBS↑	1xLPS↓, HFD↑
IL-17 signalling pathway	1xLPS↓	PBS↑		
TNF signalling pathway		4xLPS↓		
PHAGOCYTOSIS PATHWAYS				
Antigen processing and presentation	1xLPS↓	PBS↑	4xLPS↑, HFD↑	1xLPS↓
Lysosome	4xLPS↑	4xLPS↑↑	PBS↑	PBS↓↓, 1xLPS↓
Phagosome			4xLPS↑, HFD↑	1xLPS↓
Endocytosis			PBS↑, 1xLPS↓, 4xLPS↑, HFD↑	PBS↓↓,1xLPS↓, HFD↑
Proteasome			4xLPS↑, HFD↑	1xLPS↓
Fc gamma R-mediated phagocytosis	1xLPS↑, 4xLPS↓	1xLPS↑, 4xLPS↓↓		
OTHER PATHWAYS				
Protein processing in endoplasmic reticulum	1xLPS↓	PBS↑		
Neurotrophin signalling pathway			1xLPS↓, PBS↑	1xLPS↓, HFD↑
DNA replication			PBS↑	PBS↓↓, 1xLPS↓

3.5 Microglial gene expression at single-cell resolution in rat models of PD and HD

In a separate analysis, the heterogeneity of microglial cells was examined in 9-month-old BAC HD and BAC SNCA rats using single-cell RNA-sequencing (scRNA-seq). Microglia were isolated as described above **(Figure 2),** and scRNA-seq was performed using the commercial 10x Genomics solution. The raw dataset consisted of 66,528 cells collected from 8 rats (3 BAC HD, 3 BAC SNCA, and 2 wildtypes). After quality control (including removal of doublet and low-quality cells) 34,914 high-quality cells were retained for downstream analysis, with an average of 4,364 cells per rat (range 2,138-12,120 cells per animal). Using the Seurat package for analysis (Hao et al., 2021), 11 unique clusters of microglia were identified (Cluster 0 to 10) (**Figure 19. A**). However, contrary to our expectations, no pathology-specific microglial subcluster was apparent in BAC HD or BAC SNCA animals (**Figure 19. B**). However, a shift in the proportions of cells within the different microglial clusters was found for the different genotypes (**Figure 19. C**). Compared to microglia from wild-type animals, the proportion of microglia in BAC HD was significantly altered in clusters 0, 1, 2 and 4 (**Figure 19. C, D**) and in cluster 0 and 4 for BAC SNCA animals (**Figure 19. C, D**).

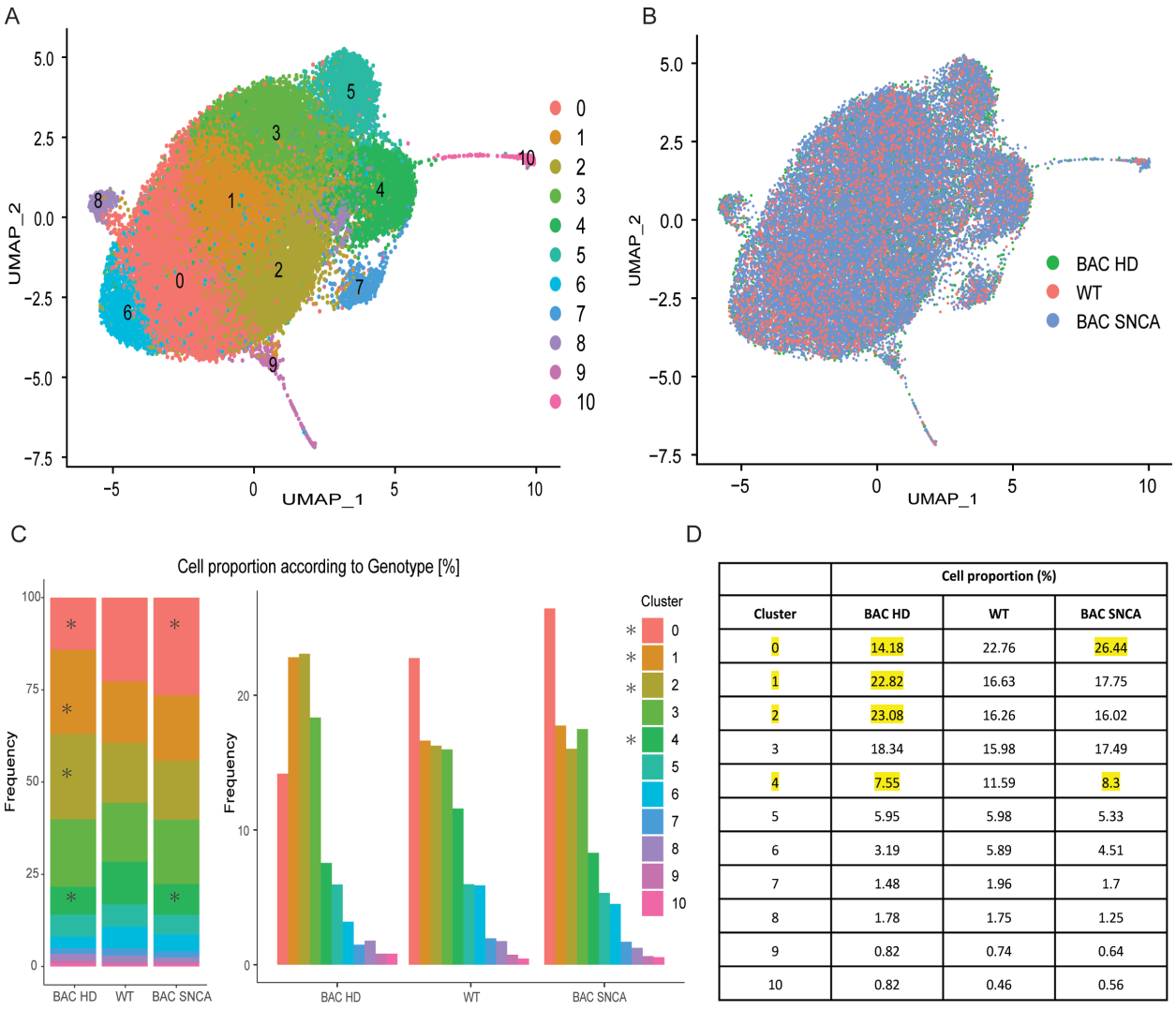

	Cell proportion (%)		
Cluster	BAC HD	WT	BAC SNCA
0	14.18	22.76	26.44
1	22.82	16.63	17.75
2	23.08	16.26	16.02
3	18.34	15.98	17.49
4	7.55	11.59	8.3
5	5.95	5.98	5.33
6	3.19	5.89	4.51
7	1.48	1.96	1.7
8	1.78	1.75	1.25
9	0.82	0.74	0.64
10	0.82	0.46	0.56

Figure 19. Microglial subclusters exhibit cellular heterogeneity as revealed by single-cell transcriptomics.

A. 33.282 microglia from eight 9-month-old rats (2 wildtype (WT), 3 BAC HD, and 3 BAC SNCA rats) were analysed and separated into 11 subclusters (0 to 10) after unsupervised clustering analysis using the Seurat R package. **B.** UMAP displayed no specific microglia subcluster in different genotypes. **C.** The proportion of cells within subclusters differs between genotypes. The proportion of cells with marked alterations within clusters was labelled with a star (*) (wild type vs BAC HD or BAC SNCA). **D.** The table showed the exact percentage of cell proportion within each cluster across genotypes. The yellow background indicates apparent alterations of cell proportion compared to wild-type animals.

To characterise the cell types of each cluster, marker genes were identified by comparing each cluster to other clusters with the FindAllmarkers function in Seurat. Specific gene markers and representative GO terms of the biological process were then identified, with most microglial subclusters showing distinct maker genes (**Figure 20**) and separable biological functions (**Figure 21**). Microglial signature genes (*P2ry12, Cx3cr1, Tmem119, Hexb*) were highly expressed in all subclusters except cluster 10. These genes were also identified as the marker genes of cluster 0,

which can therefore be classified as homeostatic microglia (Gerrits et al., 2021; Keren-Shaul et al., 2017; Mathys et al., 2019; Nguyen et al., 2020). Other clusters with apparent biological functions were cluster 5 as MHC expressing microglia, showing high expression of *Cd74, Acp5, RT1-Da, RT1-Db1* and biological process enrichment for antigen processing and presentation, corresponding to the described MHC microglial subtype or 'Activated Response Microglia' (ARM) (Ellwanger et al., 2021; Mathys et al., 2019; Safaiyan et al., 2021; Sala Frigerio et al., 2019; Wang et al., 2020a; Zhou et al., 2020). Cluster 7 showed high expression of *Irf7, Ifit2, Ifit3, Mx1,* and *Cxcl17* and was associated with biological process terms of response to virus and regulation of innate immune response, while cluster 8 showed high expression of *Ccl4, Egr1, Btg2* and was associated with biological process terms of IFN-γ response and mediated immunity; both clusters are therefore related to the previously described interferon-response microglia subtype (IRM) (Friedman et al., 2018; Mathys et al., 2017; Sala Frigerio et al., 2019). Cluster 9 likely reflects proliferating microglia (Cyc-M) because of the differential expression of *Mki67, Stmn1, Mcm5* and enrichment of the biological process term DNA replication (Elmore et al., 2014; Huang et al., 2018; Prater et al., 2021; Tay et al., 2017). Cluster 10 exhibited a low expression of microglial homeostatic genes (*P2ry12*, *Tmem119*, and *Cx3cr1*), and a high expression of white-matter associated microglia (WAM) signature genes (*Clec7a* and *Axl*), suggesting that Cluster 10 may be the WAM (Amor et al., 2022; Safaiyan et al., 2021).

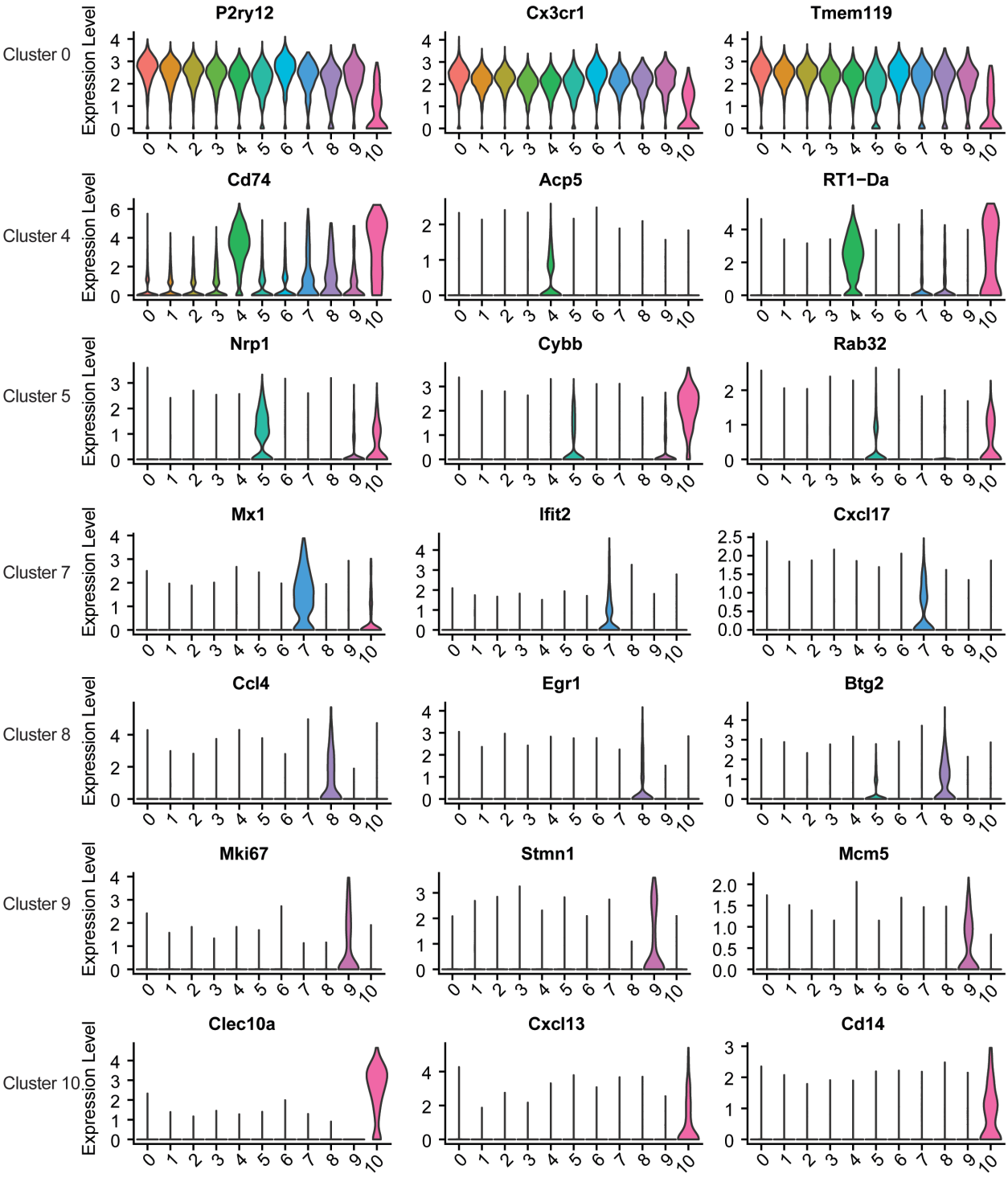

Figure 20. Specific gene markers in selected microglial subclusters.

Marker genes were identified by comparing each cluster to other clusters with the *FindALLMarkers* function from Seurat and are displayed as violin plots. The x-axis represents the gene expression level, and the y-axis represents clusters (0-10).

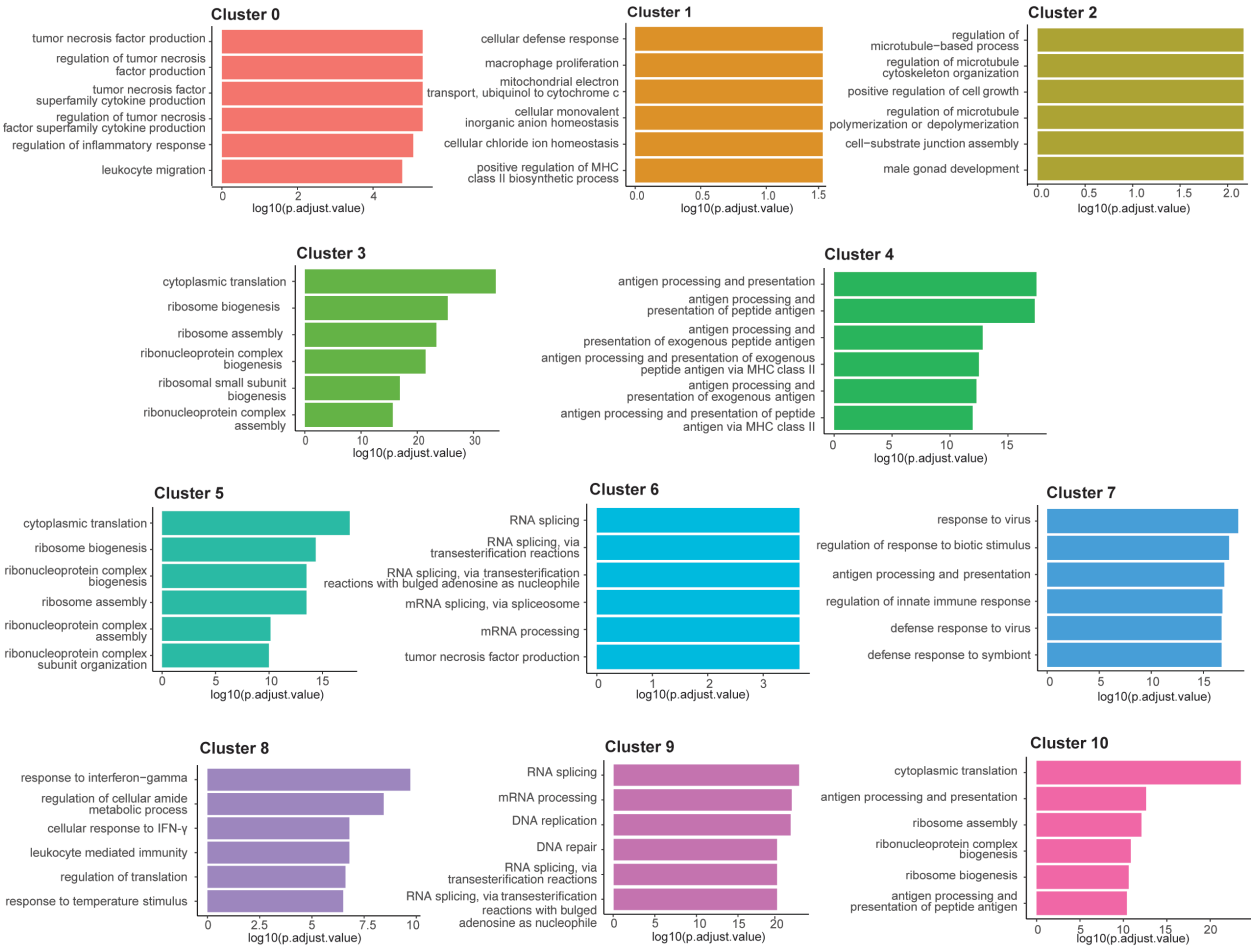

Figure 21. Functional GO enrichment analysis for each cluster based on marker genes. The top 6 GO terms of biological process for each cluster were shown in the figure.

As changes in the composition of microglial subtypes were found among genotypes (**Figure 19. C, D**), differential gene expression was also analysed within clusters between genotypes (**Figure 22**, **Figure 23**). Comparing microglia from BAC HD and wild-type animals in clusters 0, 1, 2, and 4, *RGD1563400, RT1-A1, Jund, Ccl3, Pik3ip1, Fos*, and *H1f4* were significantly upregulated in microglia from BAC HD animals in most clusters, while *RT1-CE10* and *Cd74* were significantly down-regulated in most clusters. Interestingly, the *Htt* gene was significantly upregulated in cluster 2, indicating that microglia in cluster 2 may be particularly relevant for cell-autonomous responses to *Htt* pathology.

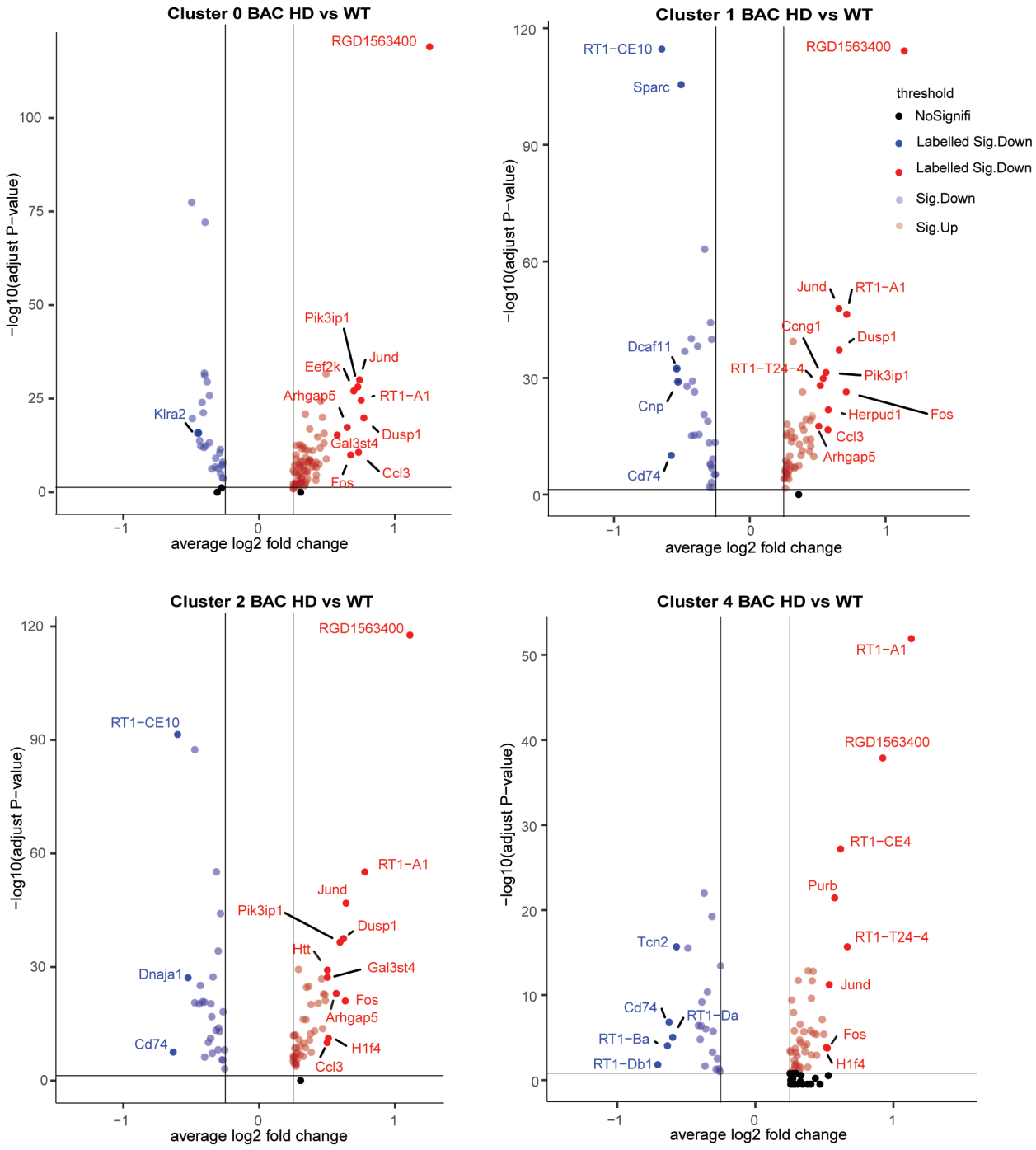

Figure 22. Differentially expressed genes (DEGs) between BAC HD and wild-type rats within selected clusters. The differential expression analysis was performed by Seurat's *FindMarkers* function. The x-axis represents statistical significance (log10 transformed adjusted P-value, based on Bonferroni correction), and the y-axis represents log fold-change of the average expression compared to wild-type rats. **"Nosignif"** means not differentially expressed genes; **"Sig.Down"** means significantly downregulated genes (threshold: average log2 fold change < -0.25 & adjusted p-value < 0.05); **"Sig.Up"** means upregulated genes (threshold: average log2 fold change > 0.25 & adjusted p-value < 0.05); **"Labelled Sig.Down"** labels the most significantly downregulated genes (threshold: average log2 fold change < -0.5 & adjusted p-value < 0.05); **"Labelled Sig.Up"** labels the most significantly upregulated genes (threshold: average log2 fold change > 0.5 & adjusted p-value < 0.05).

Comparing microglia from the BAC SNCA and wild-type animals in cluster 0 (**Figure 23**), *Ctss, LOC100360087, Efe1a1, Rpl32, and Ppia* were significantly up-regulated in BAC SNCA cells, while *Ldhb, Mt-nd4, Mt-nd1,* and *Mt-atp6* were significantly down-regulated. In cluster 4 (**Figure 23**), *Ctss, Lilrb3a, LOC108348175, Clec2l,* and *P2ry12* were significantly up-regulated in BAC SNCA microglia, while *Ldhb, Mt-nd4, Mt-nd1,* and *Mt-atp6* were significantly down-regulated.

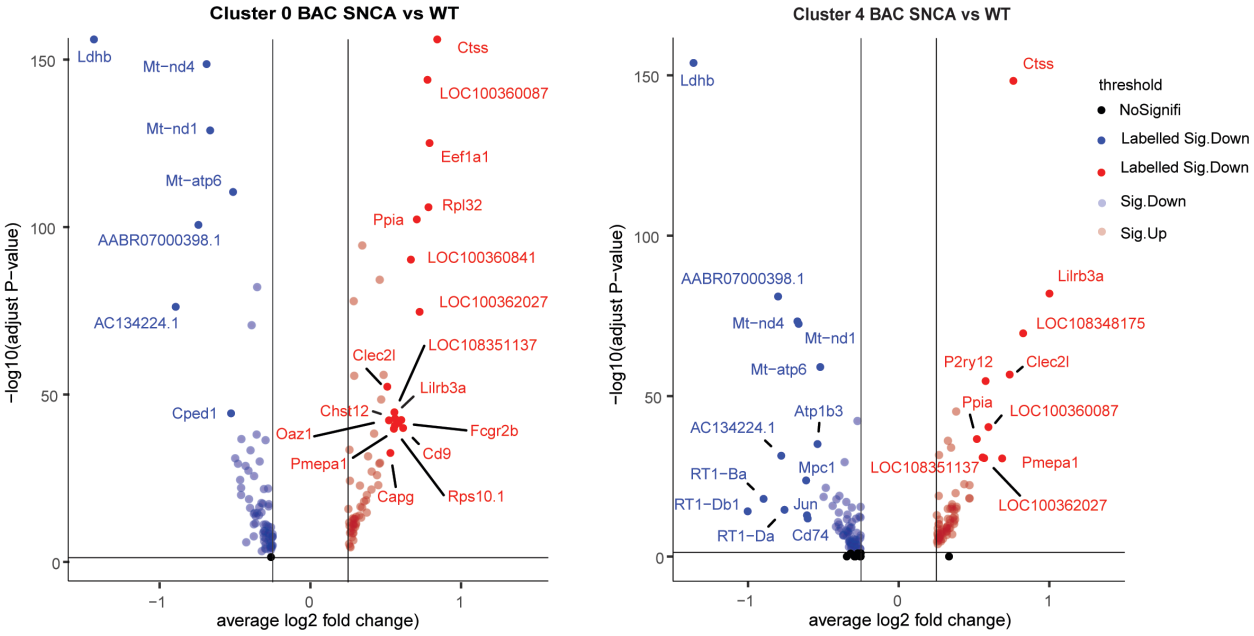

Figure 23. Differentially expressed genes (DEGs) between BAC SNCA and wild-type rats within selected clusters. The differential expression analysis was performed by Seurat's *FindMarkers* function. The x-axis represents statistical significance (log10 transform of adjusted P-value, based on Bonferroni correction), and the y-axis represents log fold-change of the average expression based on wild-type rats. **"Nosignif"** means not differentially expressed genes; **"Sig.Down"** means significantly downregulated genes (threshold: average log2 fold change < -0.25 & adjusted p-value < 0.05); **"Sig.Up"** means upregulated genes (threshold: average log2 fold change > 0.25 & adjusted p-value < 0.05); **"Labelled Sig.Down"** labels the most significantly downregulated genes (threshold: average log2 fold change < -0.5 & adjusted p-value < 0.05); **"Labelled Sig.Up"** labels the most significantly upregulated genes (threshold: average log2 fold change > 0.5 & adjusted p-value < 0.05).

Notably, compared to wild-type rats, *P2ry12* and *Ctss* were upregulated across all the microglial subclusters in the BAC SNCA rat model but relatively downregulated in the BAC HD rat model (**Figure 24. A, C**). Additionally, *Ldhb* was significantly downregulated in the BAC SNCA rat model (**Figure 24. B**), indicating those genes may play an important role in the development of α-synuclein and Htt pathology.

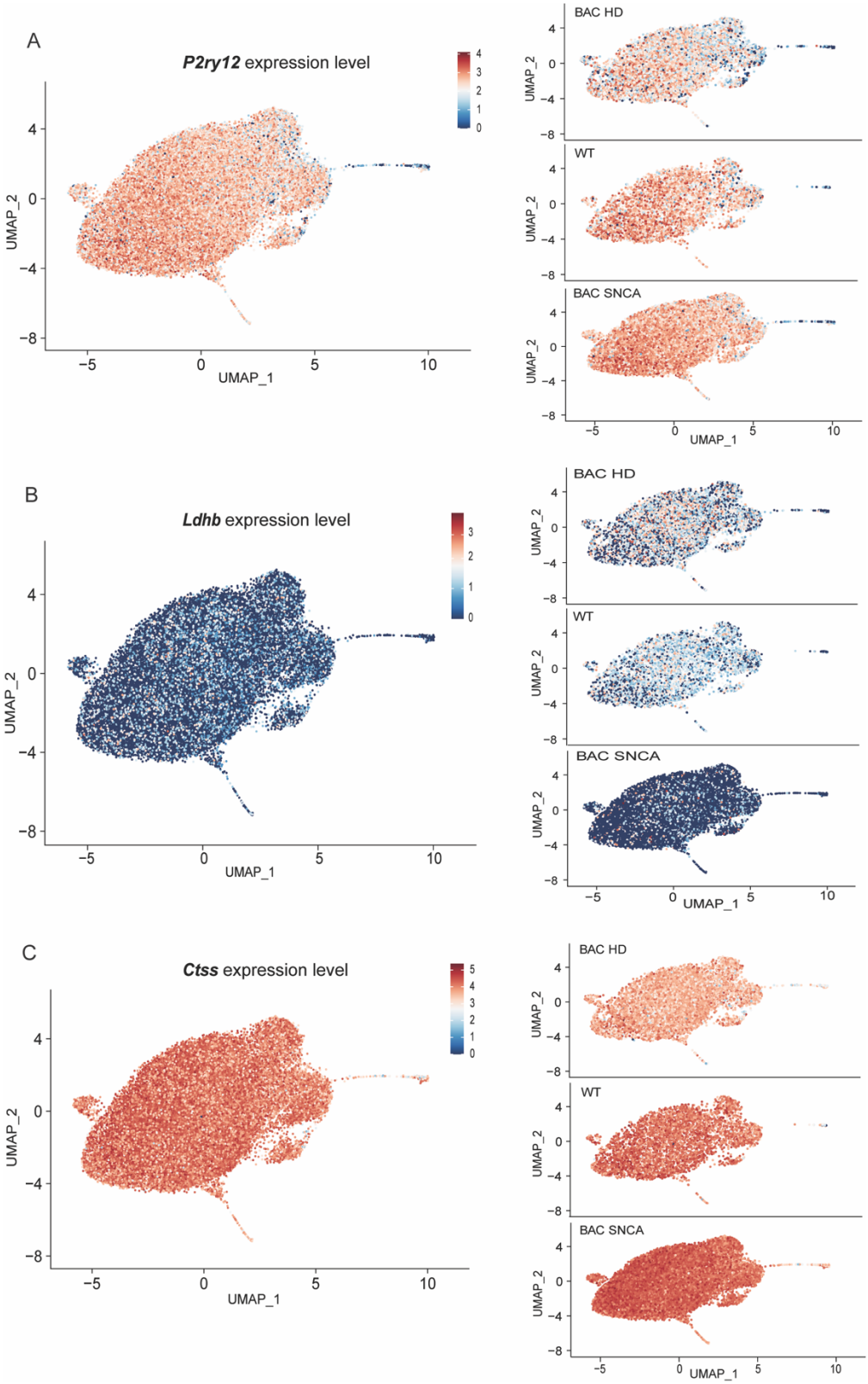

Figure 24. Expression of selected genes on UMAP plot. A. *P2ry12* expression level across genotypes. **B.** *Ldhb* expression level across genotypes. **C.** *Ctss* expression level across genotypes. The colour code indicates the average expression.

To gain a better understanding of the function of differentially expressed marker genes (DEGs) within clusters (considering all genes with an absolute value of average log2 fold change > 0.25 & adjusted p-value < 0.05), KEGG enrichment analysis was performed on all clusters (**Table 3**). Compared to wild-type rats, differentially expressed genes in most microglial subclusters in the BAC SNCA and BAC HD rat models were enriched in phagocytosis-related pathways, indicating that regulation of microglial phagocytosis function may be associated with early pathological development in both PD and HD models. Moreover, the differential enrichment pathways in both models suggested that early pathological progression in PD and HD may be affected by the regulation of different signalling pathways or by distinct regulation of the same pathway. For example, in BAC SNCA rats, metabolic pathways (Glycolysis/ Gluconeogenesis, Glucagon and HIF-1 signalling pathway) were downregulated in most microglia subclusters, whereas in BAC HD rats, inflammation-related pathways (Toll-like receptor, IL-17, TNF and MAPK signalling pathway) were up-regulated in most microglia subclusters. Furthermore, the lysosome pathway was upregulated in clusters 2, 4 and 5 of BAC SNCA but downregulated in clusters 6 and 7 of BAC HD rats (see Table 3 for a summary of regulated pathways).

Table 3: Summary of enriched pathways within clusters across genotypes. The numbers indicate the cluster.

	BAC SNCA vs WT		BAC HD vs WT	
KEGG PATHWAYS	**Downregulation**	**Upregulation**	**Downregulation**	**Upregulation**
METABOLISM PATHWAYS				
Glucagon signalling pathway	7,8			
Glycolysis/ Gluconeogenesis	5,6,7,8			
HIF-1 signalling pathway	0,2,5,6,7,8			
INFLAMMATION PATHWAYS				
NOD-like receptor signalling pathway	0,3			
Toll-like receptor signalling pathway	0			1,2,3
IL-17 signalling pathway	0,3			0,1,2,3,4,5,7
TNF signalling pathway				0,1,2,3,7
MAPK signalling pathway				2,8
PHAGOCYTOSIS PATHWAYS				
Antigen processing and presentation	0,2,3,4,5,6,8		0,1,2,3,4,5,6,7,8	2,3,4,5,7,8
Endocytosis	5		0,1,3	4,5,7,8
Lysosome		2,4,5	6,7	
Phagosome	0,4,5,6,8		0,1,2,3,4,7,8	3,4,5,7,8

4. Discussion and Conclusions

For a long time, immunological memory was believed to be a defining feature of the adaptive immune system. However, growing evidence shows that myeloid cells also exhibit memory-like characteristics (Netea et al., 2015, 2016). For instance, macrophages and monocytes might maintain a memory of previous inflammatory experiences, altering their response to secondary stimuli. Depending on the initial trigger, macrophages can be "tolerant", exhibiting hypo-responsiveness, or "trained", displaying enhanced reactivity to following stimuli (Foster et al., 2007; Ostuni et al., 2013; Yoshida et al., 2015), opening a new field of research in immunology.

Microglia, tissue-resident macrophages of the central nervous system parenchyma, are critical for neurodevelopment and maintaining tissue homeostasis. Infections or any other disruptions of the brain's homeostasis can rapidly trigger a microglial response, resulting in the release of cytokines, altered phagocytic activity, and morphological changes (Eggen et al., 2013). Recently, our lab demonstrated that microglia are capable of developing innate immune memory, which in turn could shape AD pathology in a mouse model. This study found that immune training and tolerance can modify brain cytokine levels, microglial epigenetic and gene expression profiles, metabolism, and phagocytic activity for at least 6 months (Wendeln et al., 2018). Additionally, Neher and Cunningham proposed an integrated nomenclature to describe microglial innate immune memory: the initial stimuli can trigger differential microglial states, "primed" or "desensitised". The primed microglia show enhanced responsiveness to a second stimulus (*immune training*). In contrast, desensitised microglia show reduced responsiveness to a second stimulus (*immune tolerance*) (Neher and Cunningham, 2019).

Since microglia also play an essential role in various neurodegenerative diseases (Heneka et al., 2014;Iadecola and Anrather, 2011; Prinz and Priller, 2014; Prinz et al., 2019; Xu et al., 2021), it is conceivable that microglial innate immune memory could affect the pathological hallmarks of other neurodegenerative diseases such as Parkinson's disease and Huntington's disease. However, this has not previously been investigated. Thus, the purpose of this thesis was to examine the impact of microglial innate immune memory in animal models of PD and HD.

4.1 The acute microglial immune response to peripheral insults

The same LPS injection protocol as in our lab's original study describing innate immune memory was used in this project. Initially, it was found that different LPS administration paradigms resulted in distinct immune reprogramming of microglia in adult mice, which was shown by increased vs decreased production of several cytokines (Püntener et al., 2012; Wendeln et al., 2018). In terms of serum cytokines, they reported that the first LPS (1 x LPS) challenge resulted in increased protein levels of pro-inflammatory cytokines (IFN-γ, IL-1β, TNF-α), and the pro-inflammatory cytokines were no longer increased at the second (2 x LPS), third (3 x LPS) and fourth challenges (4 x LPS) in their mouse model, demonstrating the induction of endotoxin tolerance in the peripheral immune system (Püntener et al., 2012; Wendeln et al., 2018). Similar changes were observed in the serum cytokines from our animal models in the 3-month cohort. For example, a single injection of LPS (0.5 mg/kg) resulted in increased production of several cytokines, but repeated injections of LPS (2 x LPS and 4 x LPS) resulted in suppressed production of several cytokines (**Figure 3**, **Figure 4**)

In contrast to the peripheral immune system, the original study reported no significant increase in brain cytokine levels in 1 x LPS-treated compared to PBS-treated control animals, but significant increases in brain cytokine levels following 2 x LPS injection but decreased cytokine release following 3 x LPS or 4 x LPS injection, indicating that different times of LPS injection induce distinct immune responses (1 x LPS: *immune priming*; 2 x LPS: *immune training*; 3 x or 4 x LPS, *immune tolerance*) (Püntener et al., 2012; Wendeln et al., 2018). However, in our rat models, brain cytokine levels were significantly increased in 1xLPS and decreased in 2 x LPS and 4 x LPS, indicating that repeated immune stimulation (2 x LPS or 4 x LPS) only induced immune tolerance in the brain. Although there was a modest increase in KC/GRO levels in the blood and brain of the 2 x LPS group compared to the 1 x LPS group in the BAC HD model, it was not statistically significant and required further validation with more samples. These indicate that the rat immune system differs in its response to the same LPS dose, and dose-response experiments may have to be performed to trigger the classical priming-training and desensitizing-tolerance paradigms.

Nevertheless, at the level of transcriptomic responses, the 1 x, and 4 x LPS stimuli resulted in clearly distinguishable molecular microglial phenotypes. In particular, acute microglial immune

responses were not significantly different between transgenic (BAC SNCA or BAC HD) rats and wild-type animals in PD and HD 3-month cohorts, suggesting that microglial responses are comparable across genotypes at the pre-pathological stage. Combining our WGCNA results and the summary table of enrichment analysis (**Table 1**), we found that different amounts of LPS injections induced different microglia phenotypes, which have been described in previous studies (Schaafsma et al., 2015; Wendeln et al., 2018; Zhang et al., 2021). For example, in 1 x LPS of wildtype or transgenic rats, primed microglia showed upregulation of inflammation-related genes (*Ilb, Tnf, Rela*), inflammatory signalling pathways (NOD, NFκB, TNF, and Toll-like receptor signalling pathways) as well as phagocytic signalling pathways, while in 2 x LPS, microglia showed downregulation of these genes and related signalling pathways. These results were also consistent with brain cytokine levels (IL-1β, TNF-α) in the 1 x LPS and 2 x LPS groups. Thus, in our study, a single injection of LPS may have induced microglial immune training, whereas repeated injections of LPS (2 x LPS and 4 x LPS) induced immune tolerance.

In addition to the previously used LPS stimuli, we also investigated the microglial responses to high fat or "Western" diet (HFD). Recently, Christ et al. reported elevated circulating levels of many cytokines after 4 weeks of Western diet feeding in mice (Christ et al., 2018). However, in our dataset, in the 3-month cohort of rats receiving a 30-day HFD, the blood level of IFN-γ was in fact decreased compared to rats on a standard diet (SD), and no significant changes in brain cytokines were found. In transcriptome analysis, only very few differentially expressed genes were found when comparing rats on SD to those on HFD, either by differential gene expression analysis or co-expression analysis (WGCNA). These results suggested that a short-term high-fat diet (30 days) did not induce conspicuous immune responses in the periphery or in microglia in our rat models. While it is also possible that we did not observe small scale changes, in principle, our gene expression analysis detected a large number of genes even at low expression levels.

Previous studies have shown that pathogen type, dosage and duration of exposure can establish distinct innate immune memory states in microglia (Lajqi et al., 2019; Püntener et al., 2012; Schaafsma et al., 2015; Wendeln et al., 2018; Zhang et al., 2021). Another study showed that the interval between challenges is also crucial for the innate immune memory state of microglia (Heng et al., 2021). Comparing our results in rat models with previous studies in mice suggests that species may also play an important role in the development of microglial innate immune

memory. For example, the same dose of LPS (i.p, 0.5mg/kg) administered intraperitoneally for two consecutive days (2 x LPS) elicited microglial immune training in mice (Schaafsma et al., 2015; Wendeln et al., 2018) but microglial immune tolerance in our rat models. Additionally, in separate research, microglial immune tolerance was observed in mice with 2 x LPS (i.p, 1mg/kg) within a 1-month interval (Zhang et al., 2021). Similarly, a previous study in mice and our study on rats used similar high-fat diets, but rats did not show significant alterations in cytokine levels in the brain and periphery. In other words, the same stimulation or previous inflammatory experience may activate distinct microglial immune programs in different species. Therefore, it is critical to evaluate not only the presence of innate immune memory in microglia but also to determine the distinct immune programs triggered by various stimuli.

4.2 Innate immune memory effects in models of Parkinson's and Huntington's disease

Our cytokine data suggested that microglial innate immune memory triggered by peripheral stimulation may persist over time in both rat models, which was also observed in the lab's original study on mice (Wendeln et al., 2018). In the current work, six months after the first peripheral insults (1 x LPS, 4 x LPS), innate immune memory effects were still apparent for some cytokines in the serum and brain of wild-type rats. Moreover, some cytokines (IL-13, TNF-α) in wild-type and BAC HD rats showed significant differences between the 1 x LPS and 4 x LPS groups, indicating that distinct immune memory states may be triggered by these immune stimuli. Previous studies also reported increased pro-inflammatory cytokines in serum and cerebrospinal fluid (CSF) in PD patients (King and Thomas, 2017). Similarly, in the plasma and CSF of HD patients, the levels of IL-6, IL-8 and tumour necrosis factor (TNF)-α were found to be elevated, showing a state of immune activation (Björkqvist et al., 2008). However, in the experimental control groups of our rats (receiving PBS injections), no significant changes in brain cytokine levels were found in either BAC SNCA or BAC HD rats compared to WT rats. Additionally, the impact of pathology as a secondary stimulus synergising with past inflammatory events (immune memory triggered at 3 months of age) was not evident at the cytokine level. This may be due to the 9-month-old rat models, which are at an early stage of pathology for PD or HD, or because pathology-related responses on immune memory are evident in other cytokines that we did not detect. However, another exciting possibility is that increased cytokine levels in PD and HD patients may reflect

immune exposures in the past and therefore immune memory states in the periphery (as evident in our peripherally stimulated animals), supporting the hypothesis that infections or inflammatory diseases throughout the lifespan may contribute to the risk to develop neurodegenerative diseases.

Similar to the analysis of acute immune responses at 3 months of age, I also examined long-term changes in gene expression in microglia isolated from 9-month-old wild-type (WT), BAC SNCA, and BAC HD animals. In the 9-month cohort (WT vs BAC SNCA or HD), there were differences in gene co-expression levels between the control group (PBS), suggesting that pathology associated with PD (α-synuclein) or HD (Htt) by itself led to alterations of the microglia phenotype. Moreover, there were also pronounced differences in microglial gene co-expression modules between different treatment groups (1 x LPS, 4 x LPS, HFD) when comparing microglia from animals of the same genotype, suggesting that pathology-related responses of microglia were differentially altered by peripheral immune stimulation triggered 6 months earlier.

BAC SCNA rats develop insoluble full-length α-synuclein aggregates in all brain regions with age (Nuber et al., 2013). Interestingly, previous studies have shown that the inflammatory response of microglia is involved in the degeneration of dopaminergic neurons in PD (Mosley et al., 2012; Stone et al., 2009). That is, chronic immune activation of microglia may directly contribute to neuronal degeneration. For example, it has been demonstrated that aggregation of α-synuclein, in addition to inducing neuronal toxicity, can lead to a pro-inflammatory response in the brain parenchyma by triggering microglial activation, which may exacerbate the pathogenic process of PD (Daniele et al., 2015). Interestingly, in our study, in the 9-month PD model cohort (WT vs BAC SNCA), functional analysis of co-expressed genes revealed that pathology-associated microglial phenotypes were upregulating genes involved in the unfolded protein response (UPR). Similarly, in KEGG and GO enrichment analysis, differentially expressed genes in pathology-related modules were also enriched in antigen processing and presentation, protein processing in the endoplasmic reticulum and protein folding. The unfolded protein response has been demonstrated to be involved in cellular models of PD (Ryu et al., 2002), and in PD patients, activation of the UPR is strongly associated with the accumulation and aggregation of α-synuclein (Hoozemans et al., 2007), but has so far not been demonstrated in microglial cells.

In addition, modifications of microglial phenotypes due to immune memory (triggered by peripheral immune stimulation 6 months earlier) were also evident at the transcriptomic level. It is important to note that at the pre-pathological stage, microglial responses were comparable across all genotypes, indicating that the different immune memory states were triggered by equivalent initial immune responses. In particular, with the development of α-synuclein pathology, microglial responses (at transcriptome level) differed significantly between wildtype and BAC SNCA rats, confirming that α-synuclein pathology can act as the secondary immune stimulus and thereby reveal innate immune memory states. For example, in 4 x LPS-treated BAC SNCA rats, microglia showed upregulation of genes within the Parkinson's disease pathway, metabolic pathways (such as oxidative phosphorylation, citrate/TCA cycle) as well as lysosome functions, whereas inflammation-related pathways (such as NOD-like receptor signalling pathway and TNF signalling pathway) were down-regulated. Moreover, some co-expressed gene modules in BAC SNCA rats were differentially regulated by 1 x LPS and 4 x LPS, including the purple, magenta, and yellow modules (**Figure 9. C**). These modules were mainly enriched for genes involved in pathways such as oxidative phosphorylation, Fc-γ receptor-mediated phagocytosis, and GO terms such as metabolic processes and transmembrane transport.

It is well known that microglia perform diverse cellular functions in neurodegenerative disease, including phagocytosis and clearance of abnormal proteins (amyloid β, α-synuclein and others) and maintaining homeostasis in the central nervous system (Prinz et al., 2017, 2019, 2021; Wake et al., 2013). These immune functions have a high energy demand, which can be regulated by mitochondria. Many pieces of evidence also have demonstrated that mitochondrial dysfunction is a hallmark of neurodegenerative diseases (Lin and Beal, 2006; Weydt et al., 2006). Moreover, mitochondrial dysfunction in microglia has been described in several animal models of neurodegeneration (AD (Flannery and Trushina, 2019), PD (Sarkar et al., 2017), HD (Weydt et al., 2006)), and the connection with neuroinflammation is a sophisticated and dynamic process (Lin et al., 2022). In our work, most of the affected metabolic pathways are associated with mitochondria, suggesting that different microglial innate immune memory states may influence the development of PD pathology by regulating mitochondrial function. It will be very important to define the relationship between these changes in microglial metabolism and pathological outcomes by evaluating pathological hallmarks in the different treatment groups.

In the 9-month HD model cohort (WT vs BAC HD), KEGG and GO enrichment analysis showed that microglia from BAC HD animals had higher oxidative phosphorylation and higher mitophagy but lower glycolysis. Moreover, microglia from BAC HD rats had lower DNA replication, lower endocytosis, and all inflammatory pathways (NOD, Toll, chemokines), as well as endocytosis pathways, were also expressed at lower levels. Those results suggest that the development of huntingtin pathology in the BAC HD model may be related to altered mitochondrial function and immune suppression in microglia, as indicated in a recent publication (Lin et al., 2022). Similar to the BAC SNCA 9m cohort, pathology-related responses of microglia were modulated by innate immune memory states in BAC HD animals. Compared to microglial transcriptome data from PBS-treated animals, metabolic and inflammation-related genes and pathways were downregulated in the 1 x LPS-treated BAC HD rats, indicating that the microglial immune response to Htt pathology was modulated by the initial LPS treatment. While this modulation is in principle, consistent with the concept of innate immune memory (Neher and Cunningham, 2019; Netea et al., 2015; Saeed et al., 2014; Wendeln et al., 2018), the downregulation of inflammation-related pathways rather indicates immune tolerance, not immune training as observed in the original study in mice in response to a single LPS dose (Wendeln et al., 2018). This is in line with the observed microglial acute immune response (3-month cohort) in our rat models, where a single LPS injection (i.p, 1 x LPS) may have been sufficient to evoke a desensitised state of microglia, followed by subsequent induction of immune tolerance by a secondary stimulus (i.e., a second LPS dose or brain pathology). In the black and red co-expression gene modules **(Figure 16. C)**, although 4 x LPS did not show a strong correlation or significant P-values, regulation of gene expression was opposite to 1 x LPS treatment, indicating that these two gene co-expression modules are differentially regulated by 1 x LPS and 4 x LPS in BAC HD rats. The genes in these modules are mainly enriched in phagocytosis (antigen processing and presentation, phagosome, endocytosis) and inflammation-related pathways and GO terms (NOD-like, Toll-like receptor signalling pathways), suggesting that different microglial innate immune memory states could affect the development of HD pathology by regulating these microglial functions. It is well established that microglial phagocytosis can modulate neurodegenerative disease pathogenesis and that its role is two-sided (Butler et al., 2021), i.e., phagocytosis may be beneficial by removing debris and protein aggregates (Galloway et al., 2019; Janda et al., 2018; Napoli and Neumann, 2009; Neher et al., 2011; Wolf et al., 2017), but may also be detrimental by removing synapses

and neurons in vivo (Brown and Neher, 2012, 2014; Rajendran and Paolicelli, 2018; Vilalta and Brown, 2018). Furthermore, microglial phagocytosis is closely related to both neuronal and microglial cell states, since different microglial states exhibit varying phagocytic capacity, while different neuronal states exhibit different phagocytic signals (Butler et al., 2021). Similarly, neuroinflammation has a dual function in neurodegenerative diseases (Kwon and Koh, 2020), as it may either protect the brain by removing or suppressing various pathogens (Russo and McGavern, 2016; Wyss-Coray and Mucke, 2002), or it might result in a persistent or amplified inflammatory response, exacerbating the severity of the disease (Glass et al., 2010; Kempuraj et al., 2016; Stephenson et al., 2018).

Thus, in my PhD work, 1 x LPS and 4 x LPS induced innate immune memory may have beneficial or detrimental effects on HD (as well as PD) pathology. My results confirm the capacity of microglia for innate immune memory and show for the first time that immune memory states are dependent both on the initial stimulus and secondary pathology, as shown by different sets of pathways being regulated by the same primary stimuli in models of PD and HD. The precise mechanisms of such regulation are likely dependent on epigenetic modifications in microglia, leading to enhanced or reduced chromatin accessibility. Such changes, combined with the activation of different sets of transcription factors by PD and HD pathology, are likely to result in the observed patterns of innate immune memory states and warrant further investigation. Overall, the results presented here are consistent with data from the original study by Wendeln et al. demonstrating the regulation of molecular microglial phenotypes at the transcriptomic level (Wendeln et al., 2018). Wendeln et al. also found that training promotes, while tolerance alleviates AD neuropathology, and whether the different immune memory states in microglia affect pathological hallmarks in our models of PD and HD needs to be further investigated.

4.3 Microglial heterogeneity in models of PD and HD

Developments in single-cell transcriptome technology have increased our understanding of micro glial heterogeneity across physiological and pathological processes, revealing that microglia in th e brain exhibit distinct microglial states (subpopulations) at various developmental stages, anato mical regions, and pathological conditions (Chen and Colonna, 2021; Geirsdottir et al., 2019; Ha mmond et al., 2019; Jordão et al., 2019; Masuda et al., 2020; Prater et al., 2021). Our bulk RNA-

seq data also demonstrated alterations in microglial gene expression and function in the PD and HD model in the absence of peripheral immune stimuli, i.e., when comparing microglia from con trol WT and transgenic animal cohorts. However, our bulk RNA-seq data showed relatively mino r gene expression changes in microglia in response to HD and PD pathology alone. One possible explanation of these minor changes would be that they are driven by a limited number of activate d microglia, such as a single or a few microglial subpopulations reacting to brain pathology and, t herefore, when analysing microglia in bulk, effects may be "diluted" across the whole microglial population. Thus, in order to gain a better understanding of the role of microglia in Parkinson's di sease (PD) and Huntington's disease (HD), we used single-cell RNA sequencing to profile the mi croglial transcriptome comprehensively and to investigate the microglial cell subtypes associated with PD or HD pathology.

A number of single-cell analyses have now revealed microglial heterogeneity in the brain across different conditions (Ellwanger et al., 2021; Friedman et al., 2018; Hammond et al., 2019; Keren-Shaul et al., 2017; Krasemann et al., 2017; Li et al., 2019; Mathys et al., 2017; Safaiyan et al., 2021; Sala Frigerio et al., 2019; Wang et al., 2020b; Zhou et al., 2020), especially in AD. But few single-cell studies have focused on different microglial phenotypes in PD and HD disease. Our single-cell RNA-sequencing approach now assessed microglial heterogeneity in the early stage of the PD and HD disease model (9-month-old rats). Contrary to our expectation, no pathology-specific microglial subpopulation was observed in BAC HD or BAC SNCA rats. This might be because the time point of analysis (9-month) corresponds to an early stage of pathological development with a minor influence on the transcriptome, as also shown by our bulk RNA-seq data. Alternatively, it is conceivable that while extracellular amyloid-β plaques in AD trigger strong immune responses in microglia, protein aggregates in PD and HD that are largely intracellular, result only in subtle microglial changes, possibly due to neuronal signals rather than the aggregates themselves.

However, despite the absence of distinct pathology-associated phenotypes in the PD and HD models, I observed a shift in the proportion of microglia in BAC SNCA and BAC HD in cluster 0 (HM) and cluster 4 (ARM) compared to microglia in wild-type animals. Therefore, these two microglial subpopulations may play an important role in the early pathological stages of PD and HD rat models. Single-cell analysis of microglia in AD patients (Brase et al., 2021; Del-

Aguila et al., 2019; Gerrits et al., 2021; Lau et al., 2020; Mathys et al., 2019; Nguyen et al., 2020 ; Zhou et al., 2020) and AD mouse models (Ellwanger et al., 2021; Keren-Shaul et al., 2017; Lee et al., 2021; Mathys et al., 2017; Mrdjen et al., 2018; Sala Frigerio et al., 2019; Sierksma et al., 2020; Zhou et al., 2020) originally described the DAM and ARM subtypes, where DAM showed downregulation of microglial homeostatic genes such as *P2ry12/P2ry13*, *Cx3cr1*, and *Tmem119*, while ARM showed upregulation of genes such as Cd74, H2-Ab1, and HLA-DRB1. However, upregulation of homeostatic genes such as *P2ry12* and *Cx3cr1* were also found in a separate study in AD patients (Zhou et al., 2020). These results are consistent with some of my results on the PD and HD rat models. Compared to wild-type rats, our results also revealed alterations of cell proportion in the ARM cluster in both models, and *P2ry12* was downregulated in microglial from BAC HD but upregulated in microglia from BAC SNCA rats in most clusters (**Figure 24. A**). A recent study of human tissue revealed that *P2ry12* may be a genetic risk factor for PD, with gene expression being downregulated in microglia (Lopes et al., 2022). It is well known that *P2ry12* is a key receptor in microglia-microenvironment interactions, and its importance for microglial function has been described in many publications (Badimon et al., 2020; Gómez Morillas et al., 2021). These results indicate that brain ageing or certain age-associated brain pathologies may be affected by the regulation of the *P2ry12* expression in microglia. However, this needs to be validated by more studies and larger sample sizes. Notably, compared to wild type and BAC HD rats, *Ldhb* was significantly downregulated across the clusters in BAC SNCA rats (**Figure 24. B**). Interestingly, decreased mRNA levels of *Ldhb* also have been found in blood cells from patients with early PD (Smith et al., 2018), and another very recent mouse study showed that LDHB deficiency could cause oxidative stress and neurodegeneration-associated mitochondrial dysfunction (Park et al., 2022). These results indicate that *Ldhb* and associated mitochondrial dysfunction may play a vital role in the early pathogenesis of PD.

To better understand their function, differential gene expression analysis of marker genes was performed between the different genotypes within the clusters, followed by KEGG enrichment analysis. The results indicated that microglia from BAC SNCA showed upregulation of metabolic pathways, whereas microglia from BAC HD showed downregulation of inflammatory pathways (**Table 3**). In both models, phagocytosis-related pathways were also affected, and distinct effects were found for lysosome function, being increased in BAC SNCA rats but decreased in BAC HD

rats, which is consistent with the regulation of gene expression of the lysosomal gene *Ctss* at single cell level (**Figure 24. C**). These findings suggest that, while PD and HD are both neurodegenerative diseases characterised by motor disorders, the pathological development of PD may be more closely associated with microglial metabolic dysregulation, whereas the pathological development of HD may be more closely associated with inflammatory responses during the early pathological stages. Additionally, the *Htt* gene expression was considerably increased in cluster 2 of BAC HD rats, indicating that cluster 2 may be a microglial subpopulation involved in the development of HD. This finding indicates that a microglial subpopulation with high mHTT expression exists in the early stages of our HD rat model, and this subpopulation may drive the development of HD pathology, which supports the hypothesis that cell-autonomous dysfunction of microglia plays an important role in the pathogenesis of HD (Palpagama et al., 2019; Yang et al., 2017). While these experiments indicate that microglia show distinct phenotypes in the early stages of PD and HD, future work will need to define how exactly these transcriptomic changes affect microglial functions, whether specific microglial subpopulations are associated with pathological hallmarks, and how these microglia impact disease.

4.4 Conclusion, Study Limitations and Outlook

When combined with previous studies, the work of my PhD thesis supports the existence of innate immune memory in microglia across a variety of disease models and species and extends the concept to HD and PD pathology. My results therefore indicate that microglial innate immune memory could impact on diverse neurological diseases in humans, but the same stimulus or inflammatory experience may induce distinct microglia immune programs in different species. Therefore, it will be crucial to identify the various microglial immune memory states induced by distinct stimuli and to define their role in the pathogenesis and development of neurodegenerative diseases. Moreover, distinct microglia innate immune memory states may have beneficial or detrimental effects on PD and HD pathology, and how the observed alterations in microglial responses affect pathology in these models will be a crucial next step in this project. This should involve detailed histological as well as biochemical characterisation of α-synuclein and huntingtin aggregates.

Although my thesis presented and validated some of the hypotheses in the field of microglial innate immune memory and microglial heterogeneity, some limitations of this study were also recognised. First, the sample sizes of cytokine measurements and single-cell RNA-seq were small, particularly for the 3-month cohort (**Figure 3. A, C**; **Figure 4. A, C**). Larger sample sizes would not only improve the strength of statistical tests but also confirm whether the extreme values are outliers or have biological effects, e.g., **Figure 3. C, D** and **Figure 4. C**. Second, I presented the cytokine and microglia transcriptome data for the HFD group, but I did not discuss them in depth because too few samples met quality criteria within several HFD groups before data processing (Figure 16. n=2 in HFD wildtype and BAC HD). Therefore, the sample size was insufficient for analysis and discussion. We have replicated and re-sequenced the low-quality samples, and these data have been successfully integrated into the full data set but currently awaiting analysis. Third, some potential confounding factors are still present in our experiments and data, such as inaccurate time of LPS injections (exact to the hour) due to the huge animal cohorts, different batches of microglia isolation, RNA isolation, library preparation and sequencing. Although I have corrected the unknown batch effects, unknown confounders could still affect the gene expression results presented here. Fourth, regarding the mechanisms of innate immune memory, analysis of the epigenetic profiles of microglia may provide further insights into the molecular processes that drive microglial responses. In fact, samples for these analyses were collected as part of my project, but their analysis was not completed yet. It will complement the data presented here by revealing if epigenetic modification of the same molecular pathways could mediate the observed changes in gene transcription. Fifth, while my PhD thesis presents a comprehensive analysis of microglial transcriptomes, validation of selected genes and pathways (for example, through in situ hybridisation or using immunohistochemistry) need to be performed not only to exclude the possibility of experimental artefacts but also to examine the anatomical location of microglia with altered gene expression profiles. In particular, the relationship of microglia that show altered gene expression with neurons bearing α-synuclein or huntingtin aggregates would be of high interest, also with regards to the signals that may be inducing microglial responses in these rat models. In addition, I identified some potential key genes in the modules with WGCNA and ranked their importance in the pathways, but these hub genes need to be validated with different methods such as machine learning (Farhadian et al., 2021), different algorithms from the plugins of Cytoscape (Chin et al., 2014) or through functional inactivation (e.g. through knockout studies).

In future work, single-cell RNA-seq and single nuclei RNA-seq should also be used to gain more insight into microglial heterogeneity and how microglia respond to various stimuli in different diseases or stages of the disease. Such studies should include the characterisation of microglial phenotypes at different stages of disease pathology to examine how the microglial response may change over time (as only a very early stage of pathology was analysed here). Moreover, future studies should include comparisons with microglial profiles in human tissue (which can be analysed by single nucleus sequencing) to establish whether results from animal models are transferable to patients. Such studies may help us understand the microglial role in the pathogenesis of distinct neurodegenerative diseases and provide directions for their therapy.

Statement of my contribution

In principle, the work presented in this project was assisted by Ms. Reema Chowdhury, but as most animal experiments were conducted in our laboratory and animal facility (and because Ms. Chowdhury is not qualified to work with animals), I was primarily responsible for the management and the animal experiments of this project. In detail, specific tasks were performed as outlined below:

Experimental design: by Dr. Jonas Neher and Dr. Julia Schulze-Hentrich.

Animal treatment and caretaking: Reema Chowdhury (under my supervision) and I were in charge of all the animals together, including weighing, HFD feeding, animal fixation (me) and injections (Reema).

Genotyping: I performed genotyping for BAC HD 9m cohort, other cohorts were genotyped by Reema Chowdhury.

Tissue collection: I performed the animal anaesthesia, sacrifice and brain isolation with assistance from Katleen Wild.

Microglia isolation: Reema did the brain homogenisation, and I performed the microglial isolation procedure, including FACS sorting, with some assistance from Reema Chowdhury.

RNA isolation: I isolated RNA for all the samples, including quality control.

cDNA library preparation and sequencing (bulk and single RNA-seq): Bulk RNA-seq was performed by Jessica Cielenga and scRNA-seq was done by Dr. Yogesh Singh from NGS Competence Centre Tübingen (NCCT).

ELISA: I did the sample preparation and Marius Lambert measured them with Mesoscale Discovery.

Data processing: Quality control, mapping and alignment were done by Dr. Thomas Hentrich from the Institute of Medical Genetics and Applied Genomics for bulk RNA-seq and scRNA-seq.

Data analysis: Data integration and clustering of scRNA-seq were performed by Desirée Brösamle from our lab. All other extensive analyses presented here were done by me (including cytokine, WGCNA, enrichment analysis, etc.).

List of Figures

List of Tables

Bibliography

Akira, S., Uematsu, S., and Takeuchi, O. (2006). Pathogen recognition and innate immunity. Cell *124*, 783–801.

Alam, M., and Schmidt, W.J. (2002). Rotenone destroys dopaminergic neurons and induces parkinsonian symptoms in rats. Behav. Brain Res. *136*, 317–324.

Alegre-Abarrategui, J., Christian, H., Lufino, M.M.P., Mutihac, R., Venda, L.L., Ansorge, O., and Wade-Martins, R. (2009). LRRK2 regulates autophagic activity and localizes to specific membrane microdomains in a novel human genomic reporter cellular model. Hum. Mol. Genet. *18*, 4022–4034.

Amor, S., McNamara, N.B., Gerrits, E., Marzin, M.C., Kooistra, S.M., Miron, V.E., and Nutma, E. (2022). White matter microglia heterogeneity in the CNS. Acta Neuropathol. *143*, 125–141.

Aran, D., Looney, A.P., Liu, L., Wu, E., Fong, V., Hsu, A., Chak, S., Naikawadi, R.P., Wolters, P.J., Abate, A.R., et al. (2019). Reference-based analysis of lung single-cell sequencing reveals a transitional profibrotic macrophage. Nat. Immunol. *20*, 163–172.

Askew, K., Li, K., Olmos-Alonso, A., Garcia-Moreno, F., Liang, Y., Richardson, P., Tipton, T., Chapman, M.A., Riecken, K., Beccari, S., et al. (2017). Coupled proliferation and apoptosis maintain the rapid turnover of microglia in the adult brain. Cell Rep. *18*, 391–405.

Ayata, P., Badimon, A., Strasburger, H.J., Duff, M.K., Montgomery, S.E., Loh, Y.-H.E., Ebert, A., Pimenova, A.A., Ramirez, B.R., Chan, A.T., et al. (2018). Epigenetic regulation of brain region-specific microglia clearance activity. Nat. Neurosci. *21*, 1049–1060.

Badimon, A., Strasburger, H.J., Ayata, P., Chen, X., Nair, A., Ikegami, A., Hwang, P., Chan, A.T., Graves, S.M., Uweru, J.O., et al. (2020). Negative feedback control of neuronal activity by microglia. Nature *586*, 417–423.

Bates, G.P. (2005). History of genetic disease: the molecular genetics of Huntington disease - a history. Nat. Rev. Genet. *6*, 766–773.

Bates, G.P., Dorsey, R., Gusella, J.F., Hayden, M.R., Kay, C., Leavitt, B.R., Nance, M., Ross, C.A., Scahill, R.I., Wetzel, R., et al. (2015). Huntington disease. Nat. Rev. Dis. Primers *1*, 15005.

Bennett, E.J., Shaler, T.A., Woodman, B., Ryu, K.-Y., Zaitseva, T.S., Becker, C.H., Bates, G.P., Schulman, H., and Kopito, R.R. (2007). Global changes to the ubiquitin system in Huntington's disease. Nature *448*, 704–708.

Benraiss, A., Wang, S., Herrlinger, S., Li, X., Chandler-Militello, D., Mauceri, J., Burm, H.B., Toner, M., Osipovitch, M., Jim Xu, Q., et al. (2016). Human glia can both induce and rescue aspects of disease phenotype in Huntington disease. Nat. Commun. *7*, 11758.

Benskey, M.J., Perez, R.G., and Manfredsson, F.P. (2016). The contribution of alpha synuclein to neuronal survival and function - Implications for Parkinson's disease. J. Neurochem. *137*, 331–359.

Berger, Z., Smith, K.A., and Lavoie, M.J. (2010). Membrane localization of LRRK2 is associated with increased formation of the highly active LRRK2 dimer and changes in its phosphorylation. Biochemistry *49*, 5511–5523.

Berwick, D.C., Heaton, G.R., Azeggagh, S., and Harvey, K. (2019). LRRK2 Biology from structure to dysfunction: research progresses, but the themes remain the same. Mol. Neurodegener. *14*, 49.

Biskup, S., Moore, D.J., Celsi, F., Higashi, S., West, A.B., Andrabi, S.A., Kurkinen, K., Yu, S.-W., Savitt, J.M., Waldvogel, H.J., et al. (2006). Localization of LRRK2 to membranous and vesicular structures in mammalian brain. Ann. Neurol. *60*, 557–569.

Bistoni, F., Vecchiarelli, A., Cenci, E., Puccetti, P., Marconi, P., and Cassone, A. (1986). Evidence for macrophage-mediated protection against lethal Candida albicans infection. Infect. Immun. *51*, 668–674.

Björkqvist, M., Wild, E.J., Thiele, J., Silvestroni, A., Andre, R., Lahiri, N., Raibon, E., Lee, R.V., Benn, C.L., Soulet, D., et al. (2008). A novel pathogenic pathway of immune activation detectable before clinical onset in Huntington's disease. J. Exp. Med. *205*, 1869–1877.

Boka, G., Anglade, P., Wallach, D., Javoy-Agid, F., Agid, Y., and Hirsch, E.C. (1994). Immunocytochemical analysis of tumor necrosis factor and its receptors in Parkinson's disease. Neurosci. Lett. *172*, 151–154.

Bowdish, D.M.E., Loffredo, M.S., Mukhopadhyay, S., Mantovani, A., and Gordon, S. (2007). Macrophage receptors implicated in the "adaptive" form of innate immunity. Microbes Infect. *9*, 1680–1687.

Brase, L., You, S.-F., Del-Aguila, J.L., Dai, Y., Novotny, B.C., Sariano-Tarraga, C., Dykstra, T., Fernandez, M.V., Budde, J.P., Bergmann, K., et al. (2021). A landscape of the genetic and cellular heterogeneity in Alzheimer disease. MedRxiv.

Brockmann, K., Apel, A., Schulte, C., Schneiderhan-Marra, N., Pont-Sunyer, C., Vilas, D., Ruiz-Martinez, J., Langkamp, M., Corvol, J.-C., Cormier, F., et al. (2016). Inflammatory profile in LRRK2-associated prodromal and clinical PD. J. Neuroinflammation *13*, 122.

Brockmann, K., Schulte, C., Schneiderhan-Marra, N., Apel, A., Pont-Sunyer, C., Vilas, D., Ruiz-Martinez, J., Langkamp, M., Corvol, J.C., Cormier, F., et al. (2017). Inflammatory profile discriminates clinical subtypes in LRRK2-associated Parkinson's disease. Eur. J. Neurol. *24*, 427-e6.

Brown, G.C., and Neher, J.J. (2012). Eaten alive! Cell death by primary phagocytosis: “phagoptosis”. Trends Biochem. Sci. *37*, 325–332.

Brown, G.C., and Neher, J.J. (2014). Microglial phagocytosis of live neurons. Nat. Rev. Neurosci. *15*, 209–216.

Bruttger, J., Karram, K., Wörtge, S., Regen, T., Marini, F., Hoppmann, N., Klein, M., Blank, T., Yona, S., Wolf, Y., et al. (2015). Genetic Cell Ablation Reveals Clusters of Local Self-Renewing Microglia in the Mammalian Central Nervous System. Immunity *43*, 92–106.

Butler, C.A., Popescu, A.S., Kitchener, E.J.A., Allendorf, D.H., Puigdellívol, M., and Brown, G.C. (2021). Microglial phagocytosis of neurons in neurodegeneration, and its regulation. J. Neurochem. *158*, 621–639.

Butovsky, O., Jedrychowski, M.P., Moore, C.S., Cialic, R., Lanser, A.J., Gabriely, G., Koeglsperger, T., Dake, B., Wu, P.M., Doykan, C.E., et al. (2014). Identification of a unique TGF-β-dependent molecular and functional signature in microglia. Nat. Neurosci. *17*, 131–143.

Carlson, M., Falcon, S., Pages, H., and Li, N. (2019). org. Hs. eg. db: Genome wide annotation for Human. R Package Version *3*.

Chang, D., Nalls, M.A., Hallgrímsdóttir, I.B., Hunkapiller, J., van der Brug, M., Cai, F., International Parkinson’s Disease Genomics Consortium, 23andMe Research Team, Kerchner, G.A., Ayalon, G., et al. (2017). A meta-analysis of genome-wide association studies identifies 17 new Parkinson’s disease risk loci. Nat. Genet. *49*, 1511–1516.

Chen, Y., and Colonna, M. (2021). Microglia in Alzheimer’s disease at single-cell level. Are there common patterns in humans and mice? J. Exp. Med. *218*.

Chin, C.-H., Chen, S.-H., Wu, H.-H., Ho, C.-W., Ko, M.-T., and Lin, C.-Y. (2014). cytoHubba: identifying hub objects and sub-networks from complex interactome. BMC Syst. Biol. *8 Suppl 4*, S11.

Christ, A., Günther, P., Lauterbach, M.A.R., Duewell, P., Biswas, D., Pelka, K., Scholz, C.J., Oosting, M., Haendler, K., Baßler, K., et al. (2018). Western Diet Triggers NLRP3-Dependent Innate Immune Reprogramming. Cell *172*, 162-175.e14.

Colonna, M., and Butovsky, O. (2017). Microglia function in the central nervous system during health and neurodegeneration. Annu. Rev. Immunol. *35*, 441–468.

Conrath, U., Beckers, G.J.M., Langenbach, C.J.G., and Jaskiewicz, M.R. (2015). Priming for enhanced defense. Annu. Rev. Phytopathol. *53*, 97–119.

Cookson, M.R. (2015). LRRK2 pathways leading to neurodegeneration. Curr. Neurol. Neurosci. Rep. *15*, 42.

Cremades, N., Chen, S.W., and Dobson, C.M. (2017). Structural Characteristics of α-Synuclein Oligomers. Int. Rev. Cell Mol. Biol. *329*, 79–143.

Creus-Muncunill, J., and Ehrlich, M.E. (2019). Cell-Autonomous and Non-cell-Autonomous Pathogenic Mechanisms in Huntington's Disease: Insights from In Vitro and In Vivo Models. Neurotherapeutics *16*, 957–978.

Croisier, E., Moran, L.B., Dexter, D.T., Pearce, R.K.B., and Graeber, M.B. (2005). Microglial inflammation in the parkinsonian substantia nigra: relationship to alpha-synuclein deposition. J. Neuroinflammation *2*, 14.

Crotti, A., Benner, C., Kerman, B.E., Gosselin, D., Lagier-Tourenne, C., Zuccato, C., Cattaneo, E., Gage, F.H., Cleveland, D.W., and Glass, C.K. (2014). Mutant Huntingtin promotes autonomous microglia activation via myeloid lineage-determining factors. Nat. Neurosci. *17*, 513–521.

Dalrymple, A., Wild, E.J., Joubert, R., Sathasivam, K., Björkqvist, M., Petersén, A., Jackson, G.S., Isaacs, J.D., Kristiansen, M., Bates, G.P., et al. (2007). Proteomic profiling of plasma in Huntington's disease reveals neuroinflammatory activation and biomarker candidates. J. Proteome Res. *6*, 2833–2840.

Daniele, S.G., Béraud, D., Davenport, C., Cheng, K., Yin, H., and Maguire-Zeiss, K.A. (2015). Activation of MyD88-dependent TLR1/2 signaling by misfolded α-synuclein, a protein linked to neurodegenerative disorders. Sci. Signal. *8*, ra45.

Deczkowska, A., Keren-Shaul, H., Weiner, A., Colonna, M., Schwartz, M., and Amit, I. (2018). Disease-Associated Microglia: A Universal Immune Sensor of Neurodegeneration. Cell *173*, 1073–1081.

Del-Aguila, J.L., Li, Z., Dube, U., Mihindukulasuriya, K.A., Budde, J.P., Fernandez, M.V., Ibanez, L., Bradley, J., Wang, F., Bergmann, K., et al. (2019). A single-nuclei RNA sequencing study of Mendelian and sporadic AD in the human brain. Alzheimers Res Ther *11*, 71.

Deng, H., Wang, P., and Jankovic, J. (2018). The genetics of Parkinson disease. Ageing Res. Rev. *42*, 72–85.

De Biase, L.M., Schuebel, K.E., Fusfeld, Z.H., Jair, K., Hawes, I.A., Cimbro, R., Zhang, H.-Y., Liu, Q.-R., Shen, H., Xi, Z.-X., et al. (2017). Local Cues Establish and Maintain Region-Specific Phenotypes of Basal Ganglia Microglia. Neuron *95*, 341-356.e6.

Del Río-Hortega Bereciartu, J. (2020). Pío del Río-Hortega: The Revolution of Glia. Anat Rec (Hoboken) *303*, 1232–1241.

Dempsey, P.W., Vaidya, S.A., and Cheng, G. (2003). The art of war: Innate and adaptive immune responses. Cell. Mol. Life Sci. *60*, 2604–2621.

Devine, M.J., Gwinn, K., Singleton, A., and Hardy, J. (2011). Parkinson's disease and α-synuclein expression. Mov. Disord. *26*, 2160–2168.

Dickson, D.W. (2018). Neuropathology of Parkinson disease. Parkinsonism Relat. Disord. *46 Suppl 1*, S30–S33.

DiFiglia, M., Sapp, E., Chase, K.O., Davies, S.W., Bates, G.P., Vonsattel, J.P., and Aronin, N. (1997). Aggregation of huntingtin in neuronal intranuclear inclusions and dystrophic neurites in brain. Science *277*, 1990–1993.

Dobrovolskaia, M.A., and Vogel, S.N. (2002). Toll receptors, CD14, and macrophage activation and deactivation by LPS. Microbes Infect. *4*, 903–914.

Dorsey, E.R., Sherer, T., Okun, M.S., and Bloem, B.R. (2018). The emerging evidence of the parkinson pandemic. J Parkinsons Dis *8*, S3–S8.

Dzamko, N., Inesta-Vaquera, F., Zhang, J., Xie, C., Cai, H., Arthur, S., Tan, L., Choi, H., Gray, N., Cohen, P., et al. (2012). The IkappaB kinase family phosphorylates the Parkinson's disease kinase LRRK2 at Ser935 and Ser910 during Toll-like receptor signaling. PLoS ONE *7*, e39132.

Dzamko, N., Gysbers, A., Perera, G., Bahar, A., Shankar, A., Gao, J., Fu, Y., and Halliday, G.M. (2017). Toll-like receptor 2 is increased in neurons in Parkinson's disease brain and may contribute to alpha-synuclein pathology. Acta Neuropathol. *133*, 303–319.

Eggen, B.J.L., Raj, D., Hanisch, U.K., and Boddeke, H.W.G.M. (2013). Microglial phenotype and adaptation. J. Neuroimmune Pharmacol. *8*, 807–823.

Ellwanger, D.C., Wang, S., Brioschi, S., Shao, Z., Green, L., Case, R., Yoo, D., Weishuhn, D., Rathanaswami, P., Bradley, J., et al. (2021). Prior activation state shapes the microglia response to antihuman TREM2 in a mouse model of Alzheimer's disease. Proc Natl Acad Sci USA *118.*

Elmore, M.R.P., Najafi, A.R., Koike, M.A., Dagher, N.N., Spangenberg, E.E., Rice, R.A., Kitazawa, M., Matusow, B., Nguyen, H., West, B.L., et al. (2014). Colony-stimulating factor 1 receptor signaling is necessary for microglia viability, unmasking a microglia progenitor cell in the adult brain. Neuron *82*, 380–397.

Erny, D., Hrabě de Angelis, A.L., Jaitin, D., Wieghofer, P., Staszewski, O., David, E., Keren-Shaul, H., Mahlakoiv, T., Jakobshagen, K., Buch, T., et al. (2015). Host microbiota constantly control maturation and function of microglia in the CNS. Nat. Neurosci. *18*, 965–977.

Eschbach, J., and Danzer, K.M. (2014). α-Synuclein in Parkinson's disease: pathogenic function and translation into animal models. Neurodegener Dis *14*, 1–17.

Fan, H., and Cook, J.A. (2004). Molecular mechanisms of endotoxin tolerance. J. Endotoxin Res. *10*, 71–84.

Farhadian, M., Rafat, S.A., Panahi, B., and Mayack, C. (2021). Weighted gene co-expression network analysis identifies modules and functionally enriched pathways in the lactation process. Sci. Rep. *11*, 2367.

Flannery, P.J., and Trushina, E. (2019). Mitochondrial dynamics and transport in Alzheimer's disease. Mol. Cell. Neurosci. *98*, 109–120.

Foster, S.L., Hargreaves, D.C., and Medzhitov, R. (2007). Gene-specific control of inflammation by TLR-induced chromatin modifications. Nature *447*, 972–978.

Franciosi, S., Ryu, J.K., Shim, Y., Hill, A., Connolly, C., Hayden, M.R., McLarnon, J.G., and Leavitt, B.R. (2012). Age-dependent neurovascular abnormalities and altered microglial morphology in the YAC128 mouse model of Huntington disease. Neurobiol. Dis. *45*, 438–449.

Friedman, B.A., Srinivasan, K., Ayalon, G., Meilandt, W.J., Lin, H., Huntley, M.A., Cao, Y., Lee, S.-H., Haddick, P.C.G., Ngu, H., et al. (2018). Diverse brain myeloid expression profiles reveal distinct microglial activation states and aspects of alzheimer's disease not evident in mouse models. Cell Rep. *22*, 832–847.

Füger, P., Hefendehl, J.K., Veeraraghavalu, K., Wendeln, A.-C., Schlosser, C., Obermüller, U., Wegenast-Braun, B.M., Neher, J.J., Martus, P., Kohsaka, S., et al. (2017). Microglia turnover with aging and in an Alzheimer's model via long-term in vivo single-cell imaging. Nat. Neurosci. *20*, 1371–1376.

Galloway, D.A., Phillips, A.E.M., Owen, D.R.J., and Moore, C.S. (2019). Phagocytosis in the brain: homeostasis and disease. Front. Immunol. *10*, 790.

GBD 2016 Neurology Collaborators (2019). Global, regional, and national burden of neurological disorders, 1990-2016: a systematic analysis for the Global Burden of Disease Study 2016. Lancet Neurol. *18*, 459–480.

Geirsdottir, L., David, E., Keren-Shaul, H., Weiner, A., Bohlen, S.C., Neuber, J., Balic, A., Giladi, A., Sheban, F., Dutertre, C.-A., et al. (2019). Cross-Species Single-Cell Analysis Reveals Divergence of the Primate Microglia Program. Cell *179*, 1609-1622.e16.

Gerhard, A., Pavese, N., Hotton, G., Turkheimer, F., Es, M., Hammers, A., Eggert, K., Oertel, W., Banati, R.B., and Brooks, D.J. (2006). In vivo imaging of microglial activation with [11C](R)-PK11195 PET in idiopathic Parkinson's disease. Neurobiol. Dis. *21*, 404–412.

Gerrits, E., Brouwer, N., Kooistra, S.M., Woodbury, M.E., Vermeiren, Y., Lambourne, M., Mulder, J., Kummer, M., Möller, T., Biber, K., et al. (2021). Distinct amyloid-β and tau-associated microglia profiles in Alzheimer's disease. Acta Neuropathol. *141*, 681–696.

Ginhoux, F., and Guilliams, M. (2016). Tissue-Resident Macrophage Ontogeny and Homeostasis. Immunity *44*, 439–449.

Ginhoux, F., Greter, M., Leboeuf, M., Nandi, S., See, P., Gokhan, S., Mehler, M.F., Conway, S.J., Ng, L.G., Stanley, E.R., et al. (2010). Fate mapping analysis reveals that adult microglia derive from primitive macrophages. Science *330*, 841–845.

Glass, C.K., Saijo, K., Winner, B., Marchetto, M.C., and Gage, F.H. (2010). Mechanisms underlying inflammation in neurodegeneration. Cell *140*, 918–934.

Goetz, C.G. (2011). The history of Parkinson's disease: early clinical descriptions and neurological therapies. Cold Spring Harb. Perspect. Med. *1*, a008862.

Gomez-Nicola, D., and Perry, V.H. (2015). Microglial dynamics and role in the healthy and diseased brain: a paradigm of functional plasticity. Neuroscientist *21*, 169–184.

Gómez-Suaga, P., Luzón-Toro, B., Churamani, D., Zhang, L., Bloor-Young, D., Patel, S., Woodman, P.G., Churchill, G.C., and Hilfiker, S. (2012). Leucine-rich repeat kinase 2 regulates autophagy through a calcium-dependent pathway involving NAADP. Hum. Mol. Genet. *21*, 511–525.

Gómez Morillas, A., Besson, V.C., and Lerouet, D. (2021). Microglia and neuroinflammation: what place for P2RY12? Int. J. Mol. Sci. *22.*

Gourbal, B., Pinaud, S., Beckers, G.J.M., Van Der Meer, J.W.M., Conrath, U., and Netea, M.G. (2018). Innate immune memory: An evolutionary perspective. Immunol. Rev. *283*, 21–40.

Guneykaya, D., Ivanov, A., Hernandez, D.P., Haage, V., Wojtas, B., Meyer, N., Maricos, M., Jordan, P., Buonfiglioli, A., Gielniewski, B., et al. (2018). Transcriptional and Translational Differences of Microglia from Male and Female Brains. Cell Rep. *24*, 2773-2783.e6.

Hagemeyer, N., Hanft, K.-M., Akriditou, M.-A., Unger, N., Park, E.S., Stanley, E.R., Staszewski, O., Dimou, L., and Prinz, M. (2017). Microglia contribute to normal myelinogenesis and to oligodendrocyte progenitor maintenance during adulthood. Acta Neuropathol. *134*, 441–458.

Hammond, T.R., Dufort, C., Dissing-Olesen, L., Giera, S., Young, A., Wysoker, A., Walker, A.J., Gergits, F., Segel, M., Nemesh, J., et al. (2019). Single-Cell RNA Sequencing of Microglia throughout the Mouse Lifespan and in the Injured Brain Reveals Complex Cell-State Changes. Immunity *50*, 253-271.e6.

Hanamsagar, R., Alter, M.D., Block, C.S., Sullivan, H., Bolton, J.L., and Bilbo, S.D. (2017). Generation of a microglial developmental index in mice and in humans reveals a sex difference in maturation and immune reactivity. Glia *65*, 1504–1520.

Hanisch, U.-K., and Kettenmann, H. (2007). Microglia: active sensor and versatile effector cells in the normal and pathologic brain. Nat. Neurosci. *10*, 1387–1394.

Hao, Y., Hao, S., Andersen-Nissen, E., Mauck, W.M., Zheng, S., Butler, A., Lee, M.J., Wilk, A.J., Darby, C., Zager, M., et al. (2021). Integrated analysis of multimodal single-cell data. Cell *184*, 3573-3587.e29.

Hashimoto, D., Chow, A., Noizat, C., Teo, P., Beasley, M.B., Leboeuf, M., Becker, C.D., See, P., Price, J., Lucas, D., et al. (2013). Tissue-resident macrophages self-maintain locally throughout adult life with minimal contribution from circulating monocytes. Immunity *38*, 792–804.

Haynes, S.E., Hollopeter, G., Yang, G., Kurpius, D., Dailey, M.E., Gan, W.-B., and Julius, D. (2006). The P2Y12 receptor regulates microglial activation by extracellular nucleotides. Nat. Neurosci. *9*, 1512–1519.

Healy, D.G., Falchi, M., O'Sullivan, S.S., Bonifati, V., Durr, A., Bressman, S., Brice, A., Aasly, J., Zabetian, C.P., Goldwurm, S., et al. (2008). Phenotype, genotype, and worldwide genetic penetrance of LRRK2-associated Parkinson's disease: a case-control study. Lancet Neurol. *7*, 583–590.

Heneka, M.T., Kummer, M.P., and Latz, E. (2014). Innate immune activation in neurodegenerative disease. Nat. Rev. Immunol. *14*, 463–477.

Heng, Y., Zhang, X., Borggrewe, M., van Weering, H.R.J., Brummer, M.L., Nijboer, T.W., Joosten, L.A.B., Netea, M.G., Boddeke, E.W.G.M., Laman, J.D., et al. (2021). Systemic administration of β-glucan induces immune training in microglia. J. Neuroinflammation *18*, 57.

Hickman, S.E., Kingery, N.D., Ohsumi, T.K., Borowsky, M.L., Wang, L., Means, T.K., and El Khoury, J. (2013). The microglial sensome revealed by direct RNA sequencing. Nat. Neurosci. *16*, 1896–1905.

Hoffner, G., Island, M.-L., and Djian, P. (2005). Purification of neuronal inclusions of patients with Huntington's disease reveals a broad range of N-terminal fragments of expanded huntingtin and insoluble polymers. J. Neurochem. *95*, 125–136.

Hoozemans, J.J.M., van Haastert, E.S., Eikelenboom, P., de Vos, R.A.I., Rozemuller, J.M., and Scheper, W. (2007). Activation of the unfolded protein response in Parkinson's disease. Biochem. Biophys. Res. Commun. *354*, 707–711.

Huang, Y., Xu, Z., Xiong, S., Sun, F., Qin, G., Hu, G., Wang, J., Zhao, L., Liang, Y.-X., Wu, T., et al. (2018). Repopulated microglia are solely derived from the proliferation of residual microglia after acute depletion. Nat. Neurosci. *21*, 530–540.

Iadecola, C., and Anrather, J. (2011). The immunology of stroke: from mechanisms to translation. Nat. Med. *17*, 796–808.

Ibáñez, P., Bonnet, A.M., Débarges, B., Lohmann, E., Tison, F., Pollak, P., Agid, Y., Dürr, A., and Brice, A. (2004). Causal relation between alpha-synuclein gene duplication and familial Parkinson's disease. Lancet *364*, 1169–1171.

Ibáñez, P., Lesage, S., Janin, S., Lohmann, E., Durif, F., Destée, A., Bonnet, A.-M., Brefel-Courbon, C., Heath, S., Zelenika, D., et al. (2009). Alpha-synuclein gene rearrangements in dominantly inherited parkinsonism: frequency, phenotype, and mechanisms. Arch. Neurol. *66*, 102–108.

Ifrim, D.C., Quintin, J., Joosten, L.A.B., Jacobs, C., Jansen, T., Jacobs, L., Gow, N.A.R., Williams, D.L., van der Meer, J.W.M., and Netea, M.G. (2014). Trained immunity or tolerance: opposing functional programs induced in human monocytes after engagement of various pattern recognition receptors. Clin. Vaccine Immunol. *21*, 534–545.

Imamura, K., Hishikawa, N., Sawada, M., Nagatsu, T., Yoshida, M., and Hashizume, Y. (2003). Distribution of major histocompatibility complex class II-positive microglia and cytokine profile of Parkinson's disease brains. Acta Neuropathol. *106*, 518–526.

Islam, M.S., and Moore, D.J. (2017). Mechanisms of LRRK2-dependent neurodegeneration: role of enzymatic activity and protein aggregation. Biochem. Soc. Trans. *45*, 163–172.

Iwasaki, A., and Medzhitov, R. (2015). Control of adaptive immunity by the innate immune system. Nat. Immunol. *16*, 343–353.

Janda, E., Boi, L., and Carta, A.R. (2018). Microglial phagocytosis and its regulation: A therapeutic target in parkinson's disease? Front. Mol. Neurosci. *11*, 144.

Jansen, A.H.P., van Hal, M., Op den Kelder, I.C., Meier, R.T., de Ruiter, A.-A., Schut, M.H., Smith, D.L., Grit, C., Brouwer, N., Kamphuis, W., et al. (2017). Frequency of nuclear mutant huntingtin inclusion formation in neurons and glia is cell-type-specific. Glia *65*, 50–61.

Jordão, M.J.C., Sankowski, R., Brendecke, S.M., Sagar, Locatelli, G., Tai, Y.-H., Tay, T.L., Schramm, E., Armbruster, S., Hagemeyer, N., et al. (2019). Single-cell profiling identifies myeloid cell subsets with distinct fates during neuroinflammation. Science *363.*

Kannarkat, G.T., Boss, J.M., and Tansey, M.G. (2013). The role of innate and adaptive immunity in Parkinson's disease. J Parkinsons Dis *3*, 493–514.

Kempuraj, D., Thangavel, R., Natteru, P.A., Selvakumar, G.P., Saeed, D., Zahoor, H., Zaheer, S., Iyer, S.S., and Zaheer, A. (2016). Neuroinflammation Induces Neurodegeneration. J. Neurol. Neurosurg. Spine *1.*

Keren-Shaul, H., Spinrad, A., Weiner, A., Matcovitch-Natan, O., Dvir-Szternfeld, R., Ulland, T.K., David, E., Baruch, K., Lara-Astaiso, D., Toth, B., et al. (2017). A Unique Microglia Type Associated with Restricting Development of Alzheimer's Disease. Cell *169*, 1276-1290.e17.

Kigerl, K.A., Gensel, J.C., Ankeny, D.P., Alexander, J.K., Donnelly, D.J., and Popovich, P.G. (2009). Identification of two distinct macrophage subsets with divergent effects causing either neurotoxicity or regeneration in the injured mouse spinal cord. J. Neurosci. *29*, 13435–13444.

Kim, C., Ho, D.-H., Suk, J.-E., You, S., Michael, S., Kang, J., Joong Lee, S., Masliah, E., Hwang, D., Lee, H.-J., et al. (2013). Neuron-released oligomeric α-synuclein is an endogenous agonist of TLR2 for paracrine activation of microglia. Nat. Commun. *4*, 1562.

King, E., and Thomas, A. (2017). Systemic inflammation in lewy body diseases: A systematic review. Alzheimer Dis. Assoc. Disord. *31*, 346–356.

Kleinnijenhuis, J., Quintin, J., Preijers, F., Joosten, L.A.B., Ifrim, D.C., Saeed, S., Jacobs, C., van Loenhout, J., de Jong, D., Stunnenberg, H.G., et al. (2012). Bacille Calmette-Guerin induces NOD2-dependent nonspecific protection from reinfection via epigenetic reprogramming of monocytes. Proc Natl Acad Sci USA *109*, 17537–17542.

Koros, C., Simitsi, A., and Stefanis, L. (2017). Genetics of Parkinson's Disease: Genotype-Phenotype Correlations. Int. Rev. Neurobiol. *132*, 197–231.

Kraft, A.D., Kaltenbach, L.S., Lo, D.C., and Harry, G.J. (2012). Activated microglia proliferate at neurites of mutant huntingtin-expressing neurons. Neurobiol. Aging *33*, 621.e17-33.

Krasemann, S., Madore, C., Cialic, R., Baufeld, C., Calcagno, N., El Fatimy, R., Beckers, L., O'Loughlin, E., Xu, Y., Fanek, Z., et al. (2017). The TREM2-APOE pathway drives the transcriptional phenotype of dysfunctional microglia in neurodegenerative diseases. Immunity *47*, 566-581.e9.

Kumari, U., and Tan, E.K. (2009). LRRK2 in Parkinson's disease: genetic and clinical studies from patients. FEBS J. *276*, 6455–6463.

Kurtz, J. (2005). Specific memory within innate immune systems. Trends Immunol. *26*, 186–192.

Kwan, W., Träger, U., Davalos, D., Chou, A., Bouchard, J., Andre, R., Miller, A., Weiss, A., Giorgini, F., Cheah, C., et al. (2012). Mutant huntingtin impairs immune cell migration in Huntington disease. J. Clin. Invest. *122*, 4737–4747.

Kwon, H.S., and Koh, S.-H. (2020). Neuroinflammation in neurodegenerative disorders: the roles of microglia and astrocytes. Transl. Neurodegener. *9*, 1–12.

Lajqi, T., Lang, G.-P., Haas, F., Williams, D.L., Hudalla, H., Bauer, M., Groth, M., Wetzker, R., and Bauer, R. (2019). Memory-Like Inflammatory Responses of Microglia to Rising Doses of LPS: Key Role of PI3Kγ. Front. Immunol. *10*, 2492.

LaMar, D. (2015). FastQC.

Langfelder, P., and Horvath, S. (2008). WGCNA: an R package for weighted correlation network analysis. BMC Bioinformatics *9*, 559.

Lanier, L.L. (2005). NK cell recognition. Annu. Rev. Immunol. *23*, 225–274.

Lau, S.-F., Chen, C., Fu, W.-Y., Qu, J.Y., Cheung, T.H., Fu, A.K.Y., and Ip, N.Y. (2020). IL-33-PU.1 Transcriptome Reprogramming Drives Functional State Transition and Clearance Activity of Microglia in Alzheimer's Disease. Cell Rep. *31*, 107530.

Lawrence, M., Huber, W., Pagès, H., Aboyoun, P., Carlson, M., Gentleman, R., Morgan, M.T., and Carey, V.J. (2013). Software for computing and annotating genomic ranges. PLoS Comput. Biol. *9*, e1003118.

Lawson, L.J., Perry, V.H., Dri, P., and Gordon, S. (1990). Heterogeneity in the distribution and morphology of microglia in the normal adult mouse brain. Neuroscience *39*, 151–170.

Lawson, L.J., Perry, V.H., and Gordon, S. (1992). Turnover of resident microglia in the normal adult mouse brain. Neuroscience *48*, 405–415.

Lay, K., Yuan, S., Gur-Cohen, S., Miao, Y., Han, T., Naik, S., Pasolli, H.A., Larsen, S.B., and Fuchs, E. (2018). Stem cells repurpose proliferation to contain a breach in their niche barrier. ELife *7*.

Leek, J.T., Johnson, W.E., Parker, H.S., Fertig, E.J., Jaffe, A.E., Storey, J.D., Zhang, Y., and Torres, L.C. (2019). sva: Surrogate variable analysis. R Package Version *3*, 882–883.

Lee, S.-H., Meilandt, W.J., Xie, L., Gandham, V.D., Ngu, H., Barck, K.H., Rezzonico, M.G., Imperio, J., Lalehzadeh, G., Huntley, M.A., et al. (2021). Trem2 restrains the enhancement of tau accumulation and neurodegeneration by β-amyloid pathology. Neuron *109*, 1283-1301.e6.

Lin, M.T., and Beal, M.F. (2006). Mitochondrial dysfunction and oxidative stress in neurodegenerative diseases. Nature *443*, 787–795.

Lin, M.-M., Liu, N., Qin, Z.-H., and Wang, Y. (2022). Mitochondrial-derived damage-associated molecular patterns amplify neuroinflammation in neurodegenerative diseases. Acta Pharmacol. Sin.

Li, Q., and Barres, B.A. (2018). Microglia and macrophages in brain homeostasis and disease. Nat. Rev. Immunol. *18*, 225–242.

Li, Q., Cheng, Z., Zhou, L., Darmanis, S., Neff, N.F., Okamoto, J., Gulati, G., Bennett, M.L., Sun, L.O., Clarke, L.E., et al. (2019). Developmental Heterogeneity of Microglia and Brain Myeloid Cells Revealed by Deep Single-Cell RNA Sequencing. Neuron *101*, 207-223.e10.

Lloyd, A.F., and Miron, V.E. (2019). The pro-remyelination properties of microglia in the central nervous system. Nat. Rev. Neurol. *15*, 447–458.

Lopes, K. de P., Snijders, G.J.L., Humphrey, J., Allan, A., Sneeboer, M.A.M., Navarro, E., Schilder, B.M., Vialle, R.A., Parks, M., Missall, R., et al. (2022). Genetic analysis of the human microglial transcriptome across brain regions, aging and disease pathologies. Nat. Genet. *54*, 4–17.

Lopez-Atalaya, J.P., Askew, K.E., Sierra, A., and Gomez-Nicola, D. (2018). Development and maintenance of the brain's immune toolkit: Microglia and non-parenchymal brain macrophages. Dev. Neurobiol. *78*, 561–579.

Love, M.I., Huber, W., and Anders, S. (2014). Moderated estimation of fold change and dispersion for RNA-seq data with DESeq2. Genome Biol. *15*, 550.

Marakalala, M.J., Williams, D.L., Hoving, J.C., Engstad, R., Netea, M.G., and Brown, G.D. (2013). Dectin-1 plays a redundant role in the immunomodulatory activities of β-glucan-rich ligands in vivo. Microbes Infect. *15*, 511–515.

Martinez-Vicente, M., Talloczy, Z., Wong, E., Tang, G., Koga, H., Kaushik, S., de Vries, R., Arias, E., Harris, S., Sulzer, D., et al. (2010). Cargo recognition failure is responsible for inefficient autophagy in Huntington's disease. Nat. Neurosci. *13*, 567–576.

Martin, J.B., and Gusella, J.F. (1986). Huntington's disease. Pathogenesis and management. N. Engl. J. Med. *315*, 1267–1276.

Masuda, T., Sankowski, R., Staszewski, O., and Prinz, M. (2020). Microglia Heterogeneity in the Single-Cell Era. Cell Rep. *30*, 1271–1281.

Mathys, H., Adaikkan, C., Gao, F., Young, J.Z., Manet, E., Hemberg, M., De Jager, P.L., Ransohoff, R.M., Regev, A., and Tsai, L.-H. (2017). Temporal Tracking of Microglia Activation in Neurodegeneration at Single-Cell Resolution. Cell Rep. *21*, 366–380.

Mathys, H., Davila-Velderrain, J., Peng, Z., Gao, F., Mohammadi, S., Young, J.Z., Menon, M., He, L., Abdurrob, F., Jiang, X., et al. (2019). Single-cell transcriptomic analysis of Alzheimer's disease. Nature *570*, 332–337.

McGeer, P.L., Itagaki, S., Boyes, B.E., and McGeer, E.G. (1988). Reactive microglia are positive for HLA-DR in the substantia nigra of Parkinson's and Alzheimer's disease brains. Neurology *38*, 1285–1291.

Medzhitov, R., and Janeway, C. (2000). Innate immune recognition: mechanisms and pathways. Immunol. Rev. *173*, 89–97.

Meredith, G.E., and Rademacher, D.J. (2011). MPTP mouse models of Parkinson's disease: an update. J Parkinsons Dis *1*, 19–33.

Mildner, A., Huang, H., Radke, J., Stenzel, W., and Priller, J. (2017). P2Y12 receptor is expressed on human microglia under physiological conditions throughout development and is sensitive to neuroinflammatory diseases. Glia *65*, 375–387.

Miron, V.E., Boyd, A., Zhao, J.-W., Yuen, T.J., Ruckh, J.M., Shadrach, J.L., van Wijngaarden, P., Wagers, A.J., Williams, A., Franklin, R.J.M., et al. (2013). M2 microglia and macrophages drive oligodendrocyte differentiation during CNS remyelination. Nat. Neurosci. *16*, 1211–1218.

Morgan, M., Obenchain, V., Hester, J., and Pagès, H. (2017). SummarizedExperiment: SummarizedExperiment container. R Package Version *1*.

Mosley, R.L., Hutter-Saunders, J.A., Stone, D.K., and Gendelman, H.E. (2012). Inflammation and adaptive immunity in Parkinson's disease. Cold Spring Harb. Perspect. Med. *2*, a009381.

Mrdjen, D., Pavlovic, A., Hartmann, F.J., Schreiner, B., Utz, S.G., Leung, B.P., Lelios, I., Heppner, F.L., Kipnis, J., Merkler, D., et al. (2018). High-Dimensional Single-Cell Mapping of Central Nervous System Immune Cells Reveals Distinct Myeloid Subsets in Health, Aging, and Disease. Immunity *48*, 380-395.e6.

Nagatsu, T., Mogi, M., Ichinose, H., and Togari, A. (2000). Changes in cytokines and neurotrophins in Parkinson's disease. J. Neural Transm. Suppl. 277–290.

Naik, S., Larsen, S.B., Gomez, N.C., Alaverdyan, K., Sendoel, A., Yuan, S., Polak, L., Kulukian, A., Chai, S., and Fuchs, E. (2017). Inflammatory memory sensitizes skin epithelial stem cells to tissue damage. Nature *550*, 475–480.

Nalls, M.A., Blauwendraat, C., Vallerga, C.L., Heilbron, K., Bandres-Ciga, S., Chang, D., Tan, M., Kia, D.A., Noyce, A.J., Xue, A., et al. (2019). Identification of novel risk loci, causal insights, and heritable risk for Parkinson's disease: a meta-analysis of genome-wide association studies. Lancet Neurol. *18*, 1091–1102.

Napoli, I., and Neumann, H. (2009). Microglial clearance function in health and disease. Neuroscience *158*, 1030–1038.

Neher, J.J., and Cunningham, C. (2019). Priming microglia for innate immune memory in the brain. Trends Immunol. *40*, 358–374.

Neher, J.J., Neniskyte, U., Zhao, J.-W., Bal-Price, A., Tolkovsky, A.M., and Brown, G.C. (2011). Inhibition of microglial phagocytosis is sufficient to prevent inflammatory neuronal death. J. Immunol. *186*, 4973–4983.

Netea, M.G., Latz, E., Mills, K.H.G., and O'Neill, L.A.J. (2015). Innate immune memory: a paradigm shift in understanding host defense. Nat. Immunol. *16*, 675–679.

Netea, M.G., Joosten, L.A.B., Latz, E., Mills, K.H.G., Natoli, G., Stunnenberg, H.G., O'Neill, L.A.J., and Xavier, R.J. (2016). Trained immunity: A program of innate immune memory in health and disease. Science *352*, aaf1098.

Nguyen, A.T., Wang, K., Hu, G., Wang, X., Miao, Z., Azevedo, J.A., Suh, E., Van Deerlin, V.M., Choi, D., Roeder, K., et al. (2020). APOE and TREM2 regulate amyloid-responsive microglia in Alzheimer's disease. Acta Neuropathol. *140*, 477–493.

Novakovic, B., Habibi, E., Wang, S.-Y., Arts, R.J.W., Davar, R., Megchelenbrink, W., Kim, B., Kuznetsova, T., Kox, M., Zwaag, J., et al. (2016). β-Glucan Reverses the Epigenetic State of LPS-Induced Immunological Tolerance. Cell *167*, 1354-1368.e14.

Nuber, S., Harmuth, F., Kohl, Z., Adame, A., Trejo, M., Schönig, K., Zimmermann, F., Bauer, C., Casadei, N., Giel, C., et al. (2013). A progressive dopaminergic phenotype associated with neurotoxic conversion of α-synuclein in BAC-transgenic rats. Brain *136*, 412–432.

O'Neill, L.A.J., Golenbock, D., and Bowie, A.G. (2013). The history of Toll-like receptors - redefining innate immunity. Nat. Rev. Immunol. *13*, 453–460.

Orre, M., Kamphuis, W., Dooves, S., Kooijman, L., Chan, E.T., Kirk, C.J., Dimayuga Smith, V., Koot, S., Mamber, C., Jansen, A.H., et al. (2013). Reactive glia show increased immunoproteasome activity in Alzheimer's disease. Brain *136*, 1415–1431.

Ostuni, R., Piccolo, V., Barozzi, I., Polletti, S., Termanini, A., Bonifacio, S., Curina, A., Prosperini, E., Ghisletti, S., and Natoli, G. (2013). Latent enhancers activated by stimulation in differentiated cells. Cell *152*, 157–171.

Paisán-Ruíz, C., Nath, P., Washecka, N., Gibbs, J.R., and Singleton, A.B. (2008). Comprehensive analysis of LRRK2 in publicly available Parkinson's disease cases and neurologically normal controls. Hum. Mutat. *29*, 485–490.

Paldino, E., Balducci, C., La Vitola, P., Artioli, L., D'Angelo, V., Giampà, C., Artuso, V., Forloni, G., and Fusco, F.R. (2020). Neuroprotective effects of doxycycline in the R6/2 mouse model of huntington's disease. Mol. Neurobiol. *57*, 1889–1903.

Palpagama, T.H., Waldvogel, H.J., Faull, R.L.M., and Kwakowsky, A. (2019). The role of microglia and astrocytes in huntington's disease. Front. Mol. Neurosci. *12*, 258.

Parhizkar, S., Arzberger, T., Brendel, M., Kleinberger, G., Deussing, M., Focke, C., Nuscher, B., Xiong, M., Ghasemigharagoz, A., Katzmarski, N., et al. (2019). Loss of TREM2 function increases amyloid seeding but reduces plaque-associated ApoE. Nat. Neurosci. *22*, 191–204.

Parkhurst, C.N., Yang, G., Ninan, I., Savas, J.N., Yates, J.R., Lafaille, J.J., Hempstead, B.L., Littman, D.R., and Gan, W.-B. (2013). Microglia promote learning-dependent synapse formation through brain-derived neurotrophic factor. Cell *155*, 1596–1609.

Parkinson, J. (2002). An essay on the shaking palsy. 1817. J. Neuropsychiatry Clin. Neurosci. *14*, 223–236; discussion 222.

Parkin, J., and Cohen, B. (2001). An overview of the immune system. Lancet *357*, 1777–1789.

Park, J.S., Saeed, K., Jo, M.H., Kim, M.W., Lee, H.J., Park, C.-B., Lee, G., and Kim, M.O. (2022). LDHB deficiency promotes mitochondrial dysfunction mediated oxidative stress and neurodegeneration in adult mouse brain. Antioxidants (Basel) *11*.

Pavese, N., Gerhard, A., Tai, Y.F., Ho, A.K., Turkheimer, F., Barker, R.A., Brooks, D.J., and Piccini, P. (2006). Microglial activation correlates with severity in Huntington disease: a clinical and PET study. Neurology *66*, 1638–1643.

Peng, J., Liu, Y., Umpierre, A.D., Xie, M., Tian, D.-S., Richardson, J.R., and Wu, L.-J. (2019). Microglial P2Y12 receptor regulates ventral hippocampal CA1 neuronal excitability and innate fear in mice. Mol. Brain *12*, 71.

Perdiguero, E.G., and Geissmann, F. (2016). The development and maintenance of resident macrophages. Nat. Immunol. *17*, 2–8.

van der Poel, M., Ulas, T., Mizee, M.R., Hsiao, C.-C., Miedema, S.S.M., Adelia, Schuurman, K.G., Helder, B., Tas, S.W., Schultze, J.L., et al. (2019). Transcriptional profiling of human microglia reveals grey-white matter heterogeneity and multiple sclerosis-associated changes. Nat. Commun. *10*, 1139.

Polymeropoulos, M.H., Lavedan, C., Leroy, E., Ide, S.E., Dehejia, A., Dutra, A., Pike, B., Root, H., Rubenstein, J., Boyer, R., et al. (1997). Mutation in the alpha-synuclein gene identified in families with Parkinson's disease. Science *276*, 2045–2047.

Polyzos, A.A., and McMurray, C.T. (2017). The chicken or the egg: mitochondrial dysfunction as a cause or consequence of toxicity in Huntington's disease. Mech. Ageing Dev. *161*, 181–197.

Prater, K.E., Green, K.J., Smith, C.L., Sun, W., Chiou, K.L., Kwon, R.Y., Heath, L., Rose, S., Shojaie, A., Snyder-Mackler, N., et al. (2021). Subtype transcriptomic profiling of myeloid cells in Alzheimer Disease brain illustrates the diversity in active microglia phenotypes. BioRxiv.

Prinz, M., and Priller, J. (2014). Microglia and brain macrophages in the molecular age: from origin to neuropsychiatric disease. Nat. Rev. Neurosci. *15*, 300–312.

Prinz, M., Erny, D., and Hagemeyer, N. (2017). Ontogeny and homeostasis of CNS myeloid cells. Nat. Immunol. *18*, 385–392.

Prinz, M., Jung, S., and Priller, J. (2019). Microglia biology: one century of evolving concepts. Cell *179*, 292–311.

Prinz, M., Masuda, T., Wheeler, M.A., and Quintana, F.J. (2021). Microglia and Central Nervous System-Associated Macrophages-From Origin to Disease Modulation. Annu. Rev. Immunol. *39*, 251–277.

Püntener, U., Booth, S.G., Perry, V.H., and Teeling, J.L. (2012). Long-term impact of systemic bacterial infection on the cerebral vasculature and microglia. J. Neuroinflammation *9*, 146.

Quintin, J., Saeed, S., Martens, J.H.A., Giamarellos-Bourboulis, E.J., Ifrim, D.C., Logie, C., Jacobs, L., Jansen, T., Kullberg, B.-J., Wijmenga, C., et al. (2012). Candida albicans infection affords protection against reinfection via functional reprogramming of monocytes. Cell Host Microbe *12*, 223–232.

Rajendran, L., and Paolicelli, R.C. (2018). Microglia-Mediated Synapse Loss in Alzheimer's Disease. J. Neurosci. *38*, 2911–2919.

Ransohoff, R.M., and Perry, V.H. (2009). Microglial physiology: unique stimuli, specialized responses. Annu. Rev. Immunol. *27*, 119–145.

Réu, P., Khosravi, A., Bernard, S., Mold, J.E., Salehpour, M., Alkass, K., Perl, S., Tisdale, J., Possnert, G., Druid, H., et al. (2017). The lifespan and turnover of microglia in the human brain. Cell Rep. *20*, 779–784.

Ritchie, M.E., Phipson, B., Wu, D., Hu, Y., Law, C.W., Shi, W., and Smyth, G.K. (2015). limma powers differential expression analyses for RNA-sequencing and microarray studies. Nucleic Acids Res. *43*, e47.

Russo, M.V., and McGavern, D.B. (2016). Inflammatory neuroprotection following traumatic brain injury. Science *353*, 783–785.

Ryu, E.J., Harding, H.P., Angelastro, J.M., Vitolo, O.V., Ron, D., and Greene, L.A. (2002). Endoplasmic reticulum stress and the unfolded protein response in cellular models of Parkinson's disease. J. Neurosci. *22*, 10690–10698.

Saeed, S., Quintin, J., Kerstens, H.H.D., Rao, N.A., Aghajanirefah, A., Matarese, F., Cheng, S.-C., Ratter, J., Berentsen, K., van der Ent, M.A., et al. (2014). Epigenetic programming of monocyte-to-macrophage differentiation and trained innate immunity. Science *345*, 1251086.

Safaiyan, S., Besson-Girard, S., Kaya, T., Cantuti-Castelvetri, L., Liu, L., Ji, H., Schifferer, M., Gouna, G., Usifo, F., Kannaiyan, N., et al. (2021). White matter aging drives microglial diversity. Neuron *109*, 1100-1117.e10.

Sala Frigerio, C., Wolfs, L., Fattorelli, N., Thrupp, N., Voytyuk, I., Schmidt, I., Mancuso, R., Chen, W.-T., Woodbury, M.E., Srivastava, G., et al. (2019). The major risk factors for alzheimer's disease: age, sex, and genes modulate the microglia response to aβ plaques. Cell Rep. *27*, 1293-1306.e6.

Sapp, E., Kegel, K.B., Aronin, N., Hashikawa, T., Uchiyama, Y., Tohyama, K., Bhide, P.G., Vonsattel, J.P., and DiFiglia, M. (2001). Early and progressive accumulation of reactive microglia in the Huntington disease brain. J. Neuropathol. Exp. Neurol. *60*, 161–172.

Sarkar, S., Malovic, E., Harishchandra, D.S., Ghaisas, S., Panicker, N., Charli, A., Palanisamy, B.N., Rokad, D., Jin, H., Anantharam, V., et al. (2017). Mitochondrial impairment in microglia amplifies NLRP3 inflammasome proinflammatory signaling in cell culture and animal models of Parkinson's disease. Npj Parkinsons Disease *3*, 30.

Schaafsma, W., Zhang, X., van Zomeren, K.C., Jacobs, S., Georgieva, P.B., Wolf, S.A., Kettenmann, H., Janova, H., Saiepour, N., Hanisch, U.K., et al. (2015). Long-lasting pro-inflammatory suppression of microglia by LPS-preconditioning is mediated by RelB-dependent epigenetic silencing. Brain Behav. Immun. *48*, 205–221.

Schapansky, J., Nardozzi, J.D., Felizia, F., and LaVoie, M.J. (2014). Membrane recruitment of endogenous LRRK2 precedes its potent regulation of autophagy. Hum. Mol. Genet. *23*, 4201–4214.

Schmid, C.D., Sautkulis, L.N., Danielson, P.E., Cooper, J., Hasel, K.W., Hilbush, B.S., Sutcliffe, J.G., and Carson, M.J. (2002). Heterogeneous expression of the triggering receptor expressed on myeloid cells-2 on adult murine microglia. J. Neurochem. *83*, 1309–1320.

Shirendeb, U., Reddy, A.P., Manczak, M., Calkins, M.J., Mao, P., Tagle, D.A., and Reddy, P.H. (2011). Abnormal mitochondrial dynamics, mitochondrial loss and mutant huntingtin oligomers in Huntington's disease: implications for selective neuronal damage. Hum. Mol. Genet. *20*, 1438–1455.

Sierksma, A., Lu, A., Mancuso, R., Fattorelli, N., Thrupp, N., Salta, E., Zoco, J., Blum, D., Buée, L., De Strooper, B., et al. (2020). Novel Alzheimer risk genes determine the microglia response to amyloid-β but not to TAU pathology. EMBO Mol. Med. *12*, e10606.

Siew, J.J., Chen, H.-M., Chen, H.-Y., Chen, H.-L., Chen, C.-M., Soong, B.-W., Wu, Y.-R., Chang, C.-P., Chan, Y.-C., Lin, C.-H., et al. (2019). Galectin-3 is required for the microglia-mediated brain inflammation in a model of Huntington's disease. Nat. Commun. *10*, 3473.

Singleton, A.B., Farrer, M., Johnson, J., Singleton, A., Hague, S., Kachergus, J., Hulihan, M., Peuralinna, T., Dutra, A., Nussbaum, R., et al. (2003). alpha-Synuclein locus triplication causes Parkinson's disease. Science *302*, 841.

Smith, A.M., Depp, C., Ryan, B.J., Johnston, G.I., Alegre-Abarrategui, J., Evetts, S., Rolinski, M., Baig, F., Ruffmann, C., Simon, A.K., et al. (2018). Mitochondrial dysfunction and increased glycolysis in prodromal and early Parkinson's blood cells. Mov. Disord. *33*, 1580–1590.

Soto, C., and Pritzkow, S. (2018). Protein misfolding, aggregation, and conformational strains in neurodegenerative diseases. Nat. Neurosci. *21*, 1332–1340.

Stefanis, L. (2012). α-Synuclein in Parkinson's disease. Cold Spring Harb. Perspect. Med. *2*, a009399.

Stephenson, J., Nutma, E., van der Valk, P., and Amor, S. (2018). Inflammation in CNS neurodegenerative diseases. Immunology *154*, 204–219.

Stokholm, M.G., Iranzo, A., Østergaard, K., Serradell, M., Otto, M., Svendsen, K.B., Garrido, A., Vilas, D., Borghammer, P., Santamaria, J., et al. (2017). Assessment of neuroinflammation in patients with idiopathic rapid-eye-movement sleep behaviour disorder: a case-control study. Lancet Neurol. *16*, 789–796.

Stone, D.K., Reynolds, A.D., Mosley, R.L., and Gendelman, H.E. (2009). Innate and adaptive immunity for the pathobiology of Parkinson's disease. Antioxid. Redox Signal. *11*, 2151–2166.

Sturm, M., Schroeder, C., and Bauer, P. (2016). SeqPurge: highly-sensitive adapter trimming for paired-end NGS data. BMC Bioinformatics *17*, 208.

Su, P., Zhang, J., Wang, D., Zhao, F., Cao, Z., Aschner, M., and Luo, W. (2016). The role of autophagy in modulation of neuroinflammation in microglia. Neuroscience *319*, 155–167.

Su, X., Maguire-Zeiss, K.A., Giuliano, R., Prifti, L., Venkatesh, K., and Federoff, H.J. (2008). Synuclein activates microglia in a model of Parkinson's disease. Neurobiol. Aging *29*, 1690–1701.

Tai, Y.F., Pavese, N., Gerhard, A., Tabrizi, S.J., Barker, R.A., Brooks, D.J., and Piccini, P. (2007). Microglial activation in presymptomatic Huntington's disease gene carriers. Brain *130*, 1759–1766.

Tang, Y., and Le, W. (2016). Differential roles of M1 and M2 microglia in neurodegenerative diseases. Mol. Neurobiol. *53*, 1181–1194.

Tansey, M.G., and Goldberg, M.S. (2010). Neuroinflammation in Parkinson's disease: its role in neuronal death and implications for therapeutic intervention. Neurobiol. Dis. *37*, 510–518.

Tay, T.L., Mai, D., Dautzenberg, J., Fernández-Klett, F., Lin, G., Sagar, Datta, M., Drougard, A., Stempfl, T., Ardura-Fabregat, A., et al. (2017). A new fate mapping system reveals context-dependent random or clonal expansion of microglia. Nat. Neurosci. *20*, 793–803.

Team, R.C. (2013). R: A language and environment for statistical computing.

Thion, M.S., Low, D., Silvin, A., Chen, J., Grisel, P., Schulte-Schrepping, J., Blecher, R., Ulas, T., Squarzoni, P., Hoeffel, G., et al. (2018). Microbiome Influences Prenatal and Adult Microglia in a Sex-Specific Manner. Cell *172*, 500-516.e16.

Tieu, K. (2011). A guide to neurotoxic animal models of Parkinson's disease. Cold Spring Harb. Perspect. Med. *1*, a009316.

Varvel, N.H., Grathwohl, S.A., Baumann, F., Liebig, C., Bosch, A., Brawek, B., Thal, D.R., Charo, I.F., Heppner, F.L., Aguzzi, A., et al. (2012). Microglial repopulation model reveals a robust homeostatic process for replacing CNS myeloid cells. Proc Natl Acad Sci USA *109*, 18150–18155.

Vilalta, A., and Brown, G.C. (2018). Neurophagy, the phagocytosis of live neurons and synapses by glia, contributes to brain development and disease. FEBS J. *285*, 3566–3575.

Villar-Piqué, A., Lopes da Fonseca, T., and Outeiro, T.F. (2016). Structure, function and toxicity of alpha-synuclein: the Bermuda triangle in synucleinopathies. J. Neurochem. *139 Suppl 1*, 240–255.

Vonsattel, J.P., and DiFiglia, M. (1998). Huntington disease. J. Neuropathol. Exp. Neurol. *57*, 369–384.

Vonsattel, J.P., Myers, R.H., Stevens, T.J., Ferrante, R.J., Bird, E.D., and Richardson, E.P. (1985). Neuropathological classification of Huntington's disease. J. Neuropathol. Exp. Neurol. *44*, 559–577.

Wakabayashi, K., Tanji, K., Mori, F., and Takahashi, H. (2007). The Lewy body in Parkinson's disease: molecules implicated in the formation and degradation of alpha-synuclein aggregates. Neuropathology *27*, 494–506.

Wake, H., Moorhouse, A.J., Miyamoto, A., and Nabekura, J. (2013). Microglia: actively surveying and shaping neuronal circuit structure and function. Trends Neurosci. *36*, 209–217.

Waldvogel, H.J., Kim, E.H., Tippett, L.J., Vonsattel, J.-P.G., and Faull, R.L.M. (2015). The neuropathology of huntington's disease. Curr. Top. Behav. Neurosci. *22*, 33–80.

Wang, H. (2021). Microglia Heterogeneity in Alzheimer's Disease: Insights From Single-Cell Technologies. Front. Synaptic Neurosci. *13*, 773590.

Wang, G., Yu, J., Yang, Y., Liu, X., Zhao, X., Guo, X., Duan, T., Lu, C., and Kang, J. (2020a). Whole-transcriptome sequencing uncovers core regulatory modules and gene signatures of human fetal growth restriction. Clin. Transl. Med. *9*, 9.

Wang, S., Mustafa, M., Yuede, C.M., Salazar, S.V., Kong, P., Long, H., Ward, M., Siddiqui, O., Paul, R., Gilfillan, S., et al. (2020b). Anti-human TREM2 induces microglia proliferation and reduces pathology in an Alzheimer's disease model. J. Exp. Med. *217*.

Wendeln, A.-C., Degenhardt, K., Kaurani, L., Gertig, M., Ulas, T., Jain, G., Wagner, J., Häsler, L.M., Wild, K., Skodras, A., et al. (2018). Innate immune memory in the brain shapes neurological disease hallmarks. Nature *556*, 332–338.

Weydt, P., Pineda, V.V., Torrence, A.E., Libby, R.T., Satterfield, T.F., Lazarowski, E.R., Gilbert, M.L., Morton, G.J., Bammler, T.K., Strand, A.D., et al. (2006). Thermoregulatory and

metabolic defects in Huntington's disease transgenic mice implicate PGC-1alpha in Huntington's disease neurodegeneration. Cell Metab. *4*, 349–362.

Wickham, H. (2016). ggplot2: elegant graphics for data analysis (springer).

Wolf, S.A., Boddeke, H.W.G.M., and Kettenmann, H. (2017). Microglia in physiology and disease. Annu. Rev. Physiol. *79*, 619–643.

Wong, Y.C., and Krainc, D. (2017). α-synuclein toxicity in neurodegeneration: mechanism and therapeutic strategies. Nat. Med. *23*, 1–13.

van 't Wout, J.W., Poell, R., and van Furth, R. (1992). The role of BCG/PPD-activated macrophages in resistance against systemic candidiasis in mice. Scand. J. Immunol. *36*, 713–719.

Wu, T., Hu, E., Xu, S., Chen, M., Guo, P., Dai, Z., Feng, T., Zhou, L., Tang, W., Zhan, L., et al. (2021). clusterProfiler 4.0: A universal enrichment tool for interpreting omics data. Innovation (N Y) *2*, 100141.

Wyss-Coray, T., and Mucke, L. (2002). Inflammation in neurodegenerative disease--a double-edged sword. Neuron *35*, 419–432.

Xu, Y., Jin, M.-Z., Yang, Z.-Y., and Jin, W.-L. (2021). Microglia in neurodegenerative diseases. Neural Regen. Res. *16*, 270–280.

Yang, H.-M., Yang, S., Huang, S.-S., Tang, B.-S., and Guo, J.-F. (2017). Microglial activation in the pathogenesis of huntington's disease. Front. Aging Neurosci. *9*, 193.

Yoshida, K., Maekawa, T., Zhu, Y., Renard-Guillet, C., Chatton, B., Inoue, K., Uchiyama, T., Ishibashi, K., Yamada, T., Ohno, N., et al. (2015). The transcription factor ATF7 mediates lipopolysaccharide-induced epigenetic changes in macrophages involved in innate immunological memory. Nat. Immunol. *16*, 1034–1043.

Yu-Taeger, L., Petrasch-Parwez, E., Osmand, A.P., Redensek, A., Metzger, S., Clemens, L.E., Park, L., Howland, D., Calaminus, C., Gu, X., et al. (2012). A novel BACHD transgenic rat exhibits characteristic neuropathological features of Huntington disease. J. Neurosci. *32*, 15426–15438.

Yu, G., Wang, L.-G., Han, Y., and He, Q.-Y. (2012). clusterProfiler: an R package for comparing biological themes among gene clusters. OMICS *16*, 284–287.

Yu, G., Wang, L.-G., Yan, G.-R., and He, Q.-Y. (2015). DOSE: an R/Bioconductor package for disease ontology semantic and enrichment analysis. Bioinformatics *31*, 608–609.

Zhang, X., Kracht, L., Lerario, A.M., Dubbelaar, M.L., Brouwer, N., Wesseling, E.M., Boddeke, E.W.G.M., Eggen, B.J.L., and Kooistra, S.M. (2021). Epigenetic regulation of innate immune memory in microglia. BioRxiv.

Zheng, G.X.Y., Terry, J.M., Belgrader, P., Ryvkin, P., Bent, Z.W., Wilson, R., Ziraldo, S.B., Wheeler, T.D., McDermott, G.P., Zhu, J., et al. (2017). Massively parallel digital transcriptional profiling of single cells. Nat. Commun. *8*, 14049.

Zhou, Y., Song, W.M., Andhey, P.S., Swain, A., Levy, T., Miller, K.R., Poliani, P.L., Cominelli, M., Grover, S., Gilfillan, S., et al. (2020). Human and mouse single-nucleus transcriptomics reveal TREM2-dependent and TREM2-independent cellular responses in Alzheimer's disease. Nat. Med. *26*, 131–142.

George Huntington (1850-1916) and Hereditary Chorea: Journal of the History of the Neurosciences: Vol 9, No 1. Journal of the History of the Neurosciences.